공학박사학위논문

Risk-Based Design and Management of Chemical Processes Considering Process Life Cycle

공정주기에 따른 위험도 기반의 설계 및 관리

2019 년 2 월

서울대학교 대학원

화학생물공학부

이 영 근

Abstract

Risk-Based Design and Management of Chemical Processes Considering Process Life Cycle

Younggeun Lee
School of Chemical & Biological Engineering
The Graduate School
Seoul National University

Process safety has been considered and used to the chemical process from the design stage to the operation stage due to its importance. Several types of safety management techniques are applied and used in each stage of process life cycle. However, some techniques are qualitative, while some are quantitative, but have limitations in applications due to increased process complexity. Therefore, it is necessary to apply quantitative process safety management method considering process life cycle with process characteristics. In this thesis, risk-based design and management methodology considering process life cycle are proposed and applied for process safety management.

First, risk-based design methodology is proposed and applied to consider process safety in the conceptual design stage. The inherent safety design (ISD) methodology with quantitative risk assessment (QRA) are used to consider the

safety of process quantitatively. The risk-based design methodology is applied to organic Rankine cycle (ORC) design utilized as a method of utilizing the cold energy of liquefied natural gas (LNG). ORC design considering the thermodynamic and safety aspects is explored with a multi-objective optimization methodology to consider safety in conceptual stage. Considering the working fluid as the main factor for optimal ORC design, six working fluids in three categories (pure component, binary components, ternary components) are investigated. As a result, the ORC process considering safety aspect as well as thermodynamic aspect can be designed and selected based on the risk-based design methodology in the stage of conceptual design.

Secondly, risk-based management with risk assessment considering the seismic effect is proposed and applied to consider the specific characteristics of process in the basic design stage. The QRA are improved to assess the risk of seismic effect with domino effects, and multi-hazard impacts by using a Bayesian network (BN). This analysis is applied to a topside CO_2 injection system for underground storage, which is susceptible to seismic effects. Because frequency analysis is based on a causal relationship, the BN can be used to simultaneously consider domino effects and multi-hazard risks. As a result, the safety of the CO_2 injection process to be installed in seismic area are managed with by evaluating the risk including seismic effect in the stage of basic design.

Lastly, risk-based patrol for management is proposed and applied to consider the risk in the stage of operation. The risk-based patrol is applied to natural gas

(NG) pipeline to manage NG pipeline safety with quantitative risk. The overall structure, which is made up of probability of failure (PoF) and consequence of failure (CoF), of methodology for risk-based patrol is based on risk-based inspection (RBI) methodology. Moreover, the risk factor that affect the risk of NG pipeline in aspect of patrol are proposed and added to make the methodology more reasonable. As a result, minimum patrol period is obtained from the result of risk matrix, and the risk value give the insight of patrol plan by applying the risk-based patrol for management in the stage of operation.

Keywords: Process Life Cycle (PLC); Process Design; Risk-Based Design; Quantitative Risk Assessment (QRA); Risk-Based Management (RBM);

Student Number: 2014-21540

Contents

List of Figures

List of Tables

CHAPTER 1. Introduction

1.1. Research motivation

Chemical processes have been designed and constructed globally. The processes are diverse and have different characteristics, complexity depending on its chemicals, construction material, scale, etc. Meanwhile, safety management is always conducted to assess the risk of the process occurred from accidental outcomes for managing it. In general, safety management is applied in a process with various technique in each design stage. The techniques used in each stage are represented in Figure 1-1. As represented in Figure 1-1, the safety management techniques are differently applied with the process life cycle due to mainly the difference of information, characteristic.

Although various techniques are used according to the stage of process life cycle, the qualitative methodologies, mainly, are still used for safety management. With this reason, it is difficult to analyze and assess the degree of process safety or process risk numerically. So, the comparison of process risk on alternatives is complex, and difficult to be definite. Moreover, quantitative methodology is used in some process stages, but the methodology is applied with same risk management method to diverse process with different complexity. Therefore, safety management method should be applied according to process characteristics considering process life cycle in quantitative manner. This thesis proposes risk-based design and management with quantitative

methodology considering process life cycle for chemical processes with different characteristics.

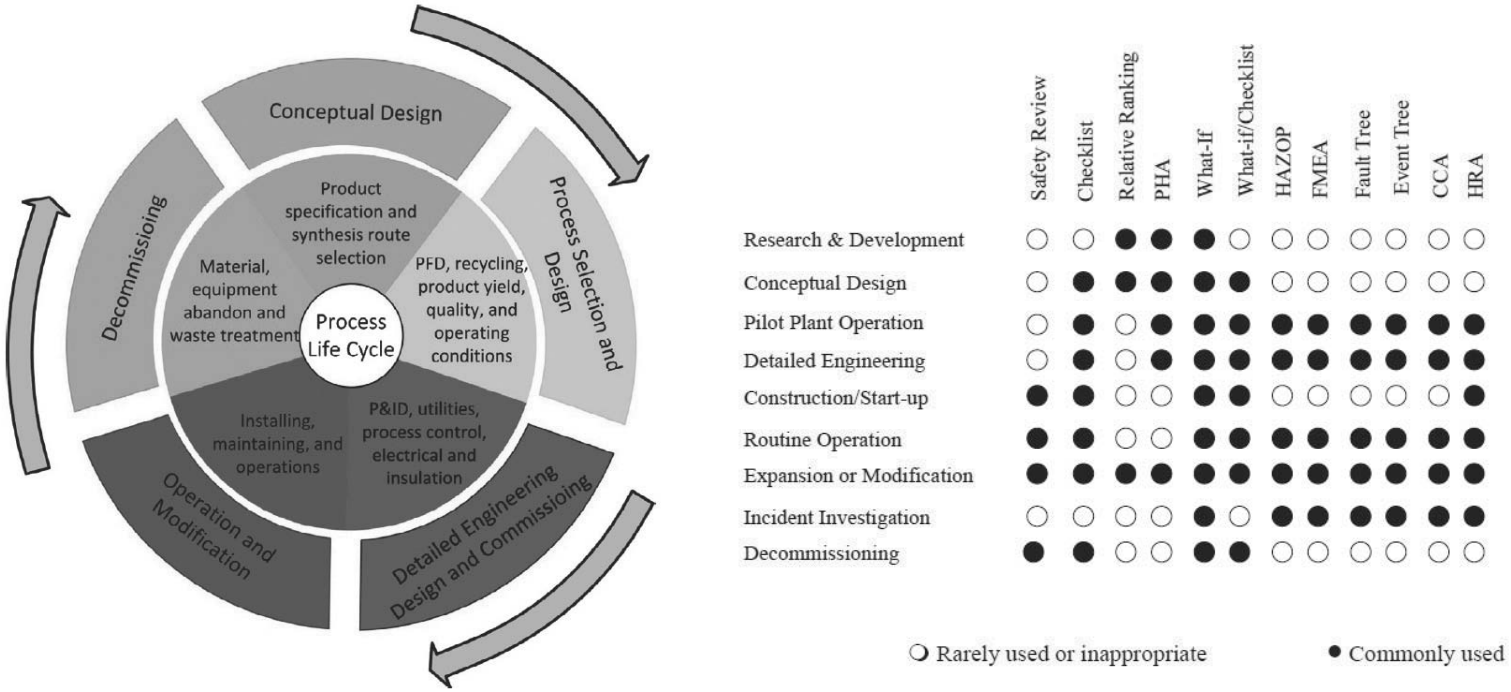

Figure 1-1. Process life cycle with safety management techniques.

1.2. Research objectives

In this thesis, risk-based design and management are proposed according to process life cycle for chemical processes to manage the safety in the process. In other words, risk-based methods considering process characteristic, process life cycle are proposed and applied. In the aspect of process life cycle, conceptual design stage, basic design stage, and operation stage are studied to perform risk-based management considering process life cycle.

First, in conceptual design stage, the risk-based design methodology is proposed and studied to consider safety of a process. The risk-based methodology is applied to organic Rankine cycle (ORC) design for utilizing LNG cold energy to assess inherent risk as one of main factors of process conceptual design.

Second, in basic design, the risk-based management studied in CO_2 injection system on topside offshore platform. Because the platform is constructed in offshore seismic area, risk occurred from seismic effect should be included in the risk of the injection process. So, modified methodology is proposed to assess the risk in CO_2 injection system with considering seismic effect.

Last, in operation stage, the risk-based management with patrol is studied for natural gas (NG) pipeline. Currently, the patrol is performed based on regulation with no basis. So, risk-based patrol methodology is proposed and applied to NG pipeline for safety management considering process life cycle and characteristics of NG pipeline.

1.3. Outline of the thesis

Chapter 1 provides the research motivation and objective of this thesis. In Chapter 2, risk-based design using inherent safety design (ISD) methodology with quantitative risk assessment (QRA) are proposed to consider the safety in the stage of conceptual design. The risk-based design is applied to organic Rankine cycle (ORC) utilizing liquefied natural gas (LNG) cold energy. Next, Chapter 3 includes the risk-based management using improved QRA considering seismic effect occurred from earthquake in the stage of basic design. CO_2 injection process in topside platform that susceptible to seismicity are investigated with the methodology to manage the risk with assessment of the risk appropriately. In Chapter 4, the proposal of risk-based patrol for management in the stage of maintenance is explained. The risk-based patrol is applied to the NG pipeline to be patrolled with risk value for proper management. Chapter 5 presents the conclusion of this thesis with the suggestion for the future work.

CHAPTER 2.
Conceptual Design Stage: Risk-based Design of Organic Rankine Cycle (ORC) Considering Inherent Safety for LNG Cold Energy Utilization

2.1. Introduction

2.1.1. Safety in conceptual design stage

The consideration of safety on conceptual design stage has been studied in previous research with various methods. One of the main attempts is a technique of inherent safer design (ISD). This methodology was proposed by Kletz (1978) for the first time. “Inherent” is defined as “existing in something as a permanent, essential, or characteristic attribute”, so inherent safer design means that the process design has safer essential characteristics by nature. From the concept of ISD, this methodology has some advantages. First, risk reduction effectiveness is the highest level in the conceptual design stage. As shown Figure 2-1, risk can be reduced by eliminating or reducing expected hazard, and the effectiveness is changed according to process life cycle. Because the expected risk means inherently expected risk in conceptual design stage, the risk reduction can be more effective than that in other stages. In addition, the effectiveness of correction is much higher than that in any other stages. This means that a correction in the process design is easier and more economic when the process has a feature/alternative for decreasing risk or increasing safety by changing its elements.

Various methods have been studied about inherent safer design in many aspects such as material, reaction, etc. Among the aspects, the assessment technique of ISD has been studied to assess the inherent risk. Edwards and Lawrence (1993) proposed the 'Prototype Index for Inherent Safety (PIIS)' for the stage of research and process development for design. PIIS considers reaction conditions and material properties with using seven parameters including inventory, temperature, pressure, yield, toxicity, flammability, and explosiveness. Heikkilä (1999) proposed the extension of the PIIS called by 'Inherent Safety Index (ISI)' to consider other factors such as layout, type of equipment, process structures. Palaniappan et al. (2002) studied the expanded methodology to add five other supplementary indices over PIIS and ISI index. Khan and Amyotte (2004) proposed the 'Integrated Inherent Safety Index (I2SI)' that have two sub-indices, the hazard index and inherent safety potential index. Shariff and Leong (2009a) developed the new index that accounts for mixture properties. Hassim and Hurme (2010) proposed an index for considering health hazards on the research stage based on material properties. However, the methodologies with index have main limitation that the risk is evaluated semi-quantitatively. Also, the concept of index is difficult to apply to different processes with different characteristics, even though some studies have proposed the indexes for assessing safety according to specific process in the conceptual design stage.

As a means of overcoming the limitations of ISD, quantitative risk assessment (QRA) has been used in previous research. QRA is widely used to assess risk in chemical processes. QRA can be performed to investigate existing

risks of a process to decide whether they are acceptable or not (CCPS. 2000). The main feature of QRA in overcoming the limitation of ISD is that quantitative values are used to assess the risk, which is more practical than using indexes. Therefore, the combination of ISD and QRA is used as a technique to assess the safety (or risk) of a process in the conceptual design stage to consider inherent process safety. Some studies have applied this methodology to specific processes to assess safety in the early design stage. Shariff and Leong (2009) proposed the application of inherent risk using QRA with a simple case study of pipelines in a hydrocarbon fractionation plant. Medina et al. (2009) researched the optimization of overall costs including damage costs from quantitative risk in addition to direct and indirect costs regarding storage tanks. Patel et al. (2010) studied the safety of extraction and solvent recovery process based on solvents to find safer alternatives. Medina-Herrera et al. (2014) applied the QRA methodology to perform risk assessment in the design of a multi-effect distillation system according to distillation conditions. Additionally, in process design, safety is not the only factor. Factors for consideration may vary according to the objective, surroundings, economic conditions, and so on. Among them, the efficiency (energy, exergy) and economic aspects are almost always considered as design factors because most processes are designed and built for economic purposes. Therefore, these factors should be considered with the safety factor in process design. Accordingly, some research proposed methodologies of process design considering several aspects (efficiency, economic, safety) simultaneously with the ISD technique. Eini et al. (2016a, 2016b) studied refrigeration cycles to find

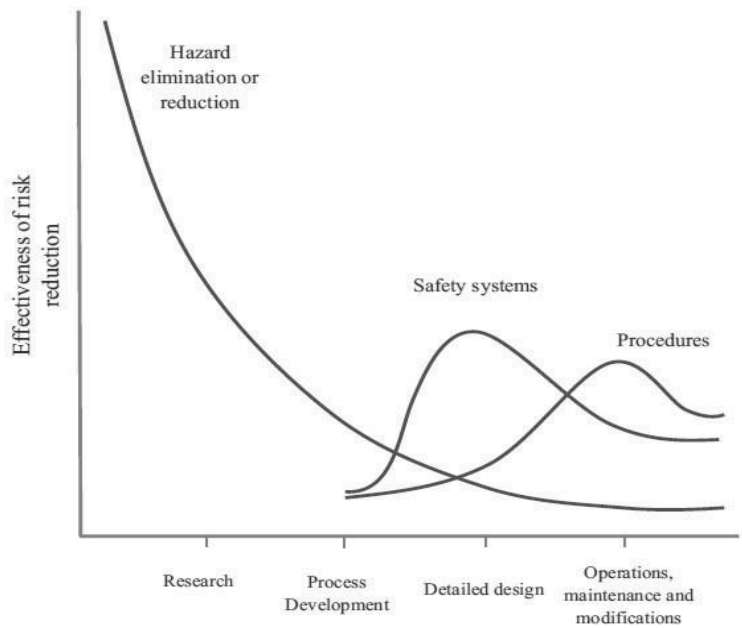

Figure 2-1. Risk reduction effectiveness in accordance with the process development stage.

an optimal design, considering several factors (safety, cost, exergy) simultaneously with multi-objective optimization. After finding Pareto optimal sets with the genetic algorithm (GA), decision-making approaches were used to select the optimal condition of the refrigeration cycle design. Eini et al. (2018) also used this methodology to design a reactor network system for allyl chloride production considering the risk and economic aspects. Martinez-Gomez et al. (2016, 2017a, 2017b, 2017c) applied the inherent safety with QRA to several processes to study the optimal design. Furthermore, a reactive distillation system for purification of biobutanol was studied to find optimal alternatives based on cost, environmental factors, and safety (Martinez-Gomez et al., 2016). A reforming process for shale gas was investigated to select an optimal reforming process among steam reforming (SR), partial oxidation (POX), and dry deforming (DR) in accordance with the H2/CO ratio considering cost and safety (Martinez-Gomez et al., 2017a). Furthermore, a reactive distillation column for silane production was studied to find optimal design conditions considering safety and cost, including cooling cost and heating cost (Martinez-Gomez et al., 2017b). Martínez-Gomez et al. (2017c) also applied a multi-objective optimization approach to compare working fluids used in geothermal facilities considering several factors including safety. Although the ISD with QRA is more reliable, but the QRA methodology has been applied without improvement or modification according to process characteristics as well as process life cycle in previous studies. In other words, the methodology should be improved and modified for a specific process in conceptual design stage.

2.1.2. Design of organic Rankine cycle (ORC) process for utilizing LNG cold energy

Energy derived from fossil fuels is used in most industries. With the growing concern on the environmental impact of fossil fuels, the usage of natural gas (NG) has increased, although coal and petroleum are still the primary energy resources. Furthermore, NG has several advantages as an energy resource, including efficient combustion, easy transportation and storage, and environmental friendliness. Nevertheless, the usage of this clean energy involves some necessary processes, mainly including liquefaction and gasification processes. In the liquefaction process, NG is liquefied to LNG (liquefied natural gas) for efficient transportation and storage. The gasification process is necessary to convert LNG to NG again for consumption. Both processes are important because they are essential in the aspect of functionality. These days, however, the gasification process has been receiving more attention in terms of using the cold energy produced during the vaporization of LNG because the cold energy is usually wasted without utilization. Therefore, previous studies have investigated various methods for recovering the LNG cold energy (Kanbur et al., 2017). Among the methods, organic Rankine cycle (ORC) is one such technology for utilizing the cold energy.

ORC is receiving attention as one of the technologies that can use low grade heat as heat source to vaporize working fluids. As the name suggests, ORC is based on the Rankine cycle, through which electric energy can be generated from heat energy. In particular, extracting energy from heat sinks comprising hydrocarbons such as LNG is efficient because organic components are used as working fluids to obtain energy. Qiang et al. (2004) analyzed some parameters

of ORC to recover the LNG cold energy with a combined power cycle such as heat source temperature and turbine inlet pressure. Shi and Che (2009) proposed ammonia-water mixture Rankine cycle for a combined power system with LNG power generation cycle. Some key variables were also analyzed, including turbine inlet pressure (ammonia, LNG) and ammonia mass fraction. Wang et al. (2013) also proposed an ammonia-water power cycle for utilizing LNG cold energy, and determined an optimum operating condition with multi-objective optimization. Liu and Guo (2011) proposed the integration of vapor absorption to a combined cycle to improve the energy recovery efficiency of LNG cold energy. A binary mixture of tetrafluoromethane (CF4) and propane was used as the working fluid. Key parameters were investigated and optimized to increase efficiency. Choi et al. (2013) performed an optimization of a cascade ORC to utilize cold energy from LNG. One-stage (C3), two-stage (C3-C3), three-stage (C3-C3-C3) ORCs were investigated to compare the power generation and exergy efficiency. Lee et al. (2014a) proposed the integration of ORC and stream cycle with LNG cold energy. Captured liquefied CO_2 from a capture process was used as the working fluid. In addition, Lee et al. (2014b) attempted to determine the optimal ternary mixture for the working fluid of the ORC system using LNG. Kim et al. (2015) proposed a cascade ORC using cryogenic energy of LNG with a binary working fluid. Mehrpooya et al. (2016) proposed a power generation cycle with CO_2 as the working fluid, utilizing low-temperature solar energy and LNG cold energy. Bao et al. (2018) studied the effects of the type and number of components for working fluids in a two-stage condensation combined cycle using a zeotropic mixture.

Generally, studies on ORC using LNG have been focused on increasing efficiency (energy, exergy), including the selection of the working fluid and using multi-component working fluids. However, the safety of ORC has not been studied despite its importance. The safety of ORC is important because ORC involves organic components that are flammable and even toxic. Moreover, ORC using LNG cold energy involves high risk of incidents that may endanger human lives because of their chemical properties. Therefore, design of ORC using LNG must be investigated from the aspect of safety and safe designs should be developed accordingly.

In this study, the methodology of risk-based design using ISD and QRA is proposed with modification for ORC design. A multi-objective optimization methodology is used to study the optimal design of ORC for utilizing LNG cold energy with considering the thermodynamic and safety aspects. According to previous studies, exergy efficiency is one of the main parameters in ORC design (Choi et al., 2013; Kim et al., 2015; Lee et al., 2014b, 2014a; Mehrpooya et al., 2016; Qiang et al., 2004; Shi and Che, 2009; Wang et al., 2013). So, exergy efficiency is used as a parameter for the thermodynamic aspect, and process risk from QRA is used as a parameter for the safety aspect. Finally, the multi-objective optimization problem with two objectives including exergy efficiency and risk is solved with design parameters of ORC.

2.2. Problem State

2.2.1. Organic Rankine Cycle (ORC)

ORC is a power cycle process that can generate electrical power from heat energy. The basic ORC consists of four components, as shown in Figure 2-2. The components include condenser, pump, vaporizer, and turbine for the working fluid to cyclically pass through.

2.2.2. Design parameters of ORC

Although the ORC process is simple, there are many parameters that affect the thermodynamic and safety aspects of ORC regarding the conceptual design. Based on previous research, the main parameters can be specified as below:

- Type of working fluid
- Combination and composition of the working fluid (if multi-components are used))
- Condition of the working fluid (mass flow rate, pressure)
- Configuration of ORC (stages, additional components)

The main parameters are mainly related to the working fluid except for configuration parameters. This means that the working fluid is the most important factor determining the characteristics of ORC. ORC characteristics can be modified by changing the type, condition, number, etc. of the working fluid. Among them, parameters, except for configuration parameters, were used as variables to find the optimal design considering two aspects in this study.

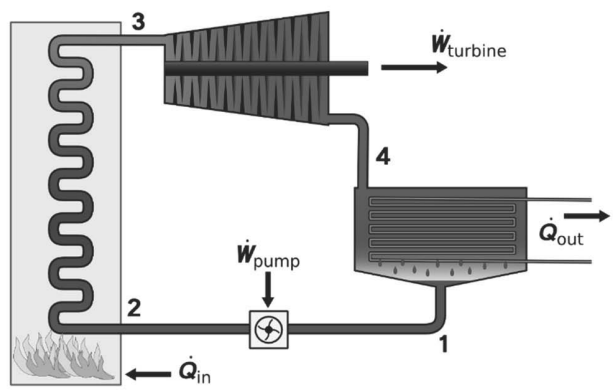

Figure 2-2. Schematic of organic Rankine cycle. A liquid stream (1) is passed through the pump for pressurization, and its state is changed to the gas phase in the vaporizer (2). Subsequently, the gas stream is expanded in the turbine to generate electricity (3) and condensed to the liquid phase again (4).

The configuration of ORC was excluded to properly focus on comparing the working fluid. In other words, the working fluid or combinations of the working fluid as well as the conditions of the working fluid, such as pressure and mass flow were investigated to find the optimal ORC design considering the safety and thermodynamic aspects.

In this study, a power generation system of organic Rankine cycle utilizing cold energy from LNG was used as the base process. LNG is used as a heat sink of the working fluid in a condenser while the LNG is vaporized. Some studies (Bao et al., 2018; Choi et al., 2013; Kim et al., 2015; Lee et al., 2014b, 2014a; Liu and Guo, 2011; Mehrpooya et al., 2016) utilized LNG as a heat sink as explained in the Introduction. A process flow diagram of ORC utilizing LNG is shown in Figure 2-3. The process involves a condenser for using LNG cold energy in addition to basic components, such as a turbine, a pump, and a vaporizer.

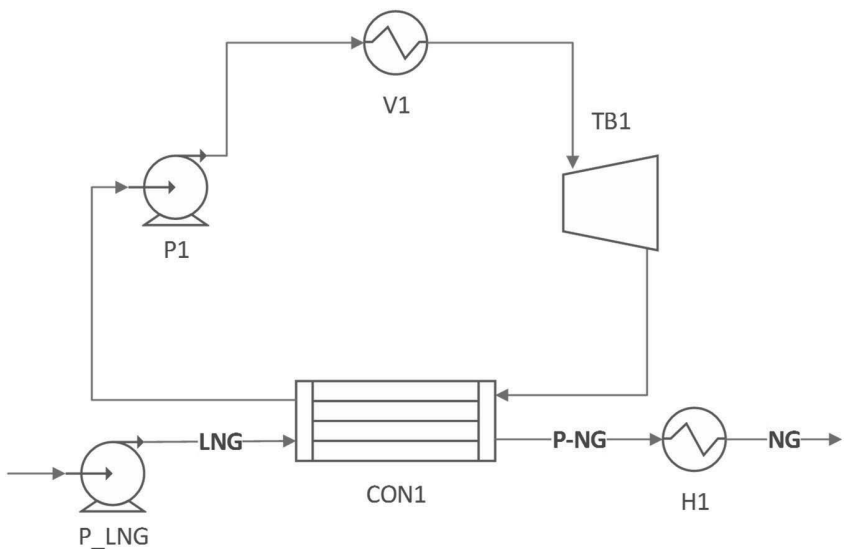

Figure 2-3. Process flow diagram of ORC.

2.2.2.1. Selection of working fluids

Candidates of the working fluid should be specified to study the ORC design in both aspects. The working fluids can be selected from previous research, in which working fluids have been selection for ORC using LNG as the heat sink (Choi et al., 2013; Lee et al., 2014b; Liu and Guo, 2011; Wang et al., 2013). Based on these studies, six fluids with two pure substances, two binary mixtures, and two ternary mixtures were selected as working fluids. The pure substance working fluid includes C_2H_6 (C2) and C_3H_8 (C3) (Choi et al., 2013), and the binary mixture working fluids include NH_3–H2O and R14-C_3H_8 (Liu and Guo, 2011; Wang et al., 2013). The ternary mixture working fluids contain R601-R23-R14 and R30-R23-R14 based on a previous study (Lee et al., 2014b). In previous studies for ORC utilizing LNG cold energy, the selection of working fluid has been studied with considering thermodynamic property of LNG used as heat sink because LNG has none iso-thermal condensing nature. The six working fluids are selected based on the result of the studies, and the selected six working fluids are mainly studied as the reliable and efficient candidates of working fluids for LNG cold energy utilization in each category (pure, binary, ternary component). The working fluids are described in Table 2-1.

Table 2-1. Type or category of working fluids.

Type or Combination		Name	Chemical formula	MM	NBP (℃)	T_C (℃)	P_C (Mpa)	LFL
Pure	C_2H_6 (C2)	Ethane	C_2H_6	30.07	-88.5	32.18	4.87	2.9
	C_3H_8 (C3)	Propane	CH_3-CH_2-CH_3	44.10	-42.1	96.7	4.24	2.37
Binary	NH_3-H_2O	Ammonia	NH_3	17.03	-33.34	132.4	11.2	15
	R14-C_3H_8	R14	CF_4	88	-128.1	-	3.75	-
Ternary	R601-R23-R14	R601	CH_3-CH_2-CH_2-CH_2-CH_3	72.15	36	196.6	3.37	1.4
	R30-R23-R14	R23	CHF_3	70.01	-82.1	25.9	4.84	-
		R30	CH_2Cl_2	84.93	40.2	237	6.08	13

2.2.2.2. Parameter specification

Some parameters have to be specified before commencing the multi-objective study. First, the composition of LNG used as the heat sink is specified in Table 2-2. The main components are methane and ethane, which account for almost 96%. And, low pressure (LP) steam (87.7 C°), which is a low-grade heat source, is used as the heat source to evaporate the working fluid in the vaporizer. The adiabatic efficiency of the pump and turbine are assumed to be 80%. Moreover, minimum approach temperature in the condenser and vaporizer is specified as 5 C° during heat exchange. The parameters are presented in Table 2-3.

Table 2-2. Composition of LNG.

Component	Mole fraction
CH_4	0.8877
C_2H_6	0.0754
C_3H_8	0.0259
n-C_4H_{10}	0.0056
i-C_4H_{10}	0.0045
n-C_5H_{12}	0.0001
i-C_5H_{12}	0.0001
N_2	0.0007

Table 2-3. Assumptions made in the ORC process.

Variables	Values
LNG pressure	30 bar
Pressure drop in the heat exchanger	0
Equation of state	Peng-Robinson
Adiabatic efficiency of the pumps	80 %
Adiabatic efficiency of the turbine	80 %
Minimum approach temperature in the condenser and vaporizer	5°C
Pressure of the LNG entering the condenser	30 bar
Turbine outlet pressure	1 bar

2.3. Methodology

A schematic of the overall algorithm is presented in Figure 2-4. Overall, the algorithm is organized to solve the multi-objective optimization problem with two objectives, including the thermodynamic and safety aspects, by finding a Pareto optimal solution (Pareto frontier). The algorithm is processed in MATLAB (Mathworks, USA) with the integration of ASPEN Plus™ (AspenTech, USA) to simulate the ORC modeling and obtain thermodynamic parameters used in the calculation of objective functions according to decision variables. Further information about calculation of thermodynamic parameters can be obtained in the reference from AspenTech, which explains physical property method used in Aspen Plus™ (Aspen Technology, 2013). In this section, methodologies contained in the algorithm are described in detail.

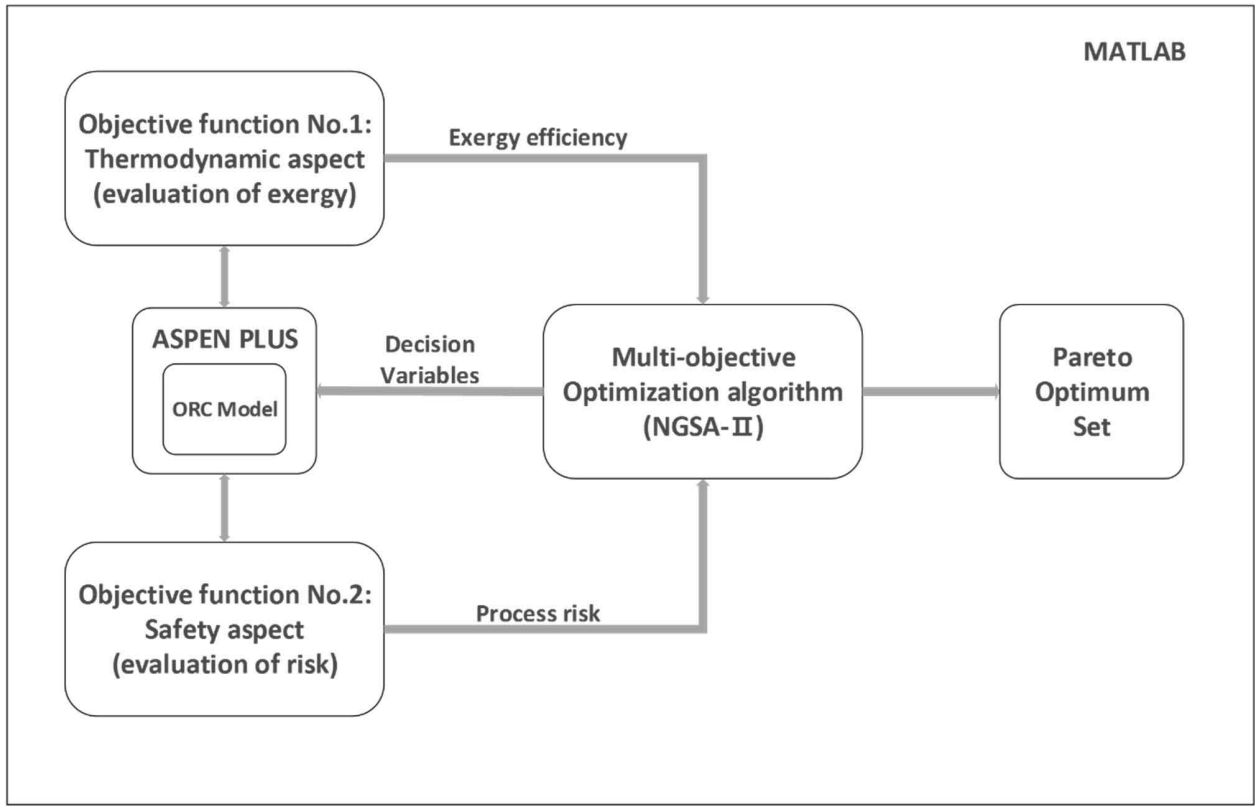

Figure 2-4. Schematic of the algorithm for solving the multi-objective optimization problem to decide the optimal design of ORC.

2.3.1. Multi-objective optimization (MOO) formulation

Multi-objective optimization is an optimization method that has more than one objective function. A generalized MOO can be formulated in mathematical terms as follows:

$$\begin{aligned} & min[f_1(x), f_2(x), \dots, f_n(x)] \\ & x \in S, \\ & S = \{x \in R^m : h(x) = 0, g(x) \geq 0\} \\ & C = \{y \in R^n : y = f(x), x \in S\} \end{aligned} \quad \textbf{(2-1)}$$

where n is the number of objective functions (>1), C is the image of the feasible set. $h(x)$ and $g(x)$ are constraints of the problem. Generally, a global solution that maximizes or minimizes all the objectives does not exist in MOO. Instead, Pareto optimal solutions can be determined, which are locally optimized and maximize or minimize only parts of objectives. The mathematical definition of a (strict) Pareto optimum is that a point x^* for the multi-objective problem if and only if there is no $x \in S$, such that $f_i(x) \leq f_i(x^*)$ for all $i \in \{1, \dots, n\}$, with at least one strict inequality (Caramia and Dell'Olmo, 2008). Therefore, obtaining a Pareto optimum set is one of the final goals in this study.

In this study, two objective functions are required to optimize the safety and thermodynamic aspects. The first objective function is specified as exergy efficiency that is determined by parameters of the working fluid to evaluate the process efficiency. The process risk calculated from quantitative risk assessment (QRA) technique is specified as the second objective function to consider the safety aspect. Sections 3.1.1–3.1.3 provide detailed information of

objectives, including the calculation of the objectives and the solving of the optimization problem.

2.3.1.1. Objective 1 – Exergy efficiency

Exergy, which is based on the second law of thermodynamics, is the maximum theoretically useful work that can be obtained in a process. Exergy can be calculated the following equations:

$$\dot{E} = \dot{m}[(H - H_0) - T_0(S - S_0)] \quad \textbf{(2-2)}$$

$$\dot{W}_{net} = \dot{W}_{turbine} - \dot{W}_{pump} \quad \textbf{(2-3)}$$

$$\boldsymbol{\eta_{exergy}} = \frac{\dot{W}_{net}}{\left(\dot{E}_{P-NG} - \dot{E}_{LNG}\right) + \dot{Q}_{vaporizer}\left(1 - \frac{T_{in}}{T_{out}}\right)} \quad \textbf{(2-4)}$$

Exergy can be calculated using Equation (2-2). Exergy efficiency is the ratio of output exergy and input exergy. Thus, exergy efficiency of the ORC process can be calculated using Equation (2-4).

Further information of exergy can be obtained from previous studies (Choi et al., 2013; Kim et al., 2015; Lee et al., 2014b, 2014a; Mehrpooya et al., 2016; Qiang et al., 2004; Shi and Che, 2009; Wang et al., 2013)

2.3.1.2. Objective 2 – Process risk from simplified QRA

QRA was used for calculating process risk. As shown in Figure 2-5, QRA involves several steps.

i. Hazard identification & Scenario selection

In this step, possible hazards are identified in the ORC process. For hazard identification, characteristics of materials used in the process as well as process specifications, such as operating pressure and temperature, should be investigated. In the case of material characteristics, two types of properties (flammable, toxic) related to hazard can be defined. The properties of working fluids are defined and arranged in Table 2-4. Among the components used in the ORC process, most components are flammable, except for R14 and R23. Furthermore, NH_3 is toxic as well as flammable. Therefore, the ORC process involves the probability of fire events and toxicity, but fire events should be prioritized because they are more likely to occur.

After analyzing material characteristics, specific scenarios should be identified with the specification of the ORC process. Because ORC is a cycle process, two states of matter (liquid, gas) exist under high and low pressure. Generally, scenarios are identified depending on the specifications of a process. So, the number of scenarios can be increased if specifications are complex to consider the all possibility. In this study, nevertheless, scenarios are selected with simplification, because the configuration is same in all cases with different working fluids. Moreover, the absolute risk value, which is hard to be calculated in conceptual design, is not the goal of this methodology. Instead, the relative

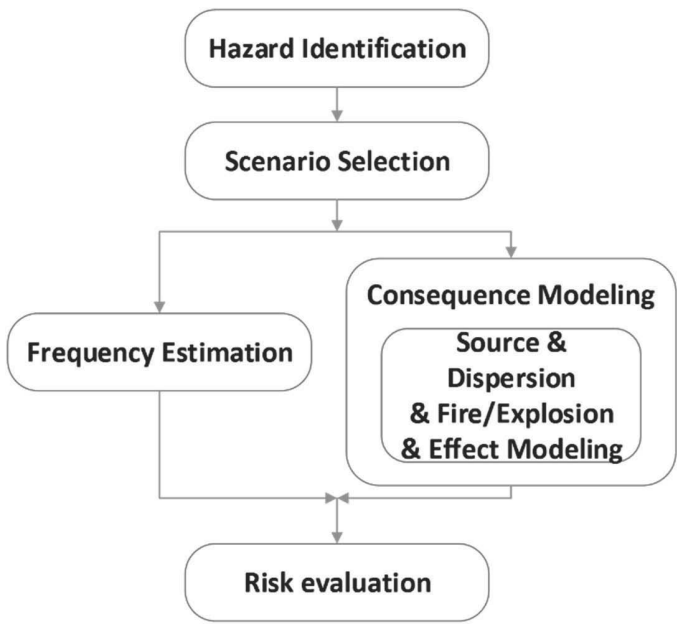

Figure 2-5. Flow diagram of quantitative risk assessment methodology.

Table 2-4. Properties of materials.

Component	Property
LNG	Flammable
C_2H_6	Flammable
C_3H_8	Flammable
NH3	Flammable, Toxic
R14	-
R23	-
R30	Flammable
R601	Flammable

risk is necessary to compare the risk values according to parameter change. In other words, the process risk can be used with different ways in conceptual design stage. In this study, most severe cases in the ORC process are considered for risk assessment because the cases can represent the risk of ORC process to compare and analyze the all ORC processes with different working fluids. This approach is different from that of other research for design of specific processes. Also, this simplified approach is more efficient for analysis and in accordance with the objective of the conceptual design stage. Namely, the ISD methodology with QRA can be improved with simplification of hazard identification on conceptual design stage for ORC design by considering the characteristics of the process. The most severe cases in this process are the accidental hazards from pipeline between the pump and vaporizer, also between the vaporizer and compressor because of the high-pressure fluids (liquid & vapor) (Figure 2-6). So, the relative risk can be compared with most severe cases (hazards from high-pressure liquid & vapor). Rupture and leak (partial rupture) with a hole are only considered as scenarios of the pipeline for simplicity.

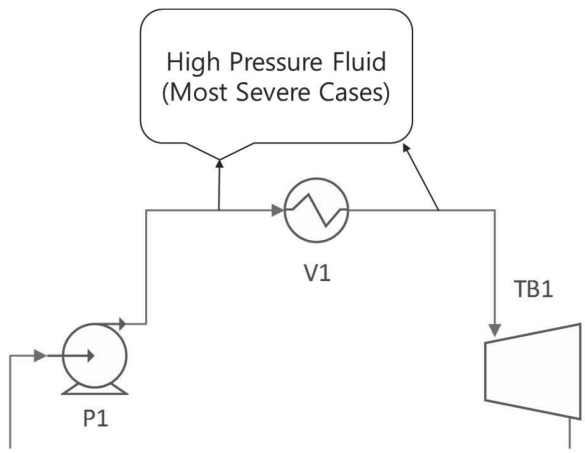

Figure 2-6. Most severe cases in the ORC process.

ii. Frequency Estimation

The next step is frequency analysis. Possible events from initial scenarios (rupture, leak) are identified with event tree analysis (ETA) for frequency analysis. Subsequently, frequency values are calculated from historical data of initial scenarios with ignition probabilities. In this study, OGP data is used for the historical data of initial scenarios (OGP, 2010). The ETA is shown in Figure 2-7. After the fluid is released as one of the modes (instantaneous, continuous), fire events occurr depending on the ignition type (immediate, delayed). The probabilities of initial scenarios, and ignition are presented in Table 2-5.

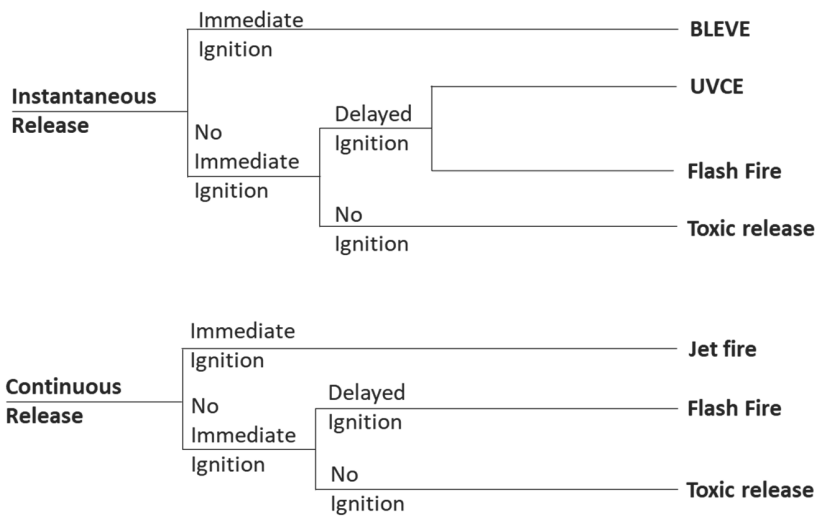

Figure 2-7. Event tree analysis (ETA).

Table 2-5. Probabilities of ignitions.

Release	Frequency	Immediate Ignition	Delayed Ignition	UVCE
Instantaneous Release	7.0×10^{-6}	0.25	0.9	0.5
Continuous Release	7.3×10^{-5}	0.1	0.75	-

iii. Consequence analysis

Consequence analysis includes source modeling, dispersion modeling, and modeling of each fire event. The release can be modeled with source modeling, and then the dispersal of material can be modeled by dispersion modeling. In case of toxic materials, information on dispersion is important in risk evaluation because the concentration of materials is a major parameter for calculating fatality. If the material is flammable, fire and explosion modeling are performed to calculate the effect of thermal radiation and overpressure. Finally, individual risk, which means the probability of the death of a person by all possible events, can be calculated to evaluate risk in the ORC process. Detailed models of the consequence analysis, except for the effect model, is described in Appendix 1. After calculating thermal radiation, overpressure for flammable materials and concentration for toxic materials, the probability of death, which indicates the effects of the outcomes, can be derived from the effect model (Equation (2-5),(2-6) & Table 2-6).

$$Y = k_1 + k_2 \ln V \tag{2-5}$$

$$P = 50\left[1 + \frac{Y-5}{|Y-5|} erf\left(\frac{|Y-5|}{\sqrt{2}}\right)\right] \tag{2-6}$$

Table 2-6. Probit model parameters

Event type	k_1	k_2	V
Thermal radiation	-14.9	2.56	$\left(\frac{t_e I^{4/3}}{10^4}\right)$
Overpressure	-77.1	6.91	p^0
Intoxication (Ammonia)	-35.9	1.85	$t_e C^2$

iv. Risk evaluation

After following previous steps, the process risk can be calculated using Equation (2-7), which is the summation of probability of death from the effect of the respective outcome. In other words, total risk comprises multiple risks associated with each outcome, which means the outcome frequency multiplied by the probability of death from the outcome. In this study, the concept of risk distance is used, because the concept can be obtained with only individual risk that don't need the information of population. Specifically, risk distance, D_{risk}, is used as the risk parameter for the safety aspect. D_{risk} is the maximum distance when $R_{overall}$ is larger than 10^{-4}/year.

$$R_{overall} = \sum_{i} (outcome\ frequency_i * probability\ of\ death\ from\ the\ outcome_i) \quad \textbf{(2-7)}$$

$$D_{risk} = maximum\ distance\ (10^{-4} < R_{overall}) \quad \textbf{(2-8)}$$

2.3.1.3. Definition of optimization problem with objectives

With two objectives, including exergy efficiency and process risk as explained earlier, multi-objective optimization problem can be formulated as follows:

$$\begin{aligned} &\text{Minimize } (f_1, f_2) \\ &f_1(\dot{n}_{wf}, P_{wf1}, P_{wf2}) = -\eta_{exergy} \\ &f_2(\dot{n}_{wf}, P_{wf1}, P_{wf2}) = R_{overall} \\ &\text{subject to} \\ &\Delta T_{min} \geq 5℃ \end{aligned} \quad \textbf{(2-9)}$$

The optimization problem is the minimization of objectives with variables affecting the values. Because high values are preferred for exergy efficiency (η_{exergy}), $-\ \eta_{exergy}$ is used as an objective (f_1) to be minimized in this study. The three variables (flow rate ($\dot{n}_{wf}$), compressor inlet pressure (P_{wf1}) and outlet pressure (P_{wf2})) determine the value of objectives, while LNG properties are fixed. Pareto optimum sets are obtained according to the combination of the working fluid. In particular, six results must be obtained from the six types of working fluids. The constraints of flowrate, turbine inlet pressure and outlet pressure are organized in Table 2-7. The ranges of the values are specified from the thermodynamic properties of each working fluids. The compositions of working fluid in the case of multi-component fluid are specified with using previous studies that the composition value made the exergy destruction minimize, or the exergy efficiency maximize.

Table 2-7. Constraint of optimization problem.

Working fluids		Constraint	Compostion
Pure	C_2H_6 (C2)	$1 \leq P_{wf} \leq 42.4$ $0.01 \leq n_{wf} \leq 0.423$	1 (pure)
	C_3H_8 (C3)	$1 \leq P_{wf} \leq 24.3$ $0.01 \leq n_{wf} \leq 0.628$	
Binary	NH_3-H_2O	$2 \leq P_{wf} \leq 30$ $0.01 \leq n_{wf} \leq 0.589$	0.95:0.05 *(Shi and Che., 2009)*
	R14-C_3H_8	$1 \leq P_{wf} \leq 70$ $0.01 \leq n_{wf} \leq 0.400$	0.73:0.27 *(Liu and Guo., 2011)*
Ternary	R601-R23-R14	$14.9 \leq P_{wf} \leq 55.5$ $0.01 \leq n_{wf} \leq 0.599$	0.067:0.707:0.227 (*Lee et al., 2014)*
	R30-R23-R14	$10.2 \leq P_{wf} \leq 63.4$ $0.01 \leq n_{wf} \leq 0.585$	0.252:0.68:0.068 (*Lee et al., 2014)*

2.3.2. Genetic Algorithm (GA)

To solve the multi-objective optimization problem, the non-dominated sorting genetic algorithm (NGSA-II), which a GA technique inspired by the evolutionist theory for the origin of species, is used as the optimization solver. In this technique, the solution set evolves, and changes through generations with selection, crossover, and mutation of species. NGSA-II was developed to solve the multi-objective optimization problem and enhance NGSA with ranking based on non-domination sorting as the fitness assignment and crowding distance as the diversity mechanism with elitism to maintain elitist solutions (Konak et al., 2006). The entire procedure of NGSA-II algorithm is shown in Figure 2-8. Further information of this algorithm is available in the literature for NGSA-II (Deb et al., 2002).

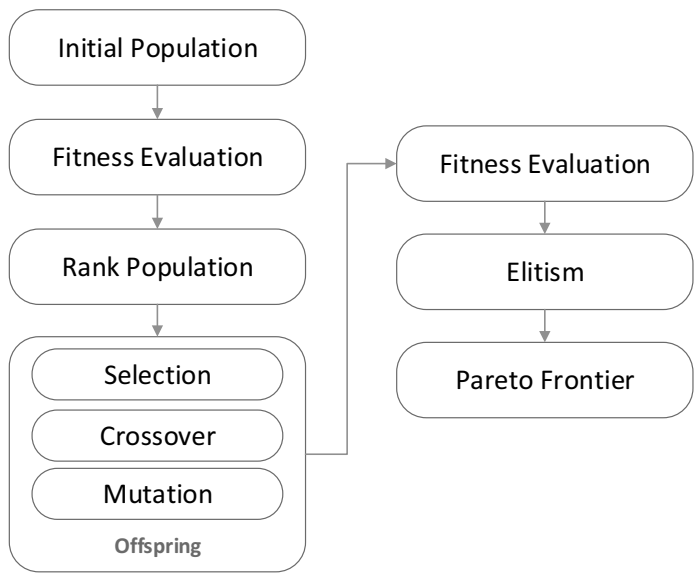

Figure 2-8. NGSA-II algorithm.

2.3.3. Decision-making method

The multi-objective optimization problem is solved with the points of the Pareto optimal set, which is different from a single optimization problem. In other words, the solution of the multi-objective optimization does not have a global optimum point. Therefore, the selection procedure for the final optimum solution should be included to design a process using a parameter of the solution. Practically, the final optimum solution can be selected with the project objective, process surrounding, and so on. Regarding the technical aspect, the decision-making technique can be used in the selection procedure.

2.3.3.1. LINMAP (Linear Programming Technique for Multidimensional Analysis of Preference)

The solution with the minimum distance from the ideal solution is selected as the final optimum solution in LINMAP. LINMAP including the distance from the ideal solution can be written as follows:

$$d_{i+} = \sum_{j=1}^{m} \left(F_{ij} - F_j^{ideal}\right)^2 \ (i = 1, \ \ldots . , \ n) \qquad \textbf{(2-10)}$$

$$i_{final} = i \in \min(d_{i+}) \qquad \textbf{(2-11)}$$

d_{i+} is the Euclidian of each solution from the ideal solution. i means the point or solution, and j means the objective. Thus, *n* is the number of Pareto optimum solutions, and *m* is the number of objectives. i_{final} is the solution of LINMAP.

2.3.3.2. TOPSIS (Technique for Order Preference by Similarity to an Ideal Solution

Unlike LINMAP, the final optimum solution in TOPSIS is the solution with the maximum value of the fraction between the distance from the ideal solution and non-ideal solution. In other words, the solution with a longer distance from the non-ideal solution is preferred in TOPSIS over that with a shorter distance from ideal solution. TOPSIS including the distance from the non-deal solution and the ratio can be written as follows:

$$d_{i-} = \sum_{j=1}^{m} \left(F_{ij} - F_j^{non-ideal}\right)^2 \ (i = 1, \ \ldots . , \ n) \qquad \textbf{(2-12)}$$

$$Y_i = \frac{d_{i-}}{d_{i+} + d_{i-}} \qquad \textbf{(2-13)}$$

$$i'_{final} = i \in \max(Y_i) \qquad \textbf{(2-14)}$$

d_{i-} is the Euclidian of each solution from the non-ideal solution. Y_i is the fraction of the distance from non-ideal solution. i'_{final} is the solution of TOPSIS.

2.3.3.3. Normalization

Before LINMAP and TOPSIS are calculated, a normalization step must be performed correctly. The objectives have different dimensions and scales, the conditions should be unified. The normalization method can be written as:

$$F_{ij}{}^{n} = \frac{F_{ij}}{\sqrt{\sum_{i=1}^{n} F_{ij}{}^{2}}} \qquad \textbf{(2-15)}$$

i and j are the same indexes as in the LINMAP and TOPSIS calculations.

2.4. Results & Discussion

2.4.1. Comparison in the same category

The working fluids can be compared in terms of the number of components and categories: C2 & C3 (pure component), NH_3-H_2O & R14-C_3H_8 (binary components), and R601-R23-R14 & R30-R23-R14 (ternary components). The results of each category are shown in Figure 9 and Table 7. Figure 9 presents graphs of the Pareto optimal front, and Table 7 presents the final optimum points (LINMAP, TOPSIS), turbine inlet pressure (P_{wf}), and flow rate of working fluid (n_{wf}) used as constraint.

The range of each objective, exergy efficiency and risk distance, in each category can be obtained from ideal and non-ideal solutions. ORC with pure component working fluids has exergy efficiency from a minimum of 12.41 % to a maximum of 22.08 %, and risk distance from a minimum of 34 m to a maximum of 149 m. The graph of pure component in Figure 9 shows that ORC with C3 as the working fluid has a wider range for both objectives than ORC with C2. Moreover, C3 has higher efficiency and risk than C2 when the solution has the highest exergy efficiency. On the other hand, C2 can be selected if the safety aspect is considered with thermodynamic aspect simultaneously, because the Pareto optimal solutions of C2 are closer to an ideal solution than of C3. It can be supported with the results of LINMAP and TOPSIS for pure component that both final optimal solutions are selected from solutions of C2. Next, binary component working fluid has exergy efficiency between 10.64 % and 22.76 % with risk distance from 19 m to 74 m. The results of binary component working fluid show R14-C_3H_8 is more efficient and safer than NH_3-H_2O in the basic

ORC because it has higher exergy efficiency and lower risk distance. Like C2 in pure component, R14-C_3H_8 can be selected as working fluid in binary component category. Lastly, the ranges of exergy efficiency and risk distance for ORC with ternary component are 12.92–20.53% (exergy efficiency) and 13–53 m (risk distance). The ranges of each objective for ORC with R601-R23-R14 & R30-R23-R14 are similar, so it's hard to select one working fluid in ternary component working fluid. Therefore, other parameters or information are required to select one working fluid between them.

The results of LINMAP and TOPSIS for each category have the same tendency that the solutions with lower risk distance are selected in each category. It can be explained that the Pareto optimal solutions lean towards the safety aspect, which means that solutions with low risk distance have shorter distance from the ideal solution (LINMAP), and non-ideal solutions have longer distances than solutions with high exergy efficiency (TOPSIS). However, it is important in aspect of decision-making that the selection of working fluid can be different according to decision circumstances, such as the decision-maker's preference and project purpose. Decision-making methods such as LINMAP and TOPSIS in this study are references, but do not provide an absolute answer regarding the decision-making process.

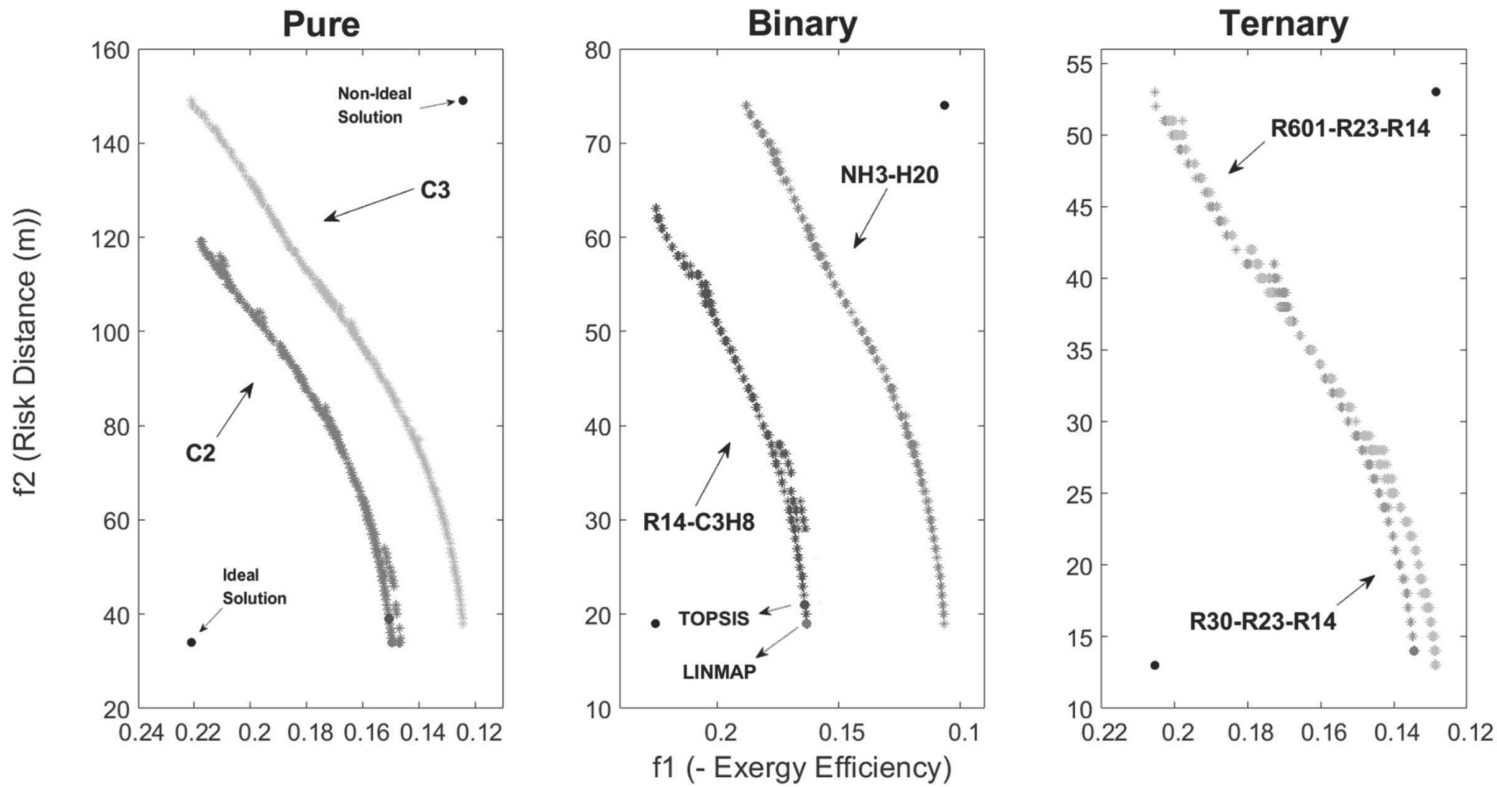

Figure 2-9. Pareto optimal solutions for each category

Table 2-8. Result of the final optimal solution for each category.

Category or Type	Working fluid	Decision-making method	Exergy efficiency (%)	Risk distance (m)	P_{wf1}/P_{wf2} (bar)	n_{wf} (kmol/h)	Ideal solution	Non-ideal solution
Pure component	C2	LINMAP	15.07	39	42.4/1.0001	0.0151	(0.2211, 34)	(0.1244, 149)
		TOPSIS	14.97	34	42.363/1.000	0.01		
Binary component	R14-C_3H_8	LINMAP	16.40	21	69.98/1.0001	0.016	(0.2252, 19)	(0.1065, 74)
		TOPSIS	16.32	19	69.84/1.0001	0.013		
Ternary component	R30-R23-R14	LINMAP & TOPSIS	13.45	14	62.67/1.000	0.0114	(0.2053, 13)	(0.1285, 53)

2.4.2. Comparison between categories

The results can be compared between different categories of the six working fluids. The Pareto optimal solutions of all working fluids can be represented in the same graph (Figure 2-10). With this graph, different working fluids in different categories as well as different working fluids in the same category can be compared. The overall ranges of exergy efficiency and risk distance of ORC with working fluids are 10.64–22.76 % and 13–149 m, respectively. The results of LINMAP and TOPSIS (Table 2-9) is the same solution with 16.52 % (exergy efficiency) and 19 m (risk distance).

ORC with R14-C_3H_8 as the working fluid exhibited the highest exergy efficiency, whereas ORC with R601-R23-R14 exhibited the lowest risk distance in the basic ORC process. This means that R14-C_3H_8 is the most efficient working fluid from the thermodynamic aspect, and R601-R23-R14 is the safest working fluid from the safety aspect. Overall, R14-C_3H_8 is the best working fluid among six working fluids because the solutions of R14-C_3H_8 are closest with an ideal solution. Moreover, it could be confirmed that the risk distance can be decreased by implementing more components as the working fluid. This is because R14 and R23 are non-flammable components. In other words, the risk is lowered if the fraction of flammable components (C_3H_8/NH_3 – binary, R601/R30 – ternary) in multiple component working fluids is lowered in same flow rate. The flow rate is an important parameter in risk calculation, and thus the risk distance is decreased if the flow rate is decreased. In addition to exergy loss in the condenser between the working fluid and LNG, this

tendency is one of the reasons for using multi-component working fluids (Bao et al., 2018; Choi et al., 2013; Kim et al., 2015; Lee et al., 2014b, 2014a; Liu and Guo, 2011; Mehrpooya et al., 2016). On the other hand, previous studies have reported that the exergy efficiency of ORC with ternary component working fluids is higher than that of pure and binary components (Lee et al., 2014a). The reason for the lower value of ternary component working fluids than other working fluids in this thesis is the difference of configuration of ORC. Other studies used complex configurations to reduce exergy loss, but this thesis used the basic ORC process.

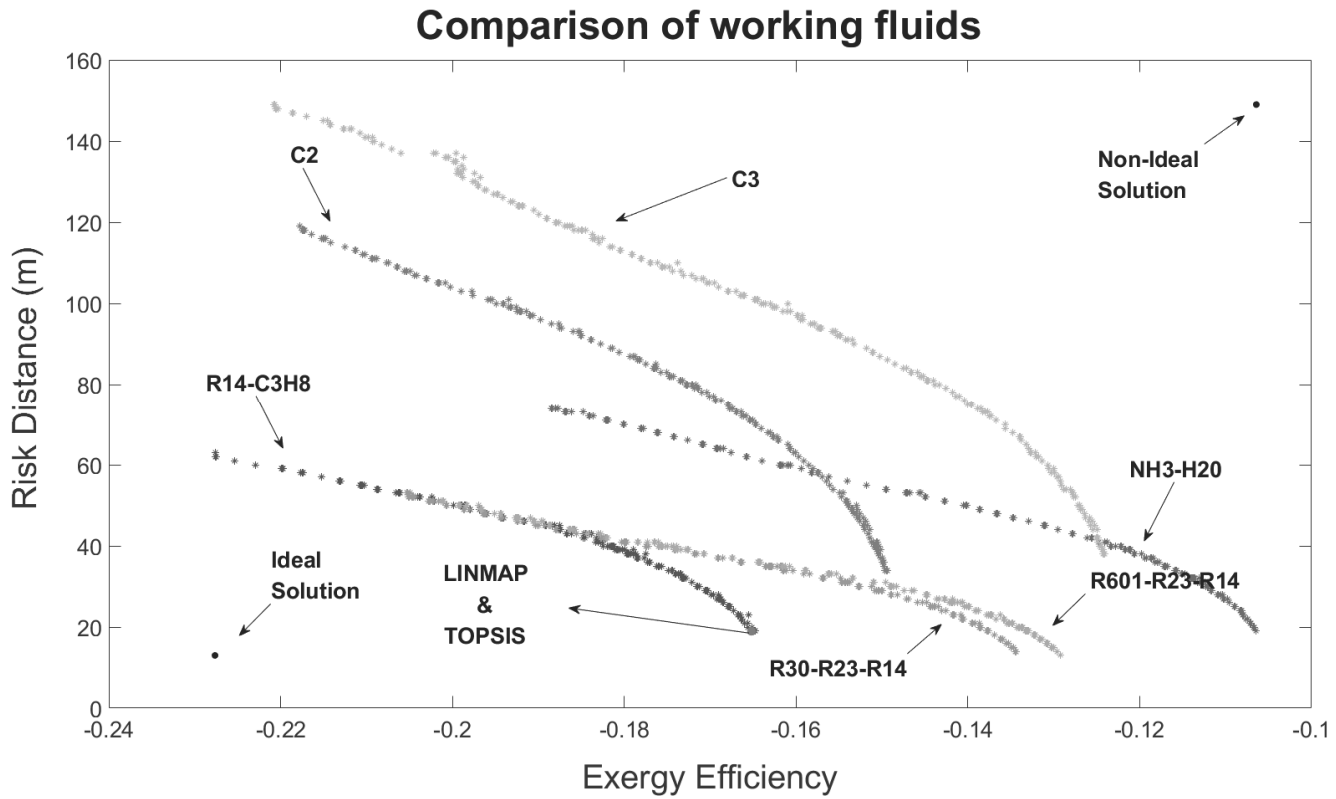

Figure 2-10. Pareto optimal solutions of six working fluids**.**

Table 2-9. Result of the final optimal solution for all working fluids.

Working fluid	Decision-making method	Exergy efficiency (%)	Risk distance (m)	P_{wf} (bar)	n_{wf} (kmol/h)	Ideal solution	Non-ideal solution
All	LINMAP & TOPSIS	16.52	19	78.01	0.013	(-0.2276, 13)	(-0.1064, 149)

2.5. Chapter conclusion

In this chapter, an ORC process is designed considering the thermodynamic and safety aspects using the multi-objective optimization methodology. Exergy efficiency, which is a parameter of the second thermodynamic law, is used to consider the thermodynamic aspect, and risk distance, which is calculated from the individual risk of the simplified QRA methodology, is used for the safety aspect. The multi-objective optimization methodology is used to consider both objectives simultaneously. The working fluid is used as the main design parameter among various parameters of ORC design. To determine the optimal working fluid for ORC design, a total of six working fluids in three categories, including pure component (C2, C3), binary component (NH_3-H_2O, R14-C_3H_8), and ternary component (R601-R23-R14, R30-R23-R14) working fluids, are selected on the basis of previous studies.

As a result, Pareto optimal solutions are obtained from the multi-objective optimization problem with two objectives (exergy efficiency, risk distance) using all the working fluids. Comparing C2 and C3, C3 provides a solution with the highest exergy efficiency, but the solutions of C2 are safer than the solutions of C3 for the same exergy efficiency. In the case of binary components, R14-C_3H_8 is more efficient and safer than R601-R23-R14. In the case of ternary components, both working fluids show similar ranges of exergy efficiency and risk distance. Moreover, as the number of components is increased, the risk distance is decreased. In particular, ORC with ternary component working fluids appeared to be safer than ORC with binary component working fluids. Furthermore, the results support the use of multi-component fluids as the

working fluid. And, overall, R14-C_3H_8 is the best working fluid among six working fluids because the solutions of R14-C_3H_8 are closest with an ideal solution. In conclusion, safety is an important factor to be considered in ORC design.

Appendix 2A

1) Source modeling

Source models are used to quantitatively define the release scenario by estimating discharge rates, total quantity released, etc. A continuous release of liquid and vapor can be calculated with the model written in Equation (2A-1).

$$\dot{m}_{liquid} = \rho A C_D \sqrt{2\left(\frac{g_c P_g}{\rho} + g h_L\right)}$$

$$\dot{m}_{vapor} = A C_D P_1 \sqrt{\frac{k g_c M}{R_g T_1}\left(\frac{2}{k+1}\right)^{(k+1)/(k-1)}} \qquad \textbf{(2A-1)}$$

$$\dot{m}_{total} = \frac{\dot{m}_{vapor} + \dot{m}_{liquid}}{2}$$

2) Dispersion modeling

Dispersion models convert the source term outputs to concentration fields downwind from the sources. Equation (1-2) represents dispersion model of instantaneous release that can model a ground level instantaneous release. $< C_i > (x, 0,0, t)$ is a function of dispersion coefficients in downwind, crosswind and axial direction (σ_x, σ_y and σ_z), wind velocity, u, time, t, and position, (x,0,0). Equation (1-3) represents a model for a point ground level from continuous release. $< C_i > (x, 0,0)$ is a function of dispersion coefficients in downwind, crosswind and axial direction (σ_x, σ_y and σ_z), wind velocity, u, and position, (x,0,0).

A. Instantaneous release

$$< C_i > (x,0,0,t) = \frac{Q^*}{\sqrt{2}(\pi)^{1.5}} exp\left[-\frac{1}{2}\left\{\left(\frac{x-ut}{\sigma_x}\right)^2 + \frac{y^2}{{\sigma_y}^2} + \frac{z^2}{{\sigma_z}^2}\right\}\right]$$

$$\sigma_x = 0.024x^{0.89} \ ,\sigma_y = 0.024x^{0.89} \ ,\sigma_z = 0.05x^{0.61} \quad \textbf{(2A-2)}$$

B. Continuous release

$$< C_c > (x,0,0) = \frac{\dot{m}_r}{\pi\sigma_y\sigma_z u} exp\left[-\frac{1}{2}\left\{\frac{y^2}{{\sigma_y}^2} + \frac{z^2}{{\sigma_z}^2}\right\}\right]$$

$$\sigma_y = \frac{0.04x}{\sqrt{1+0.0001x}} \ ,\sigma_z = \frac{0.016x}{\sqrt{1+0.0003x}} \quad \textbf{(2A-3)}$$

3) Fire & Explosion

A. BLEVE (Boiling Liquid Expanding Vapor Explosion)

Boiling liquid expanding vapor explosion (BLEVE) occurs when there is a sudden loss of containment of a pressure equipment containing a superheated liquid or liquified gas. BLEVE characterization model is represented in Equation (1-4). Emissive radiation hazard, E_r, is basically a function of mass released, Q*, the fireball's diameter, D_{max}, the duration, t_{BLEVE}, and the thermal emissive power, E.

$$D_{max} = 5.8Q^{*1/3}$$

$$X_s = \sqrt{L^2 + {H_{BLEVE}}^2} - \frac{D_{max}}{2} \quad \textbf{(2A-4)}$$

$$t_{BLEVE} = 2.6Q^{*1/6}$$

$$H_{BLEVE} = 0.75\, D_{max}$$

$$D_{initial} = 1.3\, D_{max}$$

$$\mathrm{E} = \frac{R\, Q^{*} H_{comb}}{\pi D^{2}{}_{max} t_{BLEVE}}$$

$$E_r = \tau_a E F_{21}$$

B. UVCE (Unconfined Vapor Cloud Explosion)

When a large amount of flammable vaporizing liquid or gas is rapidly released, a vapor cloud forms and disperses with the surrounding air. If this cloud is ignited before the cloud is diluted below its lower flammability limit, VCE will occur. The main hazard of UVCE is the blast by explosion. Equation (1-5) shows the model for UVCE. The overpressure, p^{o}, is a function of released mass, Q*, and the fuel heat of combustion, H_{comb}. A TNT equivalency model is used in this analysis. The fuel mass is equal to the unknown TNT mass, W, and its combustion heat, H_{TNT}.

$$\mathrm{W} = \frac{\eta_e\, Q^{*} H_{comb}}{H_{TNT}}$$

$$\mathrm{Z} = \frac{R_o}{W^{1/3}}$$

$$log_{10}(p^{o}) = \sum_{i=0}^{12} c_i\, (a + b log_{10} Z)^{i}$$

$$a = -0.2144,\ b = 1.3503 \qquad \textbf{(2A-5)}$$

$$c_i = [2.7808,\ -1.6959,\ -0.1542,\ 0.5141,$$

$$0.0989,\ -0.2939, 0.0268,\ 0.1091,$$

$$0.0016\ , -0.0215,\ 0.0001,\ 0.0017]$$

C. Flash fire

Flash fire is the nonexplosive combustion of a vapor cloud resulting from a release of flammable material into the open air. Flash fire is a complex phenomenon that lack of a well-accepted characterization model. So, flash fire is distance from dispersion model on LFL.

D. Jet Fire

Jet fire result from the combustion of material as it is being released from a pressurized process unit. Equation (1-6) represents the model of jet fire with the thermal radiation hazard. Radiation (E_r) is a function of the discharge rate ($\dot{m}_r$), the flame size (L_{flame}), the heat of combustion (H_{comb}) and the point view factor (F_P).

$$\frac{L_{flame}}{d_j} = \frac{15}{C_T}\sqrt{\frac{M_a}{M_f}}$$

$$F_P = \frac{1}{4\pi x^2}$$

$$X_s = \sqrt{L^2 + {L_{flame}}^2} \qquad \textbf{(2A-6)}$$

$$E_r = \tau_a \eta_j \dot{m}_r H_{comb} F_P$$

CHAPTER 3.
Basic Design Stage: Risk-based Management with Quantitative Risk Assessment Considering Seismic Effects for Offshore Carbon Dioxide Injection System

3.1. Introduction

3.1.1. Risk assessment in basic design stage

Among the techniques used to assess the risk, quantitative risk analysis (QRA), derived from probabilistic safety assessment (PSA) used in the nuclear industry, is mainly used for risk assessment in chemical processes on basic design stage. QRA allows investigation of the existing risks on a process to decide whether the risks are acceptable (CCPS, 2000). In the QRA method, consequence analysis and frequency analysis are used. Consequence analysis considers the effect of an expected chemical accident, whereas frequency analysis uses historical accident data to consider the occurrence probability of an expected chemical accident.

QRA has been widely applied to processes or systems in many studies owing to its reliability. Lee et al. (2015) studied risk assessment and management by QRA methodology on gas treating units in gas–oil separation plants. Risks in a topside LNG-liquefaction process of Liquefied Natural Gas Floating Production Storage and Offloading (LNG–FPSO) was analyzed by Jafari et al. (2012), including a hydrogen generator that uses natural gas in the reforming

process. Domenico et al. (2014) analyzed risk in methanol production plants by using QRA methodology. Cunha (2016) studied several risk assessment research results including frequency and consequence analysis on onshore pipelines. Similarly, risk in CO_2 transportation pipelines, including uncertainties and effects, was assessed by Koornneef et al. (2010a), and quantitative risk in CO_2 capture facilities was analyzed by Engebø et al. (2013). Likewise, the QRA has been widely used to assess the risk in various processes on basic design stage before detailed design stage in chemical industry. However, the QRA is applied to the various processes with same way, even though the processes have different characteristics that can affect the risk value. One of the characteristics considered in risk assessment is the surrounding of process. Among surroundings of process, seismic area has possibility of earthquakes that make process riskier. Generally, however, the seismic effect has not been considered in risk assessment even though some processes are vulnerable to earthquakes. Even if the effect is considered, the method to assess the risk from earthquakes should be improved. In this chapter, improved quantitative risk assessment considering seismic effects is proposed and studied for risk-based management in basic design stage.

3.1.2. Risk assessment considering seismic effect

From the 2011 Tohoku earthquake (Japan) accident to the Perugia (Italy) earthquake, earthquakes occur worldwide and cause considerable damages. With the increasing occurrence and power of earthquakes, damages from seismic effects have also risen. Thus, earthquakes have gained attention as important safety issues in industrial fields, including chemical plants. As a result, industries are considering seismic effects because resultant accidents increase the possibility of lethal events. In several studies, seismic effect has been considered in risk assessment. Fabbrocino et al. (2005) evaluated the effect of seismic action in a loss of containment accident, and Antonioni et al. (2007) considered seismic effect simply by using equipment-dependent failure probability models. A methodology to analyze life loss risk caused by airborne chemicals triggered by seismic effects was proposed by Meng et al. (2015). A QRA method considering multi-vessel failure scenarios triggered by seismic effect was proposed by Kim et al. (2016). Some researchers offered various proposals to consider seismic effect in risk assessment. However, there are still limitations in the previous studies. Few papers have considered multi-hazard impacts triggered by seismic effect, which affects the entire industrial process simultaneously rather than independently, such as that occurring in other natural hazards (Gallina et al., 2016). In addition, the domino effect was considered on a only limited basis owing to its complexity (Kim et al., 2016). Moreover, it is difficult to consider this method in other applications because most research proposes a method for specific cases.

Multi-hazard impacts define several hazards that occur simultaneously. In a process containing multiple equipment types, hazard scenarios generally occur separately on specific equipment. However, in the case of hazards by earthquake, several hazardous scenarios can occur simultaneously as results of simultaneous leakage or rupture of several pieces of equipment. Moreover, the domino effect from such failure can trigger other hazards through the transfer of accidental effects (Landucci et al., 2012).

Bayesian network (BN) is used for considering multi-hazard effects and domino effects, which are important factors to be considered in hazard assessment in this thesis. A BN is a directed acyclic graph (DAG), which is a graphical model, and contains probability theory. BN can represent causal relationships, such as cause–effect relationships, and represents uncertain knowledge in probabilistic systems. Because frequency analysis is based on a causal relationship including event tree analysis (ETA), BN is used as tool for risk analysis in some research. Martins et al. (2014) studied application of a regasification system with methodology based on hybrid BNs of iterative six-step risk analyses. Liang et al. (2017) conducted risk analysis on level crossing using BN. Some papers studied risk assessment with BN of oil and gas pipelines (Kabir et al., 2016; Li et al., 2016). Thus, BN is a proper method for analyzing multi-hazard and domino effects, because these effects are also based on cause–effect relationships. Moreover, the methodology to assess the risk of seismic effect is proposed with the generalized equation for application to various processes that is vulnerable to earthquakes.

3.1.3. Application: Offshore topside CO2 injection system for underground storage

For application, an offshore topside CO_2 injection system for underground storage in South Korea is used owing to the necessity of risk assessment on the process itself, which has not been well studied previously. Previous studies of safety in CO_2 injection systems analyzed whether the CO_2 injected underground is stable. Because use of this technology depends on stability of CO_2 storage, many studies have been published about risk and stability associated with the storage. The research include studies on diverse risk assessment of CO_2 storage in a Salah CO_2 storage project (Dodds et al., 2011; Metcalfe et al., 2013; Oldenburg et al., 2011), studies on the stored CO_2 containment risk or leakage risk from storage site and its impacts (Blackford et al., 2014; Damen et al., 2006; Little and Jackson, 2010; Tucker et al., 2013), CO_2 release risk from failure of caprock trapping the CO_2 (Rohmer and Seyedi, 2010; Smith et al., 2011), CO_2 storage risk caused by earthquakes (Nicol et al., 2011; Vilarrasa and Carrera, 2015; Zoback and Gorelick, 2012), monitoring strategies and their demonstration for management of CO_2 storage risk (Blackford et al., 2015; Hvidevold et al., 2015; Zhang et al., 2014), and studies for assessment and management of four types of risk in geologic CO_2 storage: performance, long-term containment, public perception, and market (Pawar et al., 2015).

However, CO_2 offshore storage has other risks to be considered in addition to storage stability. In particular, some risks are caused by process characteristics. The injection system has some characteristics relating to process safety because the system is installed on topside processes in storage sites near oceans, First, the space required for these process facilities is smaller

than that for onshore sites. Because of the cost issue, even in the same process, it should be placed in a smaller space. If accidental events occur in a topside system, more substantial damage can occur owing to its highly compact nature. Second, weather issues are more critical in offshore storage. Because the system is built in the sea, weather changes are diverse and rapid; therefore, this aspect of weather is also related to process safety. Despite these factors, safety or risk research of an offshore CO_2 storage system has not been conducted. Therefore, QRA on an offshore CO_2 storage system offers useful information. Moreover, earthquakes increasing in intensity have occurred near South Korea in recent times; thus, risk study of an offshore system near South Korea is meaningful for considering earthquakes in a process. Figure 3-1 represents the ranking of the power of an earthquake near the Korean Peninsula. The most powerful earthquake, and the most recent, occurred in Gyeongju in September 2016. Because this region is near a storage site (red point in Figure 3-1), risk assessment must be renewed by considering the seismic effect, which is an important parameter that increases process risk. Therefore, this particular topside CO_2 injection system is an adequate example for analysis with the proposed QRA, or modified method, which considers seismic effects.

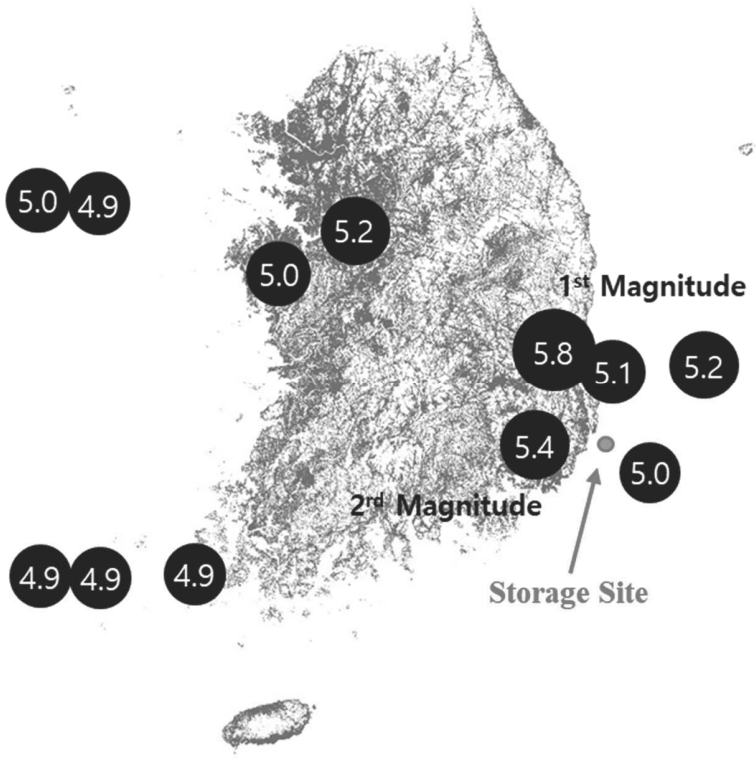

Figure 3-1. Main earthquakes occurring in South Korea until 2017.

The present study includes a proposed modified QRA methodology considering seismic effects with multi-hazard and domino effects, which is analyzed by using a BN. In addition, this methodology is applied to a topside CO_2 injection system for underground storage.

To summarize, the main contents of this study are as follows:

- QRA of topside CO_2 injection system rather than stability risk of CO_2 storage.
- Consideration of seismic effect, which is susceptible to offshore topside systems, by using the proposed modified QRA with BN.

3.2. Methodology

3.2.1. Conventional QRA procedure

The conventional QRA procedure is presented in Figure 3-2. QRA is conducted with a specific process for defining potential event incidents to evaluate the incident outcome and the risk (CCPS, 2010). QRA is performed mainly after detailed design among process design stages because sufficient information of the process can be obtained. Application of QRA in this study is conducted after the detailed design stage as well.

For assessing risk on a specific process, possible major hazards in the process must be specified in a step is known as hazard identification (HAZID) (CCPS, 2008). Possible incidental scenarios initiating hazard events, or initial scenarios, can be specified such as pipeline rupture or tank leak. Then, frequency and consequence analyses of these scenarios are performed. Frequency analysis is the calculation of the probability of hazard events from initial scenarios such as rupture or leak. Generally, the frequency rates of initial scenarios are obtained from historic data including equipment failure data from Oil and Gas Producers (OGP) and the UK's Health and Safety Executive (HSE). Consequence analysis estimates the scale of damage caused by an accident by calculating fluid concentrations along with the downwind distance, radiation intensity, and toxic dose for dispersion, fire or explosion, and toxicity events.

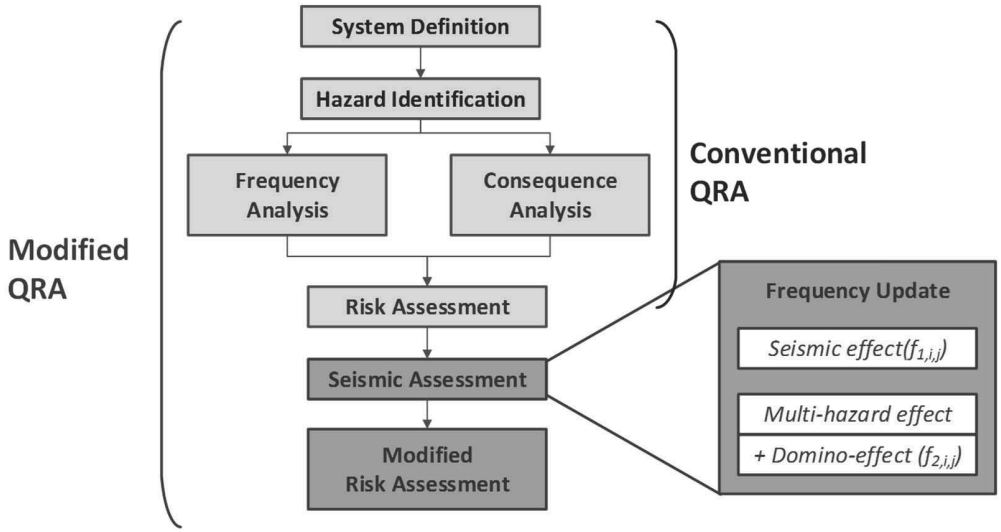

Figure 3-2. Modified and conventional quantitative risk analysis procedures.

In general, risk is categorized as individual risk (IR) and societal risk. IR is the general concept of risk, which is the risk of death or serious injury to specific individuals exposed to the risk. Individuals can be expressed as Equations (3-1) and (3-2), where IR is the total individual risk per year, IR_i is individual risk by event I, F_i is frequency (probability) of event I, and P_{fi} is probability of fatality by event I, which expresses the severity of the consequence.

$$\text{IR} = \sum_{i=1}^{N} IR_i \tag{3-1}$$

$$IR_i = F_i \times P_{fi} \tag{3-2}$$

On the contrary, societal risk is the relationship between the probability of a catastrophic incident and its consequences and is usually represented as an F–N curve. This graph plots the expected frequency (F) of the number (N) of casualties by all possible dangerous incidents in the surrounding area. F and N can be expressed as Equations (3-3) and (3-4), where N_i is the number of fatalities resulting from event I, N_p is the number of people, F_N is the frequency of all events, and F_i is the frequency of event I.

$$N_i = N_p P_{fi} \tag{3-3}$$

$$F_N = \sum_{i=1}^{N} F_i \tag{3-4}$$

In short, IR indicates the probability of death of one person by all possible events I, and societal risk describes the probability of death of a specific number

of people by all possible events I. Conventional QRA methodology is a well-studied topic. However, the content of this methodology has numerous parts and is difficult to explain in its entirety. Details of QRA methodology have been given in previous research (CCPS, 2010)

3.2.2. Modified QRA

3.2.2.1. Frequency update for seismic effect

As shown in Figure 3-2, modified QRA includes conventional QRA with additional procedures such as frequency updates for seismic effects and a BN for considering multi-hazard and domino effects. The basic concept of the QRA method including seismic effects is the addition of the frequency rate by the seismic accident scenario to the general frequency rate. Most accidental events caused by seismic effects are the same as general events because these accidental events occurring from the same initial leak (or rupture) event on equipment can be caused by seismic effects as well. For example, if an earthquake occurs, seismic power affects units of the process such as pipelines and tanks. Then, the seismic effects can result in pipeline or tank leaks or ruptures, which are same as general scenarios as initial leaks or ruptures. Thus, seismic effects can be considered simply by adding the additional frequency rate of the leak event caused by the earthquake. This is a main assumption of the present study for considering seismic effects. Equation (3-5) represents this method as a generalized equation, where f is the frequency rate considering seismic effects, f_0 is the frequency rate from historic data excluding seismic effects, and f_α is the frequency rate from seismic effects including multi-hazard and domino effects.

$$f = f_0 + f_\alpha \quad \textbf{(3-5)}$$

For considering domino and multi-hazard effects apart from seismic effects, Equation (3-5) should be more generalized. Therefore, a more general

expression of frequency of leakage considering seismic effects, domino effects, and multi hazard effects is represented in Equations (3-6), (3-7), and (3-8):

$$f_0 = \sum_i \sum_j f_{h,i,j} \tag{3-6}$$

$$f_\alpha = \sum_i \sum_j (f_{s,i,j} + f_{d,i,j}) \tag{3-7}$$

$$f = f_0 + f_\alpha = \sum_i \sum_j (f_{h,i,j} + f_{s,i,j} + f_{d,i,j}) \tag{3-8}$$

where i and j are equipment and substance, respectively. Specifically, f is the total frequency rate of the leak event including seismic effects and additional effects, $f_{h,i,j}$ is the frequency rate of the leak event from historic data, $f_{s,i,j}$ is the frequency rate from direct seismic effects, and $f_{d,i,j}$ is the frequency rate from domino and multi-hazard effects. $f_{s,i,j}$ is considered by a probit equation expressing the probability of leaks by seismic effects, and $f_{d,i,j}$ is considered by the BN technique explained in Section 2.2.2.

3.2.2.2. Bayesian network for multi-hazard and domino effects

BN is a theory that can represent probabilistic relationships by using a graphical structure. Causal relationships, including those between causes and effects, can be represented by using this theory. BN is expressed in the form of a directed acrylic graph (DAG) consisting of nodes and arcs. The nodes correspond to the variables, and the arcs represent conditional dependencies between linked nodes. The nodes consist of parent and child nodes. The parent node has an arc (or arcs) from the node to the child node, which means there is a direct causal or influential dependency of A on B. The BN is based on the Bayes theorem, which can be expressed as Equation (3-9), where $P(X|Y)$, $P(X)$ is known as the posterior probability of the parameters X given evidence Y and the prior probability of parameters X. The joint probability distribution, $P(x_1, x_2, \dots, x_n)$ of a set of variables in BN, can be described as Equation (3-10), where $Parent(x_i)$ is the parent set of variables x_i.

$$P(X|Y) = \frac{P(Y|X)P(X)}{P(Y)} \quad \textbf{(3-9)}$$

$$P(x_1, x_2, \dots, x_n) = \prod_{i=1}^{n} P\left(x_i \middle| Parent(x_i)\right) \quad \textbf{(3-10)}$$

In this study, BN is used to handle domino and multi-hazard effects. Although BN has been used in previous studies for risk assessment, it was used here to represent relationships of causes and effects to understand the progression of one cause propagating to effect through several consequences.

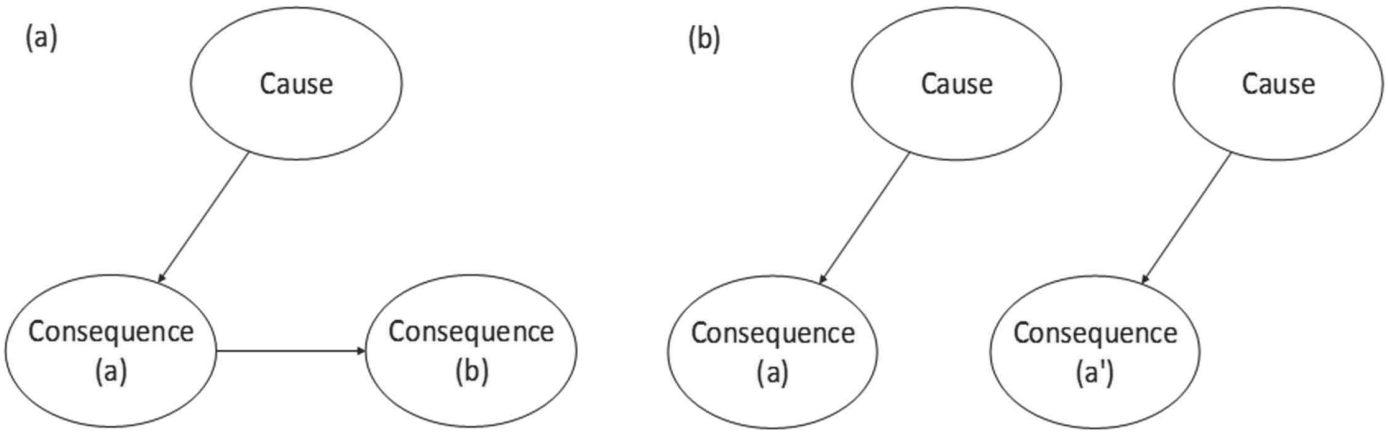

Figure 3-3. Bayesian network: (a) domino effect, (b) multi-hazard effect.

Unlike that in previous studies, dominos and multi-hazard effects are also types of causal relationships, although the relationships are hazard–hazard or effect–effect. Considering the facility aspect, the effects of a hazard from one facility propagates other facilities to create hazards. When a cause, or seismic effect, creates a consequence such as fuel tank leakage, it can be represented as BN. In case of a domino effect, the consequence leads to another consequence or event. Thus, prior consequence plays a role in another cause, which is the same as the parent node in BN (Figure 3-3(a)). In case of multi-hazard effects, BN consists of multiple parent nodes, which means that multiple causes simultaneously affect the accident conditions (Figure 3-3(b)).

3.3. Description of CO_2 injection process for underground storage

For QRA, the CO_2 injection process should be specified. The specific process, shown in Figure 3-4, is an offshore topside platform built for CO_2 storage containing a CO_2 injection system in South Korea. The storage site includes specific stratum in a deep seabed near Pohang Youngil Bay. This topside system was constructed to consider changes in the condition of CO_2 to specific conditions to meet the criteria based on geologic survey. Figure 3-4 represents the unit process block diagram of the CO_2 injection process. The input stream is supplied after several preprocessing steps, which consist of a separation step to produce a CO_2 gas phase of about 95% purity by using the post-combustion capture process and a conversion step to liquid CO_2 through a compression–dehydration–liquefaction process. The composition of CO_2 is liquid CO_2 with a purity of 99.9% and several hundred parts per million of water. The output stream is over-pressurized liquid carbon dioxide for considering the pressure and temperature of the CO_2 injection bed.

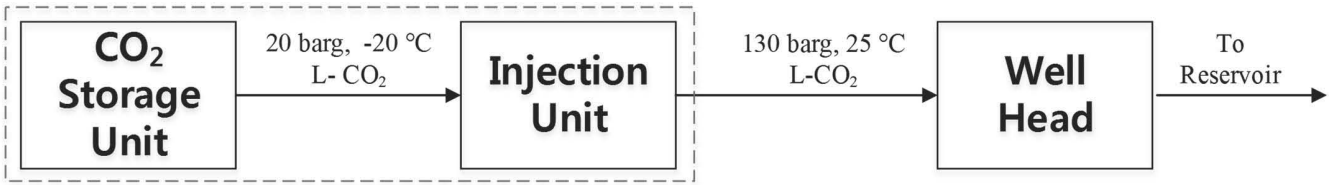

Figure 3-4. Unit process block diagram of CO_2 injection process.

Specifically, this process consists of a CO_2 storage unit, an injection unit, and a well head; the main target units are the CO_2 storage unit and the injection unit, as shown by the blue dashed line in Figure 3-4. The CO_2 temporary storage unit serves to temporarily store the liquid CO_2 transferred from the CO_2 capture and liquefaction process. Therefore, this unit consists of facilities capable of minimizing heat loss so that the CO_2 can be maintained in a liquid state. The injection unit consists of pressurization and temperature control equipment, which manipulate parameters such as pressure and temperature to target specifications. Liquid CO_2 from storage is pressurized and undergoes temperature change before injection through the well head. The CO_2 condition before injection considers the condition of the storage site, which is 130 barg, 25°C in a liquid state. The well head is a structure that provides the boundary between the injection well and the upper process.

The layout of this topside process, which is necessary for risk assessment, is shown in Figure 3-5. This system consists of several sites including operating sites, a storage unit site, an injection unit site, and a utilities site. The operating site contains an operating and monitoring room, accommodations, and a storage room. This site can accommodate five people as residents for operation, monitoring, and other duties. The storage unit site has CO_2 storage tanks, and the injection unit site has an injection unit. Utilities sites contain electricity generators, and fuel storage tanks. For analysis, the number of fuel storage tanks was assumed to be two.

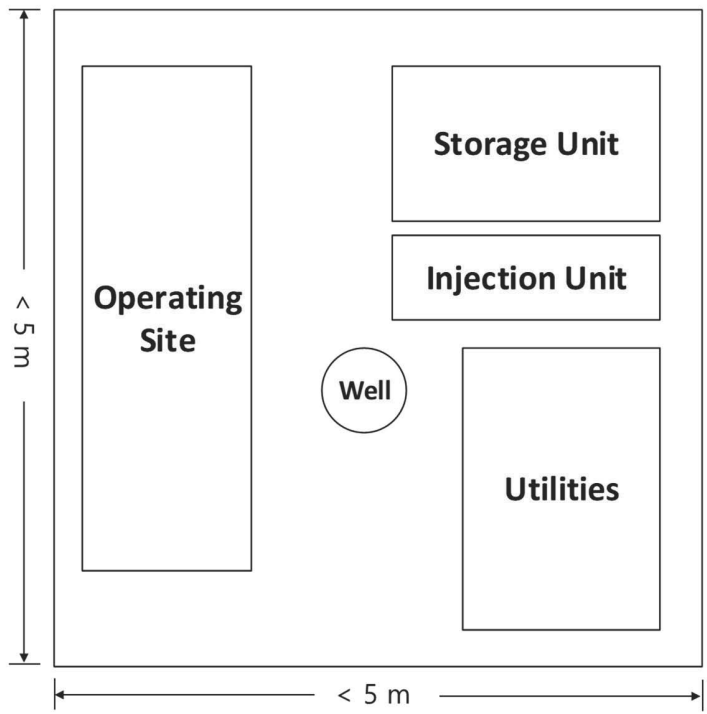

Figure 3-5. Offshore topside platform system plot plan.

3.4. Quantitative risk assessment: Application of topside CO_2 injection system

3.4.1. System definition and hazard identification

For performing QRA, the basic information related to this system and accident scenarios should be specified in addition to performing system analysis, as described in Section 3. The information and the scenarios are shown in Table 3-1, which includes weather information near Pohang Youngil basin and three accident scenarios. Weather information includes wind velocity, wind direction, and temperature, which are the main data for QRA. The three accident scenarios are leakage from the fuel storage tank, leakage from the CO_2 storage tank, and leakage from the CO_2 pipeline with the highest pressure. These accident scenarios are determined by performing a hazard and operability study (HAZOP) procedure, which is used for qualitative analysis and specifies possible hazards with causes and consequences in a process plant utilizing HAZID. After identifying hazards, several methods are suggested such as removal of the cause or reduction of the consequence. The details of HAZOP for this process have been reported previously (An, 2017). The general hazards of pressurized CO_2 (Koornneef et al., 2010b; Witkowski et al., 2015) and hydrocarbons have also been reported previously (CCPS, 2008; Dan et al., 2014; Jafari et al., 2012; Lee et al., 2015)

Table 3-1. Weather information of the offshore topside system

Accident scenario	**Unit**				**Leak size**			
	Fuel storage tank CO_2 storage unit CO_2 pipeline				Large, medium, small Large, small			
Weather Information	Item		Unit	Info	Item		Unit	Info
	Wind	Average	m/sec	2.8	Direction	SW	%	15.2
		Max	m/sec	10.5		WSW	%	20.2
	Temperature	Annual average	°C	14.2	Precipitation	Annual average	mm	1,152.0
		Monthly max/min	°C	29.4/-2.0		Day max.	mm	516.4

3.4.2. Frequency analysis

For frequency analysis, the initial failure data of each piece of equipment are necessary. In this study, the failure data, including those for the storage tank and pipeline, were obtained from OGP 2010 (Oil and Gas Producers, 2010), as represented in Table 3-2. These data are used as initiating events in event tree analysis (ETA), which is a technique performed to identify and evaluate all the possible outcomes from an initiating event. The results of the ETA, represented in Figure 3-6, are structured on the basis of several conditions such as immediate or delayed ignition. Possible accidental outcomes for fuel storage tanks include jet fire, pool fire, flash fire, explosion, and other disasters, and that CO_2 storage tanks and pipelines includes suffocation.

The conditional probability of each scenario for a fuel tank is represented in Table 3-3, which was evaluated on the basis of the release rate (kg/s). There is no conditional probability of scenarios related to CO_2 owing to material properties. The release rate was calculated by using DNV PHAST. v. 6.7 through a discharge model and employing the following reasonable assumptions:

- The ignition probabilities are determined from look-up correlations (EI, 2006).
- The probability of an immediate ignition is 0.5, and that of an explosion is 0.12 for the whole scenario based on the release rate in this analysis (Lee et al., 2015).

Table 3-2. Failure data for accident scenarios (Oil and Gas Producers, 2010).

Accident scenario	Historic data (leak size)
Fuel storage tank	3.5E-04 (small)/1.1E-04 (medium)/1.7E-04 (large)
CO_2 storage tank	
CO_2 pipeline	3.8E-05 (small)/2.7E-05 (large)

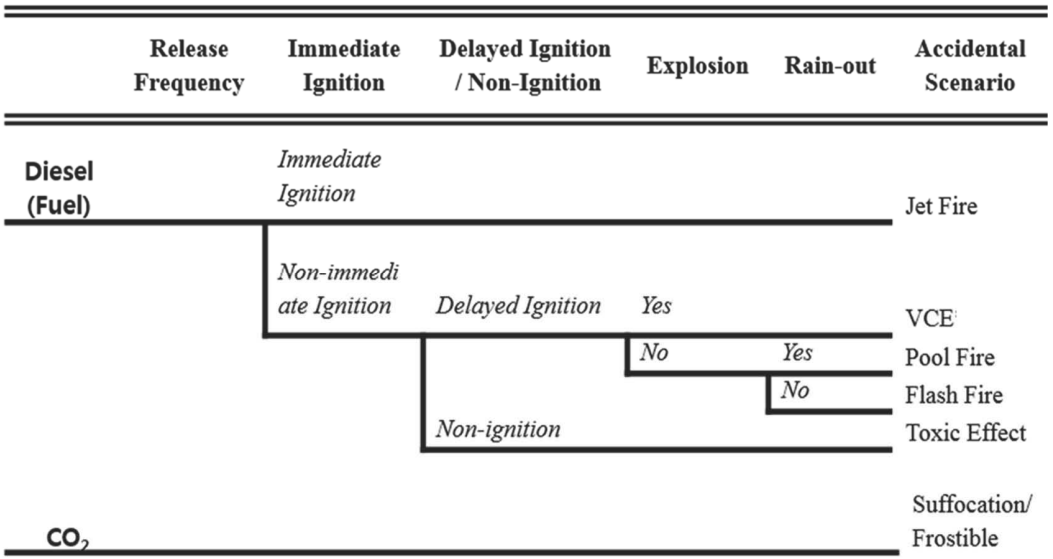

Figure 3-6. Event tree analysis**.**

Table 3-3. Conditional probabilities of each leak scenario.

Scenario	Release rate (kg/s)	Ignition	Immediate ignition	Delayed ignition	Explosion
DO Tank Leak 50 mm	7.589×10^{0}	1.224×10^{-3}	0.5	0.5	0.12
DO Tank Leak 100 mm	3.036×10^{1}	2.641×10^{-3}	0.5	0.5	0.12
DO Tank Leak 150 mm	6.930×10^{1}	4.142×10^{-3}	0.5	0.5	0.12

3.4.3. Consequence analysis

The main consequences of this study are CO_2 concentration along with downwind distance by CO_2 tank, CO_2 pipeline failure, and radiation intensities of fire or explosion by fuel tank failure. The results are shown in Figure 3-7 and Figure 3-8. Figure 3-7 shows the result of 100 mm leak scenario on a CO_2 storage tank including four different weather scenario cases. These weather scenarios contain two wind speeds, 10.5 m/s and 2.8 m/s, as represented in Table 3-1, in addition to two Pasquill stability classes, stable (F) and unstable (A), which are factors relevant to the circulation of the atmosphere. In all scenarios, the overall topside plant is covered by vaporized CO_2 because CO_2 is spread about 450–620 m from the leak point (Figure 3-7(a)). Moreover, the CO_2 concentration surrounding the topside system is more than 20,000 ppm, which can cause headaches and fatigue (Figure 3-7(b)). This level is the minimum level affecting humans; a level greater than 20,000 ppm is even more dangerous and is therefore a concentration threshold (Table 3-4 and orange dashed line in Figure 3-7). Examples of other leak and CO_2 pipeline scenarios were omitted because the results are similar to those in the 100 mm leak case; such cases differ only in terms of the magnitude of dispersion.

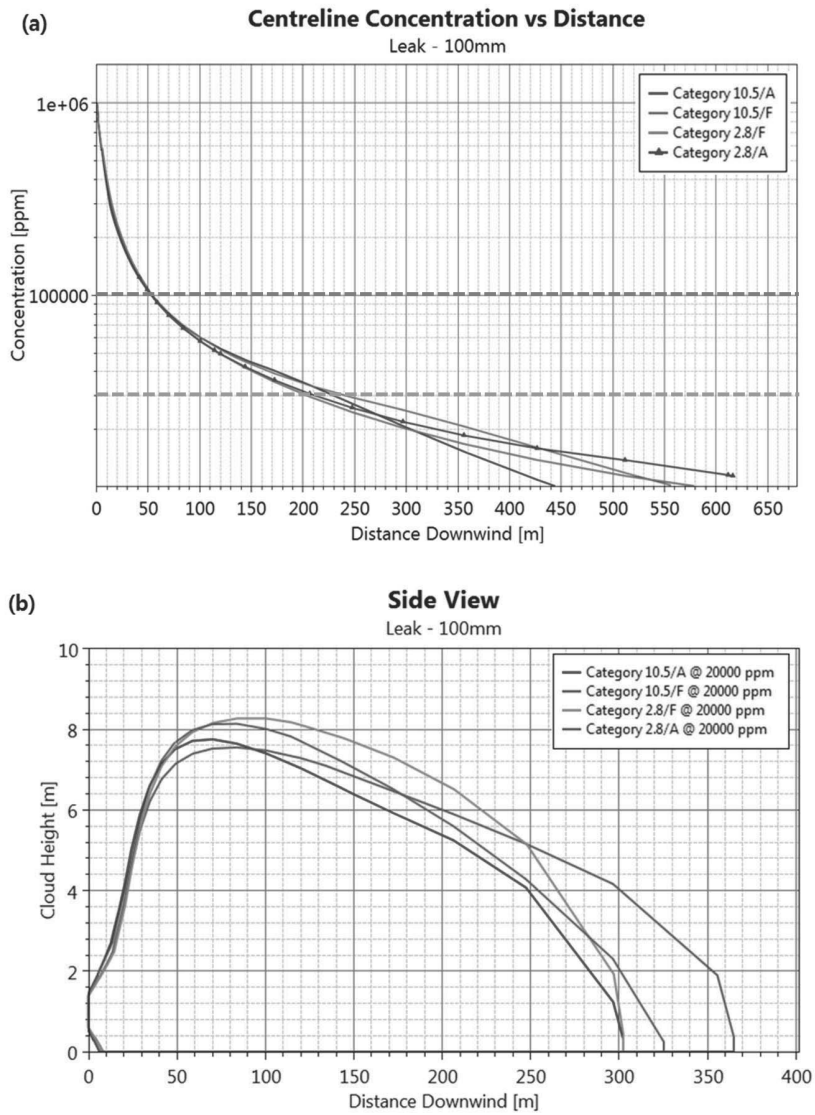

Figure 3-7. Results of consequence analysis on CO_2 storage tank: (a) centerline concentration versus distance; (b) side view.

Table 3-4. Effects of increased CO_2 concentration on humans (DNV, 2010).

CO_2 concentration in air (%) [= 10000 ppm]	**Time of exposure**	**Effects on humans**
>20	Within 1 min	Loss of consciousness, convulsions, coma, death
>10–15	1 to several minutes	Dizziness, drowsiness, muscle twitching/spasms, loss of consciousness
7–10	Several minutes	Loss of consciousness, near unconsciousness
	1.5 min to 1 h	Headache, increased pulse rate, shortness of breath, sweating, increased breathing rate
6	1–2 min	Hearing and visual disturbances
	≤16 min	Headache, breathing problems (dyspnea)
	Several hours	Tremors
4–5	Within several minutes	Headache, dizziness, elevated blood pressure, breathing discomfort (equivalent of the concentration exhaled by humans)
3	1 h	Mild headache, sweating, breathing problems at rest
2	Several hours	Headache, breathing problems upon mild exertion
0.5–1	8 h	Acceptable occupational hazard level

The results of the 100 mm leak scenario on a fuel storage tank with weather scenarios are represented in Figure 3-8. In this scenario, the two main types of fire are jet fire and pool fire; the effect graphs in the figure show radiation versus distance. Although the effect range of the jet fire is small, but the radiation is powerful near the fire point at ~5 m. Moreover, the effect range of the pool fire is relatively large, but the maximum radiative power is about 26 kW/m^2, which is smaller than jet fire value of 100 kW/m^2. The difference between the jet fire and pool fire is related to their characteristics (Pedersen, 2012). Similar to that with the CO_2 storage tank scenarios, other scenarios were omitted because the tendencies are similar. One of the notable results is that no explosion cases occurred in all leak scenarios. There are two reasons for this result. First, the storage tank had a small quantity of fuel to cause an explosion, and had atmospheric pressure, which are not favorable conditions for an explosion.

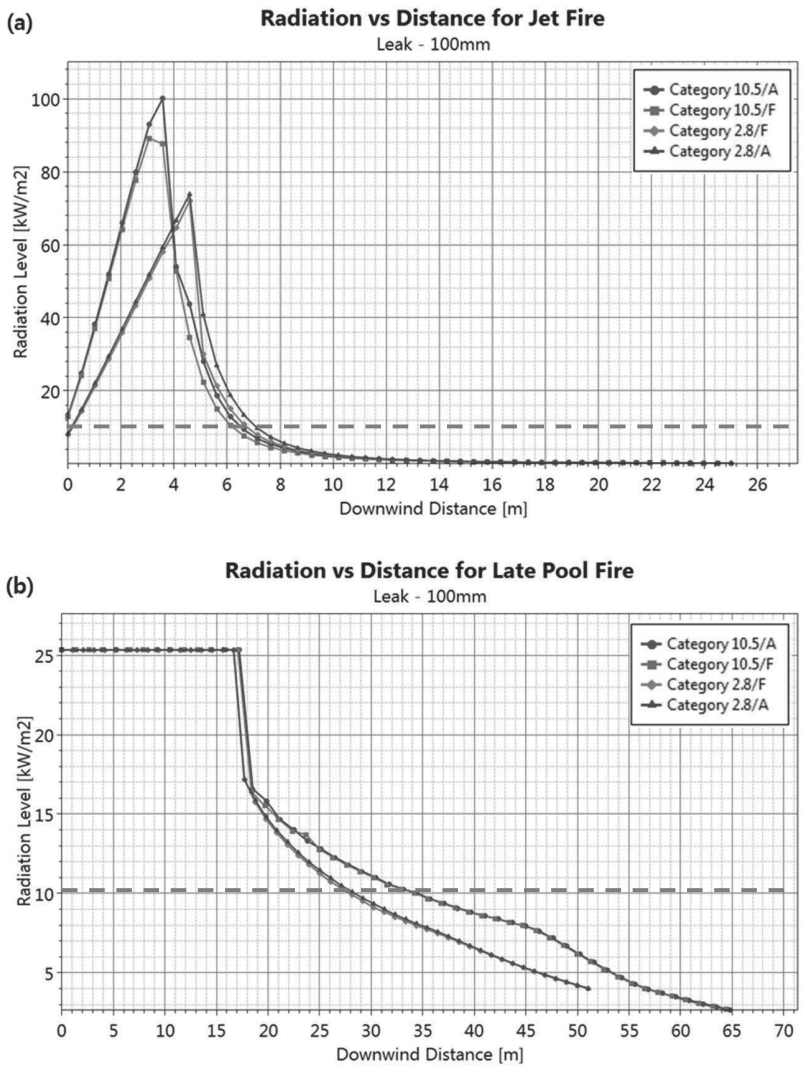

Figure 3-8. Fuel storage tank: (a) radiation versus distance for jet fire; (b) radiation versus distance for pool fire.

Table 3-5. Responses to radiation (Lentini, 2013).

Radiation (KW/m^2)	Description
170	Maximum flux measured in a post-flashover compartment
80	Thermal Protective Performance test for personal protective equipment
52	Fiberboard ignites in 5 s
29	Wood ignites, given time
20	Typical beginning of flashover at floor level of a residential room
16	Human skin: sudden pain and second-degree burn blisters after 5 s
12.5	Wood produces ignitable volatiles by pyrolysis
10.4	Human skin: Pain after 3 se, second-degree burn blisters after 9 s
6.4	Human skin: second-degree burn blisters after 18 s
4.5	Human skin: second-degree burn blisters after 30 s
2.5	Human skin: burns after prolonged exposure, radiant flux exposure typically encountered during firefighting
1.4	Sunlight, sunburns potentially within 30 min

To further analyze the consequence results, threshold analysis can be performed. In the case of the CO_2 storage tank, the minimum CO_2 concentration that causes harmful effects in humans is 20,000 ppm. However, the time of exposure, at several hours (Table 3-4), is longer than the leakage time of the CO_2 storage tank, at minimum and maximum times of 55 s and 410 s, respectively. Moreover, the standard concentration for specifying a safe distance should be decided on the basis of threat to human life. Therefore, the threshold concentration can be conservatively specified as 100,000 ppm (10%), which is expressed as the red dashed line in Figure 3-7. As a result, the safe distance is about >50 m for the CO_2 storage tank. In the case of the fuel storage tank, 10.4 kW/m^2 can be a conservative threshold standard of heat radiation (Table 3-5). Thus, the safe distances are about >7 m for jet fire and >35 m for pool fire relative to fuel storage tanks.

Apart from risk reduction, action should be taken to mitigate consequences. A leak detector or gas detector is recommended to identify leakages in facilities such as the CO_2 storage tank, pipeline, and fuel storage tank. In addition, oxygen masks and first-aid equipment are also recommended to handle all incidents.

3.4.4. Risk analysis

After the frequency and consequence analyses on the accident scenarios are conducted, risk analysis is performed. In this study, PHAST_RISK. v. 6.7 was used by QRA. The input data for risk assessment include the operating data of each equipment piece and the weather conditions specified in Section 4.3. The results of risk analysis are represented in Figure 3-9. Figure 3-9(a) shows an individual contour representing individual risk, and Figure 3-9(b) displays an F–N curve. In the individual contour, the differences in risk depend on location. Because the main risk source is the fuel storage tank, risk is higher near the tank than in other areas. This risk information can be used for locating lifeboats or setting an evacuation plan. In the case of the CO_2 tank and pipeline, the situations appear to be dangerous according to the consequence analysis, although the effect to risk is almost zero. This occurred because accident scenario fatalities such as suffocation, which is an accident scenario of CO_2, depends on the spent near the concentration. That is, CO_2 concentration by dispersion is high, but the time that can affect a person is short. Thus, the risk from events related to CO_2 is not influential for overall risk.

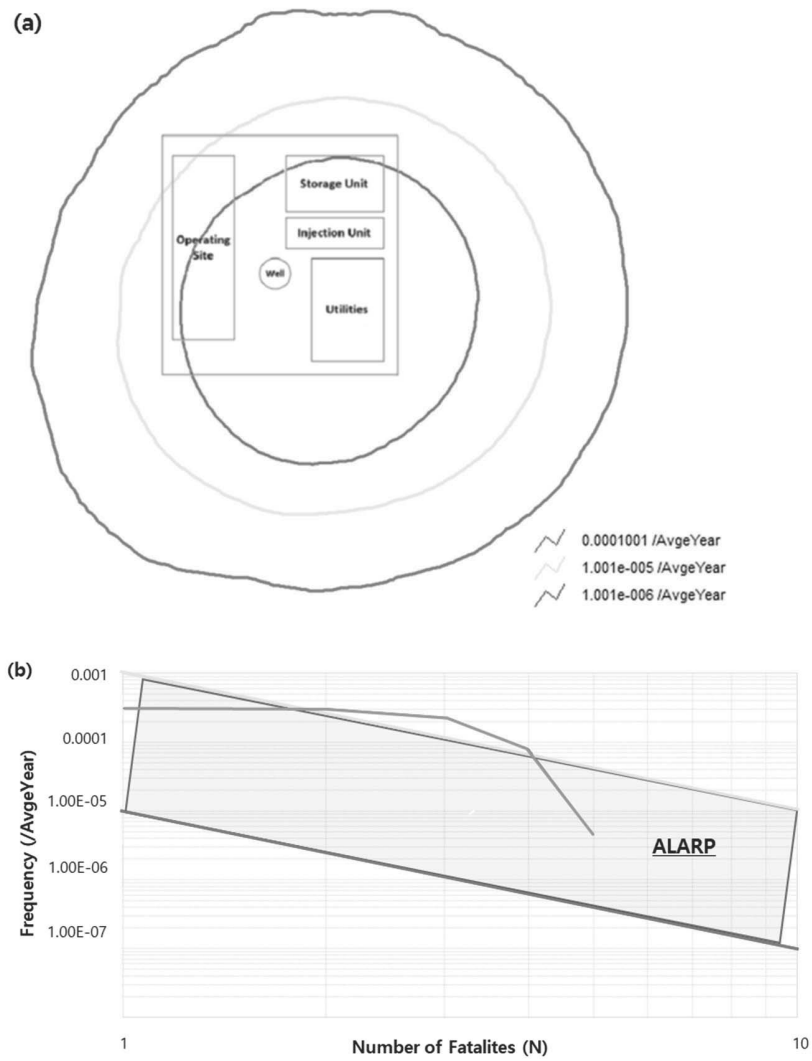

Figure 3-9. Result of conventional quantitative risk analysis: (a) Individual Contour, (b) expected frequency/number of casualties (F–N) curve.

Table 3-6. Societal risk integral (general quantitative risk analysis)

Equipment	Scenario	Risk [/AvgYr]	Risk [%]	CRDRO	CRDFP	Others
Fuel storage tank (a)	50 mm	2.174×10^{-4}	23.37	11.46	7.13	4.78
	100 mm	1.596×10^{-4}	17.16	13.45	2.15	1.55
	150 mm	7.339×10^{-5}	7.89	6.89	0.54	0.46
Fuel storage tank (b)	50 mm	2.588×10^{-4}	27.82	13.80	8.40	5.63
	100 mm	1.334×10^{-4}	14.34	11.24	1.80	1.30
	150 mm	8.767×10^{-5}	9.42	8.23	0.65	0.55
Total Risk		9.303×10^{-4}	100	65.07	20.67	14.26

CRDRO: Continuous release with Rainout Delayed Residual pOol fire effects

CRDFP: Continuous release with Rainout Delayed Flash fire with additional Pool fire effects

On the contrary, the F–N curve includes three risk lines: upper-bound risk, process risk, and lower-bound risk. Upper- and lower-bound risk are the criteria of risk. The area between these bounds is known as the as low as reasonably practicable (ALARP) region, which is a region of tolerable risk. In this study, an HSE standard was used as the ALARP region criterion. In Figure 3-9(b), part of the blue line, which is the process risk line, extends past the upper bound; specifically, the process risk is higher than tolerable risk level. Detailed information of risk is represented in Table 3-6, which shows the elements of societal risk contained in terms of equipment, scenario, and outcome. There are two main equipment, three scenarios, and four main outcomes based on ETA. The total societal risk integral value was 9.303×10^{-4}/year, and a small leak scenario at fuel storage tank (b) had the highest risk integral value of 2.588×10^{-4}/year, which accounted for 27.82% of the total societal risk. Additionally, continuous release with rainout delayed residual pool fire effects (CRDPO) accounted for the largest percentage of the total risk, at 65.07%. As a result, process risk had to be reduced to tolerable levels. Moreover, after consideration of seismic effects, the risk will be further increased. For this reason, the seismic effect should be considered in QRA. Therefore, seismic effects must be considered to calculate process risk prior to risk reduction.

3.4.5. Consideration of seismic effect using modified quantitative risk analysis

For considering seismic effects as well as multi-hazard and domino effects, updated frequency should be applied, which is included in the modified QRA procedure described in Section 2.2, and Equation (3-8). In this study, i contains three pieces of equipment such as a CO_2 tank or pipeline, and j contains two substances such as CO_2 or fuel in $f_{i,j}$, which are summarized in Table 3-7. $f_{0,i,j}$ is specified by historic data, as discussed in Section 4.1. $f_{s,i,j}$ is the leakage frequency rate by earthquake, which is expressed in Equation (3-11); AEP is the annual exceedance probability of the peak ground acceleration (PGA), which indicates the power of an earthquake; and P_{PGA} is the leak probability of the tank according to the PGA value.

$$f_{s,i,j} = AEP \times P_{PGA} \quad \textbf{(3-11)}$$

In this study, $f_{s,i,j}$ is calculated with AEP data (Rhee et al., 2012) and P_{PGA} data except for $f_{s,pipe,j}$ are specified with instrumental intensity (Wahid et al., 2017). AEP based on PGA near the CO_2 storage site is represented in Figure 3-10. The PGA is set as 0.34, which is a possible value near the storage site. The P_{PGA} value is expressed as Equation (3-12), which is an error function of Y expressed as a probit function and decided by the PGA value. The probit equations for the Y values are expressed as Equations (3-13) and (3-14) following previous studies (Antonioni et al., 2007; Fabbrocino et al., 2005). Equation (3-13) is for pressurized storage, and Equation (3-14) is for atmospheric storage. In this study, the CO_2 storage tank is used for pressurized

storage, and the fuel storage tank is used for atmospheric storage. To summarize, the P_{PGA} value reflects the probability of the specific equipment failure according to the PGA value.

$$P_{PGA} = 50\left[1 + \frac{Y-5}{|Y-5|}\mathrm{erf}\left(\frac{|Y-5|}{\sqrt{2}}\right)\right] \quad \textbf{(3-12)}$$

$$\mathrm{Y} = 5.146 + 0.884\ln(PGA) \quad [\text{Pressurized vessel}] \quad \textbf{(3-13)}$$

$$\mathrm{Y} = 7.8 + 1.43\ln(PGA) \quad [\text{Atmospheric vessel}] \quad \textbf{(3-14)}$$

Table 3-7. Frequency equations (CO_2 tank, CO_2 pipeline, fuel tank).

Equipment	Equation
CO_2 tank	$f_{tank,CO2} = f_{0,tank,CO2} + (f_{s,tank,CO2} + f_{d,tank,CO2})$
CO_2 pipeline	$f_{pipeline,CO2} = f_{0,pipe,CO2} + (f_{s,pipe,CO2} + f_{d,pipe,CO2})$
Fuel tank	$f_{tank,fuel} = f_{0,tank,fuel} + (f_{s,tank,fuel} + f_{d,tank,fuel})$

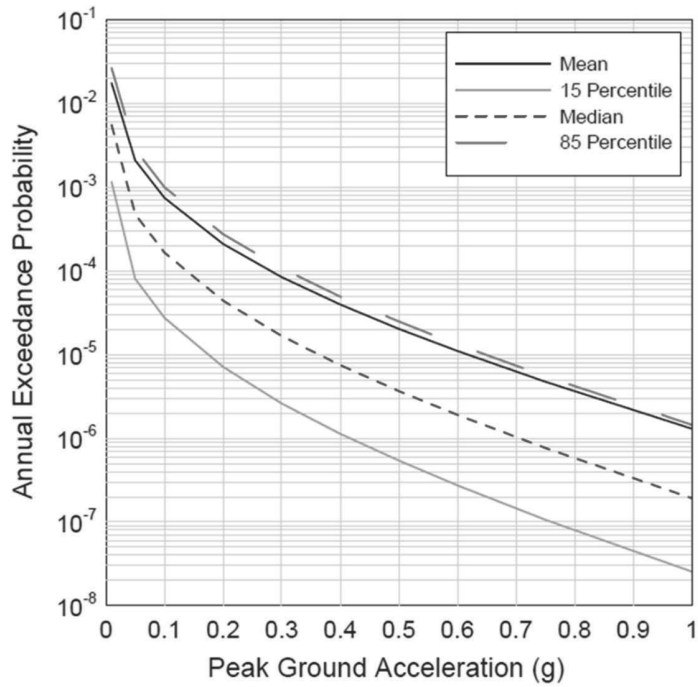

Figure 3-10. Annual exceedance probability for peak ground acceleration near the storage site (Rhee et al., 2012).

Further, $f_{d,i,j}$ is the frequency from domino effects including multi-hazard effects. This frequency considers the effects of an event by the first initiated event to the second one. For example, other fuel tanks can explode if an explosion event occurs and that exploded tank is positioned near the other one. For calculating the domino effect term, $f_{d,i,j}$, BN theory is used. Prior to calculation, relevant events must be analyzed by fault tree analysis (FTA) for organizing the proper BN structure (Figure 3-11). One of the reasons that a CO_2 leak occurs is a pressure increase through temperature increase owing to vaporization. This case can be triggered by fire effects from accidental events of a fuel tank. This event is an additional cause of CO_2 leak by domino effects. Similarly, a fuel tank can be affected from accidental events of other tanks, such as fire or explosion. Such an event is an additional cause of fuel tank leakage by domino effects. Therefore, domino effects should be considered if multiple tanks are used. Moreover, multi-hazard effects such as CO_2 tank leaks and fuel tank leaks, which are simultaneous hazards through seismic effects, are included in BN (Figure 3-12). In Figure 3-12, the parent nodes, which indicate possible causes, include seismic effects and events of fuel tank (a), which is one of two fuel tanks. Outcomes from the events of fuel tank (a) include CO_2 pipe events, CO_2 tank events, and fuel tank (b) events based on the FTA in Figure 3-10. Probabilities of events by seismic effects are specified by reference data, and those by fuel tank (a) events are determined on the basis of risk assessment results. In this analysis, the probabilities of propagation are specified in Table 3-8. For organizing BN, the following assumptions are specified as well:

- The causes contain seismic effects and event from failure of fuel tank (a).

- The consequences from seismic effects are failures of the CO_2 pipeline, CO_2 tank, and tank (a).

- The consequences from failure of fuel tank (a) are failures of the CO_2 pipeline, CO_2 tank, and tank (b).

- Failure of the CO_2 pipeline tank cannot affect any fuel tanks owing to limitations of the incident.

- Fuel tank (a) can be changed to fuel tank (b).

GeNIe Academic is used by organizing and calculating BNs. Additional information about GeNIe Academic has been reported elsewhere (BayesFusion, LLC, 2015)

Table 3-8. Probabilities of propagation.

Accident Scenario	Propagation Unit		
	CO_2 Storage Tank	CO_2 pipeline	Fuel Storage Tank
Jet fire	0.9	0.9	0.9
Pool fire	0.9	0.9	0.3
Flash fire	0.5	0.5	0.1

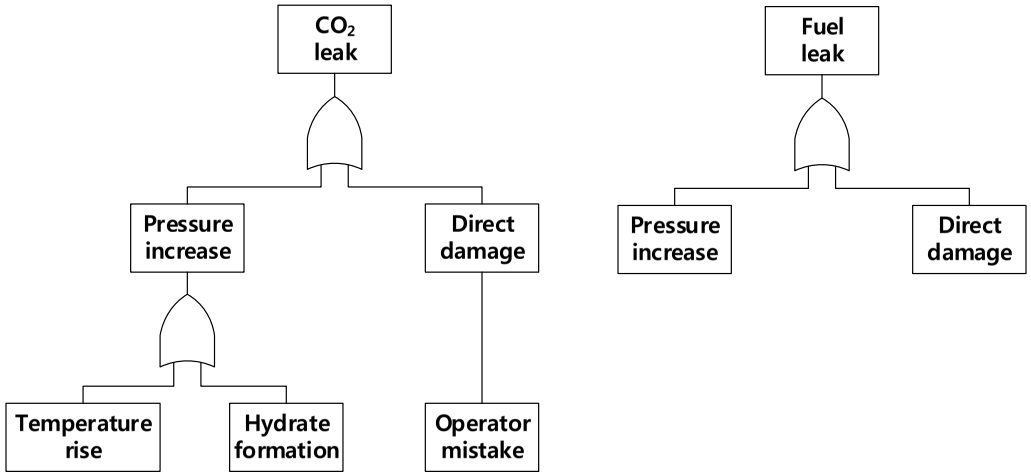

Figure 3-11. Fault tree analysis for CO_2 leak and diesel leak events.

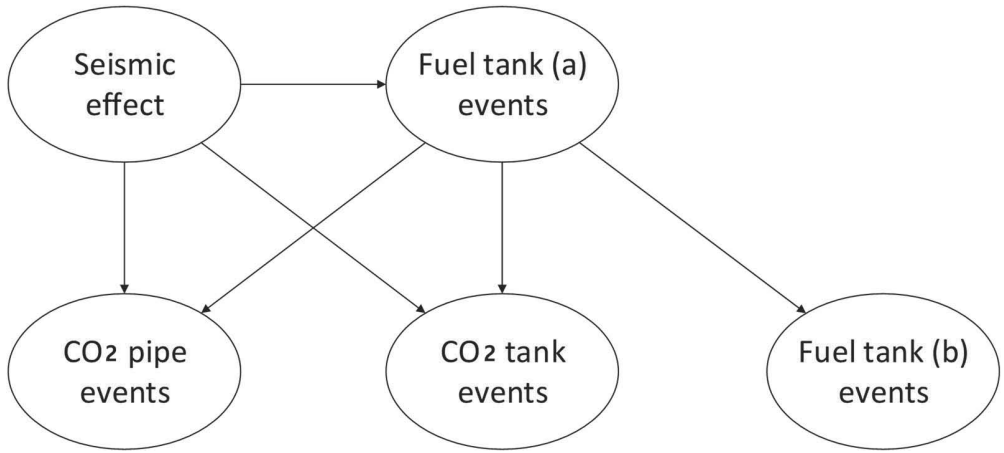

Figure 3-12. Bayesian network for domino effect.

A jet fire occurring from fuel tank (a) can affect other units such as the CO_2 storage tank, CO_2 pipeline, and fuel storage tank. A jet fire generates enough radiation intensity to cause other units to leak; therefore, the probability of propagation caused by a jet fire is 0.9, which is a conservative value. Although the pool fire has a lower radiation intensity than the jet fire, the intensity is sufficient for causing failure in a CO_2 storage tank and CO_2 pipeline owing to susceptible states such as low temperature below zero and high pressure. However, the fuel storage tank is not susceptible; thus, the probability of propagation caused by jet fire is 0.3 according to the ratio of the radiation intensity of jet fire and pool fire. Moreover, because the flash fire is weaker than the pool fire (CCPS, 2010), the probabilities of propagation by the former are specified as lower values than those for the latter.

The results of additional frequency rate related to seismic effects are shown in Table 3-9. The $f_{s,i,j}$ values, which represent the seismic effects on the leak frequency itself, were 3.174×10^{-6}/year for $f_{s,tank,CO2}$, 2.75×10^{-10}/year for $f_{s,pipe,CO2}$, and 9.906×10^{-6}/year for $f_{s,tank,fuel}$. These values were calculated on the basis of PGA and AEP using reference data. The $f_{d,i,j}$ values, which were calculated by BN, were 8.603×10^{-6}/year, 1.317×10^{-5}/year, and 9.905×10^{-7}/year for $f_{d,tank,CO2}$, $f_{d,pipe,CO2}$, and $f_{d,tank,fuel}$, respectively. A comparison of f_s and f_d revealed that the values of f_d are similar to those of f_s. This result means that the domino effects are important for the additional frequency rate.

Table 3-9. Additional frequency rates of seismic effects (f_s) and domino effects (f_d).

Seismic effect (f_s)			Domino effect (f_d)		
$f_{s,tank,CO2}$	$f_{s,pipe,CO2}$	$f_{s,tank,fuel}$	$f_{d,tank,CO2}$	$f_{d,pipe,CO2}$	$f_{d,tank,fuel}$
3.174×10^{-6}	2.75×10^{-10}	9.906×10^{-6}	8.603×10^{-6}	1.317×10^{-5}	9.905×10^{-7}

Finally, the modified frequency rates were applied to conventional QRA. Through this measure, the results of the modified QRA can be obtained, including seismic and domino effects. Figure 3-13 shows an F–N curve as the result of modified QRA (black line in the figure). Compared with the conventional QRA results, updated risk is increased through seismic effects; this result is also represented in Table 3-10. The risk integral of conventional QRA was $9.303 \times 10^{-4}/\text{year}$, and that for modified QRA was $9.667 \times 10^{-4}/\text{year}$. The risk increased about 3.9% by considering seismic effects including domino and multi-hazard effects. This value increase can cause general risk to go beyond the upper bounds of risk if the general risk is near the boundary. Moreover, stronger earthquakes are possible, the risk will increase even more. Therefore, this result shows the importance of considering seismic effects, including domino and multi-hazard effects, in QRA. After the modified QRA is completed, risk reduction should be applied to the process for mitigating the risk owing to unfavorable risk levels.

Figure 3-13. Updated expected frequency/number of casualties (F–N) curve. Seismic effects and domino effects are shown by the black line, and risk reduction strategy is represented by the green line.

Table 3-10. Societal risk integral (general, modified quantitative risk analysis, risk reduction).

Method	Risk integral (/AvgYear)
General QRA	9.303×10^{-4}
Modified QRA	9.667×10^{-4}
Risk reduction (Application of fire wall)	4.380×10^{-4}

3.4.6. Sensitivity analysis

Prior to risk reduction, sensitivity analysis was performed to show the further risk increase according to the annual exceedance probability (AEP) value. The AEP value was chosen as a parameter of this analysis because it is changeable with case. That is, the sensitivity analysis depends on the AEP value because it is a probabilistic value rather than a specific value, as shown in Figure 3-10. In this study, the median value (1.1×10^{-5}) was used as the AEP value for the purpose of representative case study.

For sensitivity analysis, AEP values are specified from the values of 15th percentile to 85th percentile. By using the different AEP values, additional frequencies from seismic effects are calculated, as is the modified risk. The results of sensitivity analysis are shown in Figure 3-14. The overall risk increased from 1% (15th percentile) to 35% (85th percentile) depending on the AEP value. In the case of the CO_2 injection system, the AEP value can be specified as more than the median because the earthquake occurrence is currently increasing at the injection site area. Similar to the sensitivity analysis results, if the AEP can be chosen as more than the median value, the modified risk can be increased to 35% higher than conventional risk. This significant risk increase shows the importance of considering seismic effects in QRA near the CO_2 injection area. In short, the modified QRA approach considering seismic effects with the domino effect is a proper approach for assessing risk, particularly in earthquake hazard areas

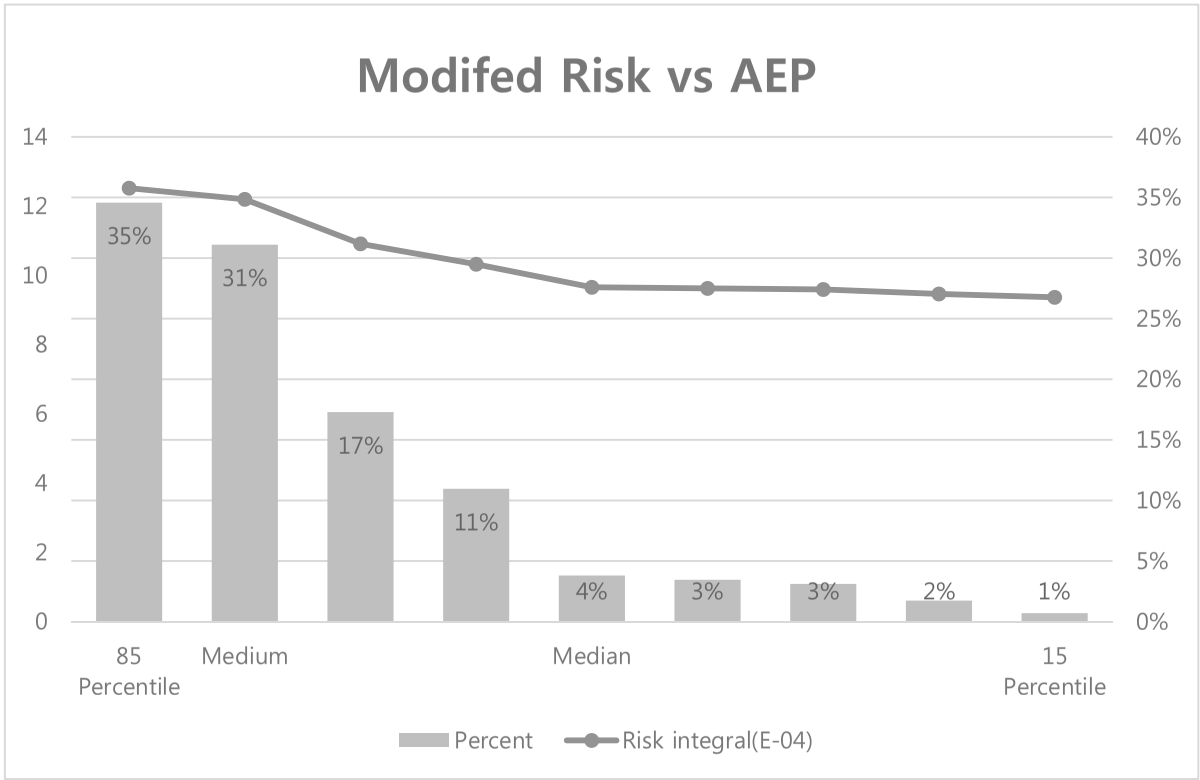

Figure 3-14. Sensitivity analysis: modified risk versus annual exceedance probability.

3.5. Risk reduction

For risk reduction, the composition of the total risk must be checked because total risk is composed of separate risks arising from each scenario. Similar to conventional QRA, CRDRP accounts for almost all risks in this process. The risk proportions of the main outcomes in the modified QRA are similar to those in conventional QRA because only the frequency rate is revised in the modified QRA. Thus, the risk reduction method must be proposed by targeting mitigation of CRDRP.

The two methods used for risk reduction include the consequence reduction approach and the frequency reduction approach, which are same as in risk assessment composition. The former approach is a method of reducing the effect of a specific event, and the latter approach is a way of reducing the probability related to the event. There are various methods in risk reduction on consequence effects (first approach). One of which is a fire protection wall for decreasing pool fire effect to the entire topside system, which can be installed near a fuel storage tank. Fire protection walls play a role in isolating fuel sources and ignition sources and for reducing fire effect despite the outbreak of fire outcome. Fire walls can be composed of several types of material such as concrete, and they can be installed at various thicknesses according to process design condition. In case of risk reduction on frequency rate (second approach), various methods are used to control the probability of events. If the probabilities are decreased, the total risk is reduced at the same time as a result of frequency reduction when the effects are constant. To lower the probability of specific

events, methods that can prevent conditions from causing accidental outcomes at each node in ETA should be applied.

In this study, fire protection walls were used, which is a first approach method. The first approach was chosen on the basis of the risk assessment results. In case of this QRA, the impact of the consequence effect was more dominant than that of the frequency rate in total risk. Therefore, application of the first approach method is more effective for mitigation of risk. The fire protection walls were assumed to be composed of concrete with slightly higher height than that of the tanks to prevent such effects. However, the thicknesses could not be specified owing to the lack of simulators.

The results of QRA after application of risk reduction methodologies are represented in Figure 3-12. The green line represents the F–N curve, which contains risk reduction effects by application of fire protection walls. After the fire protection walls were applied to the facility system, the F–N line of this process was moved to the ALARP region, indicating reasonable risk (Figure 3-12). A comparison with societal risks is included in Table 3-10. The societal risk integral of QRA with the risk reduction method was $4.380 \times 10^{-4}/\text{year}$, which is about 54.6% lower than the modified QRA result. The main reduction is attributed to CRDRP, which is one of the pool fire events. Pool fire is caused from pooling, which is an area of spilled liquid from leaking storage equipment. If a fire wall is installed around the storage equipment, the pool area created by spilled liquid is restricted by the wall. Therefore, the pool area becomes

narrower than that without the wall. This indicates that the range of influence is reduced because the pool area is smaller. Moreover, the pool fire effect is decreased in the surrounding area owing to the fire wall itself. Therefore, the overall risk is decreased to an acceptable level by using the risk reduction approach.

3.6. Chapter conclusion

In this chapter, QRA is implemented on a topside CO_2 injection system for underground storage. First, conventional QRA methods including frequency and consequence analyses is applied. Next, a modified QRA method is suggested and applied for considering seismic effects with multi-hazard and domino effects. The modified method includes additional frequency caused by earthquakes and domino effects from initiating events. Domino and multi-hazard effects are considered by a BN, which reveals a causal relationship. Moreover, risk reduction methods are applied to the CO_2 injection system to mitigate the process risk based on risk element analysis to target the main contribution risk. After the method is applied, the process risk is mitigated and meet the standard criteria set by ALARP.

As a result, the societal risk integral is $9.303 \times 10^{-4}/\text{year}$ when applying the conventional QRA. After applying the modified QRA methods containing seismic effects with multi-hazard and domino effects, the societal risk integral increases to $9.667 \times 10^{-4}/\text{year}$ by additional effects, which indicates a 3.9% increase from conventional. Moreover, the risk of the system increases by 35% according to annual exceedance probability (AEP). Therefore, additional effects including seismic effects are meaningful and should be considered, and it is necessary to calculate the risk assessment near areas prone to earthquakes. The total risk is higher than the standard criteria, according to the F–N curve result. Thus, the risk reduction method, which is an aspect of the consequence effect among two methodologies, is suggested on the basis of risk factors of this

process. Through risk reduction measures, the societal risk integral decreases to $4.380 \times 10^{-4}/\text{year}$ that meet the ALARP criteria in the F–N curve.

CHAPTER 4.
Operation stage: Risk-based management with Risk-Based Patrol (RBP) for Natural Gas (NG) Pipeline

4.1. Introduction

4.1.1. Risk-based management on operation stage

Maintenance is a main issue on operation stage for management of a process. Among ways of maintenance, inspection is one of the important and effective methods to manage the process during operation. Although inspection is important, it's impossible to inspect whole process every day in aspect of cost. So, the systematic method is necessary for inspection with considering the safety and the cost. With this background, risk-based inspection (RBI) has been studied and organized as guideline (American Petroleum Institute, 2016; Det Norske Veritas, 2010)

Risk-based inspection (RBI) is a methodology that involves quantitative assessment with the probability of failure (PoF) and the consequence of failure (CoF) related with each equipment item in a particular process unit. RBI technique categorizes equipment items by their risks, prioritizes inspection plan, and provides guidance for risk mitigation efforts, such as changes in materials, changes in operating conditions, the addition of linings, etc. RBI method includes several contents: identification and assessment of risk for all

equipment, suggestion for effective risk management, reduction of risks associated with operating processing facilities.

RBI methodology has been applied and studied in various research. Noori and Price (2006) and Gross et al (2012) studied the application of RBI to specific process units, boiler tube and spring-operated relief valves respectively. Vinod et al (2014) studied the RBI for H_2S based process plant with devising the approach for handling the influence factor related to the quantity of H_2S release. Tan et al (2011) Seo et al (2015) proposed a risk-based inspection method for subsea pipelines with time-variant corrosion model. Kamsu-Foguem (2016) proposed a RBI methodology with organized analysis using knowledge sharing for the marine oil pipeline. Mancuso et al (2016) proposed a RBI method for optimizing the inspections of underground infrastructure networks with incomplete information. This methodology uses multi-attribute value theory and portfolio decision analysis to assess the risk and decide the optimal inspection. Likewise, the RBI methodology has been utilized and studied in various processes from a unit to chemical plant for inspection.

Although the inspection has been studied with risk-based methodology, the patrol, which is also one of the mainly used maintenance ways like inspection, has been not studied in previous research. The goal of patrol is the observation of surface conditions on and adjacent to the transmission line right-of-way for indications of leaks, construction activity, and other factors affecting safety and operation. Among them, the main objective of the patrol manages the

unexpected excavation near pipeline. While the inspection controls the risk through precise safety diagnosis, patrols play a role in preventing dangerous elements around the area that the pipeline is buried. In general, patrol is regulated with a law, for example, patrol should be performed once a year in the United States. However, patrol plan is not regulated with a law as well as not studied in previous study. Also, the decision of minimum patrol period has been not studied.

4.1.2. Application: Natural gas (NG) of pipeline in South Korea

4.1.2.1. Natural gas (NG) supply

The Korea Gas Corporation (KOGAS) is in charge of the introduction and wholesale division in the LNG industry, and supplies high-pressure natural gas to each urban gas company through pipelines. In the retail sector, urban gas companies supply medium and low-pressure natural gas to users by region. And the safety of whole LNG supply chain is managed by Korea Gas Safety Corporation (KGS). The LNG supply chain is represented in Figure 4-1.

In South Korea, domestic natural gas demand has grown a compound annual growth rate (CAGR) of 11.0% from 1.61 milion-tons in 1987 to 36.81milion tons in 2017. As the urban gas became popular in the 1990s, the demand of NG grew rapidly (Figure 4-2). It is a household fuel used by more than 18.6 million consumers nationwide by 2017, but also an industrial and power generation fuel, which is an important energy source for the national economy. In the case of urban gas, as of 2017, the total supply amount is 23,572 million m^3 and the demand number is 18,567,000. Compared with 1990, this figure is about 2200% higher based on supply. From 1990s to 2008, supply and demand had increased sharply, but by 2017, demand number has slightly increased while supply amount has been fluctuating. The overall NG supply amount also has been fluctuated after the supply peaked in 2013 with rapid growth rate.

The interpretation of graph represents that the growth of the NG industry is slowing down, and this situation has become a background for management of

existing facilities rather than construction of new ones. This aspect can also be confirmed through a supply plan. Table 4-1 is a summary of the supply plans of urban gas until the year 2021. Supply is planned to increase by 2021, but it can be seen that the supply in 2021 does not exceed the maximum supply in 2013. That is, the growth of the NG (urban gas) industry is stagnant, which makes increase of interest in existing facilities. Due to this background, interest in the safety management of NG facilities is also increasing.

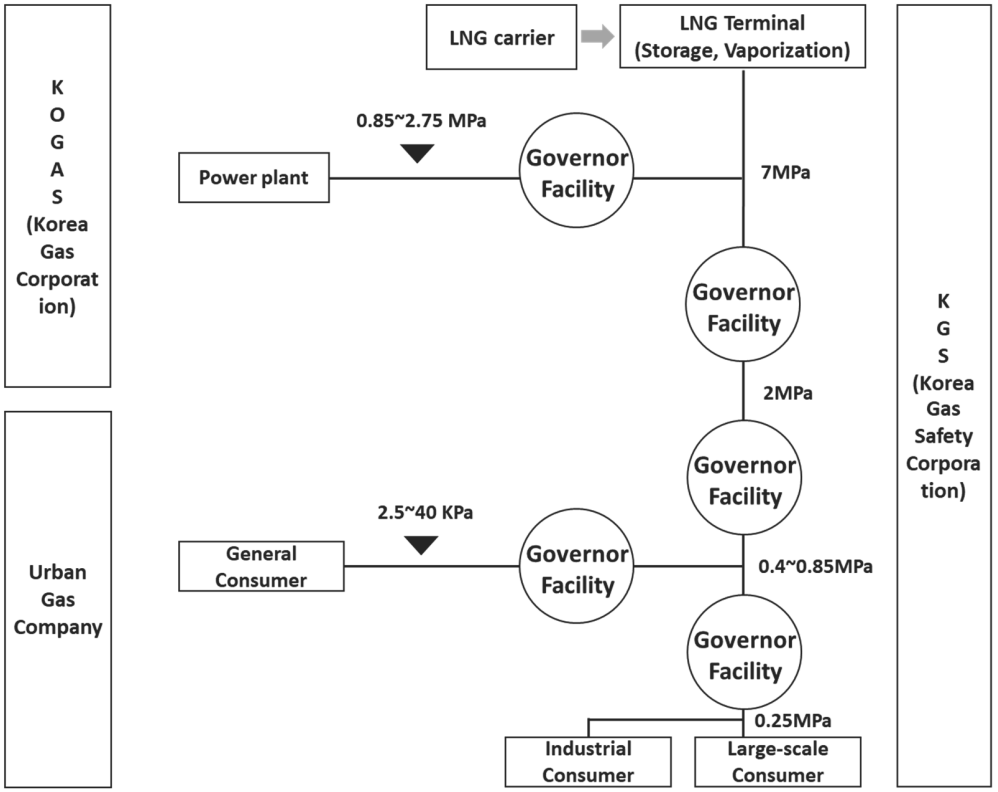

Figure 4-1. LNG supply chain (South Korea).

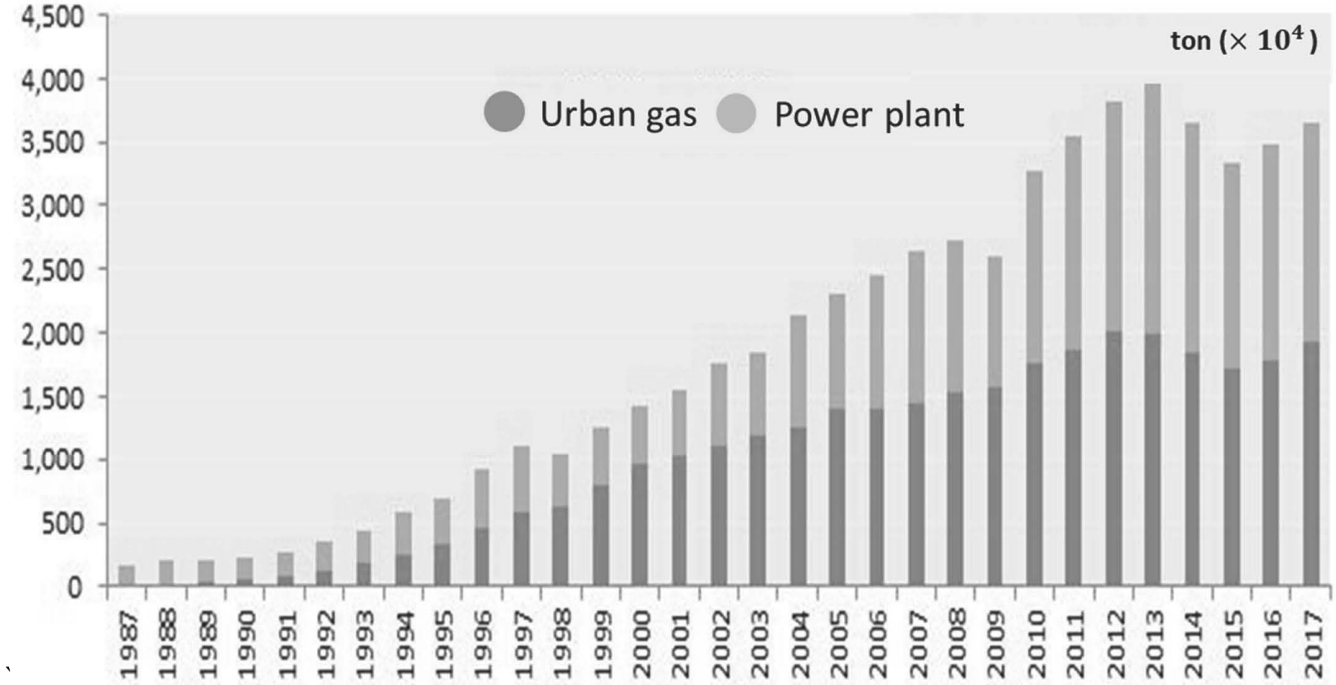

Figure 4-2. Supply amount of natural gas (NG) in South Korea (1987~2017)

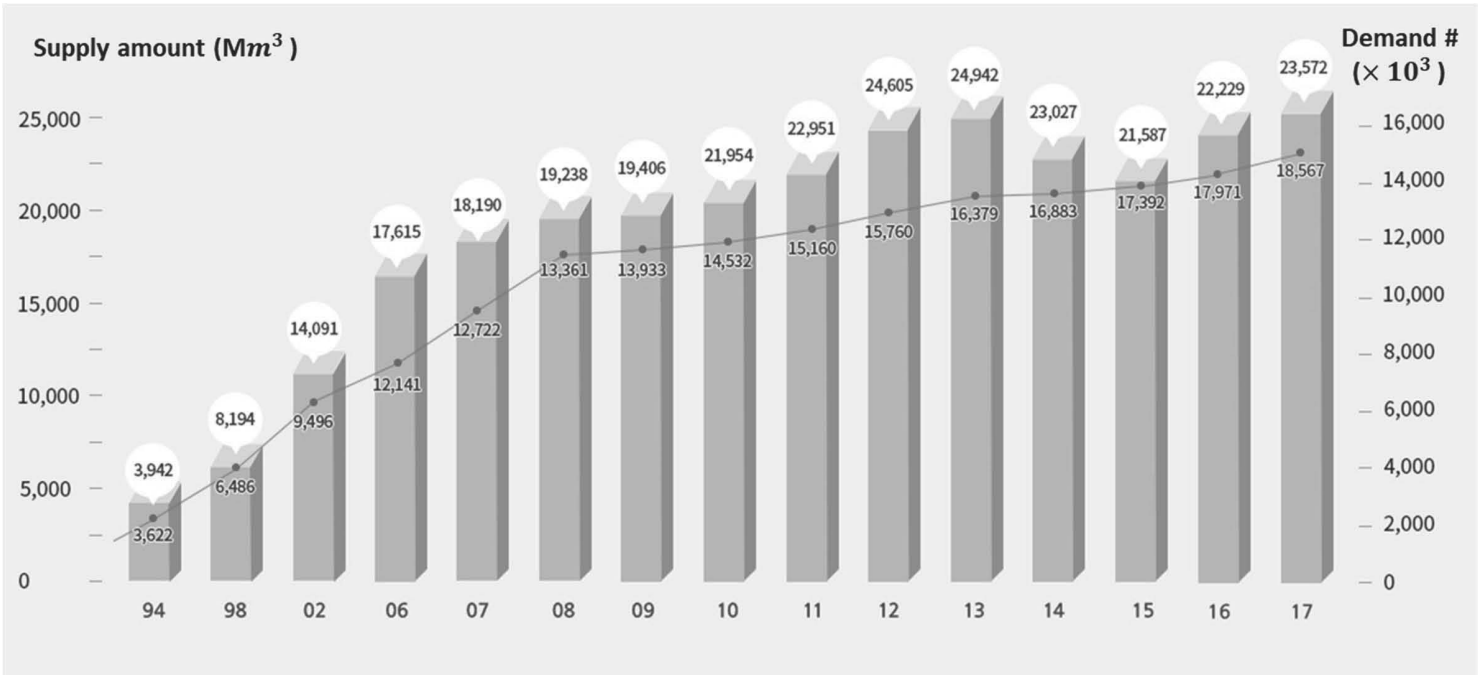

Figure 4-3. Urban gas - Supply amount (Mm^3) & Demand number ($\times 10^3$)

Table 4-1. Supply plan of urban gas (2018~2021).

Year	2018	2019	2020	2021
Supply Amount (Mm^3)	22,820	23,362	23,849	24,331
Demand Number ($\times 10^3$)	19,234	19,866	20,422	20,954

4.1.2.2. Safety management of natural gas pipeline (Lee et al., 2017)

As explained, safety management of (existing) natural gas (NG) pipeline is being an important issue in the industry. The safety management of NG pipeline in South Korea was enforced by legal regulation right after big disasters occurred. One was a disaster occurred in Ahyeon, Seoul that made 12 persons died, and 101 seriously injured in 1994. The other was happened in Daegu (1995) with 303 casualties (Dead: 101, Injury: 202). Both accidents were caused from leakage of pipeline with wrong safety management. Because these accidents made big fatality and financial loss, it was enough to be reason that government strictly regulated the safety management on NG pipeline.

However, the regulations make safety management inefficient these days. This is because, as described before, the network of pipelines has been increased and complex, but the regulation has still same basis that can't follow this circumstance. Moreover, the regulation is blocking the introduction of advanced technologies such as auto-inspection although the technology has been developed. One of the problems of the safety regulation is safety management via patrol in South Korea. Currently, the patrol on pipeline should be performed once in a day by the regulation. It's very stricter regulation than any other nations (once a year (US, Canada)), and inefficient because safety managers cannot focus on the safety management work with higher priority such as safety valve checking, excavation management. Further, this regulation has been maintained without any change during about 20 years. So, the

regulation and work of patrol should be updated. Thus, in this thesis, the risk-based patrol (RBP) is proposed for safety management of NG gas pipeline. The RBP methodology is proposed with two goals that minimum patrol period, which is specified as once a day without any backgrounds, is decided with risk level, and patrol plan is specified with depending on risk value according to pipeline.

4.2. Methodology

4.2.1. Risk-based patrol (RBP)

Risk-based patrol (RBP) is proposed to manage the pipeline with patrol based on the concept of risk. RBP is proposed as similar methodology with risk-based inspection (RBI) for pipeline maintenance in overall framework. Risk in RBP is calculated from probability of failure (PoF), and consequence of failure (CoF) as equation (4-1). It is similar with QRA methodology that risk is calculated from frequency and consequence results, but RBP has additional factor called as 'Risk Factor' in PoF. Risk factor is added to reflect the effect of some factors that make risk of pipeline higher. Further explanation is represented in following sections.

$$Risk = Probability\ of\ Failure\ (PoF) \times Consequence\ of\ Failure\ (CoF) \quad \textbf{(4-1)}$$

4.2.2. Probability of failure (PoF)

4.2.2.1. Generic failure frequency (GFF)

PoF is the frequency of the failure in pipeline. The PoF can be obtained from the product of risk factor and generic failure frequency (GFF) for specifically pipe. GFF for pipes (Dou et al., 2017) can be shown in Table 4-2. The GFF is specified by the diameter of pipe.

$$\begin{aligned} &Probability\ of\ Failure\ (PoF) \\ &= Risk\ factor\ (C_R) \\ &\times\ Generic\ Failure\ Frequency\ (GFF) \end{aligned} \quad \textbf{(4-2)}$$

4.2.2.2. Risk factor (C_R)

The risk factor is proposed to give weight to risk in risk-based patrol. So, these factors are associated with risks of NG pipeline that can be found in the midst of patrol. The factors that affect the risk are represented in Table 4-3. The factors, which are made with referring references (American Petroleum Institute, 2016; Det Norske Veritas, 2010), include excavation, population density, buried area, seismic area.

Table 4-2. Generic failure frequency (GFF) for pipe

Diameter	Rupture leak (/km year)
$D \leq 25\ \text{mm}$	1E-3
$25\ \text{mm} < D \leq 50\ \text{mm}$	1E-3
$50\ \text{mm} < D \leq 100\ \text{mm}$	3E-4
$100\ \text{mm} < D \leq 150\ \text{mm}$	1.5E-4
$150\ \text{mm} < D \leq 300\ \text{mm}$	1E-4
$D > 300\ \text{mm}$	5E-5

i. Excavation factor ($C_{R,e}$)

Excavation factor means how many excavation works are done near area of buried pipeline. If the ground is excavated and buried again, the state of ground can be changed, and the change can affect the buried NG pipeline. In addition, the completion of excavation work should be checked whether the work is finished well or not. Therefore, the number of excavation work should be considered as one of the risk factors that make the risk higher.

The standard of state of excavation factor is an average of excavation work number (E_a). If more excavation work is taken place than average number, then the pipeline near the area has more risk and high priority to manage the pipeline with patrolling. The index of excavation factor according to the state is organized in Table 4-4.

Table 4-3. Risk factor ($\boldsymbol{C_R}$)

Factor	Contents
Excavation ($C_{R,e}$)	Excavator work affects the ground and pipeline condition
Population density ($C_{R,p}$)	Effect from consequence of pipeline can be changed according to population density
Buried area ($C_{R,b}$)	Effect to ground of pipeline is different based on buried area
Seismic area ($C_{R,s}$)	The pipeline in seismic zones should be managed more carefully.

Table 4-4. Excavation factor ($C_{R,e}$)

Risk states			
1	$> E_a \times 2$	Very High	3
2	$> E_a$	High	1.5
3	$> E_a \times 0.5$	Medium	1
4	$E_a \times 0.5 <$	Low	0.8

ii. Population density factor ($C_{R,p}$)

Population density is the population number per area. The necessity and risk are increased when the population density is increased because it can be interpreted that more people are in dangerous area. For example, the pipeline with 100 persons/m^2 has higher risk and should be managed more frequently than one with 10 persons/m^2.

The state of population density is specified with average population density value (P_a). The index of the population density can be shown in Table 4-5. It has four index values based on the range of the population density.

Table 4-5. Population density ($\boldsymbol{C_{R,p}}$)

Risk states			
1	$> P_a \times 3$	Very High	2
2	$> P_a \times 2$	High	1.5
3	$> P_a$	Medium	1.2
4	$P_a <$	Low	0.9

iii. Buried area ($C_{R,b}$)

The risk of NG pipeline can be affected according to buried area. Based on buried area, the pipeline itself and the ground can be vulnerable to be damaged, destroyed. Also, some area should be paid more attention than other area.

The index of the buried area with states can be shown in Table 4-6. It has three index values based on the buried area. First, school area is selected due to its distinctiveness. The NG pipeline buried in school area should be managed with higher priority than other pipeline because the area is the main area of minors. Second, driveway and railway area are specified as another special area. The ground and pipeline near these areas get more impact from cars, train. So, the driveway, railway areas are classified as one of the special buried areas. The agricultural area is also risky buried area due to the characteristics. This area is easily collapsed due to its geological characteristics.

Table 4-6. Buried area ($C_{R,b}$)

Risk states		
1	School area	2
2	Driveway, railway area	1.8
3	Agricultural area	1.5

iv. Seismic area ($C_{R,S}$)

The seismic area is also one of the risk factors that affect the risk of the ground or pipeline buried in this area. If earthquake frequently occurs, then the possibility of collapse/destroy of the ground and pipeline can be increased.

The index of the seismic area with states is represented in Table 4-7. Risk states of seismic area are specified with the zone based on frequency of earthquake. Zone A means earthquakes has occurred 10 times with magnitude less than 5, or once with magnitude 5 or greater during a year. Zone B means earthquakes has occurred over 5 times with magnitude less than 5, and occurred less than 5 times in the case of zone C.

Table 4-7. Seismic area ($C_{R,S}$).

Risk states		
1	Seismic are - zone A	2
2	Seismic are - zone B	1.5
3	Seismic are - zone C	1.2

4.2.3. Consequence of failure (CoF)

The CoF can be obtained with several bases such as impacted area, economic loss, the number of casualties. In this study, impacted area is used as parameter for consequence of CoF from pipeline failure. Impacted area can be calculated with potential impact radius (PIR) model. PIR model is simple, because this model only requires operating pressure (p) and diameter (d) for calculation of impact radius (r) (Equation (4-3)). A and B are the parameters specified from material of fluid. In the case of natural gas, A is 0.1017, B is 0.5 m (Stephens et al., 2002).

$$r = A * [p \cdot d^2]^B \qquad \text{(m)} \qquad \textbf{(4-3)}$$

After calculation of impact radius, impact area (m^2) can be calculated to specify the CoF. Based on the impact area, consequence category is specified to classify the danger from the consequence of failure (Dou et al., 2017).

4.2.4. Risk matrix, patrol plan

After CoF and PoF are calculated, risk level can be specified with category of CoF and PoF. The both categories are divided into 5 classes. The category of PoF having category 1 to 5 can be classified with the value of PoF that the product of GFF and risk factor. The categories with the range can be shown in Table 4-8. Similarly, the CoF can be categorized like Table 4-9 which have category A to E. If the category of CoF and PoF are classified, the risk level is decided by using risk matrix (Figure 4-4). Depending on the risk level, minimum patrol period is decided to manage the pipeline with different manner. The higher risk level the pipeline has, then the shorter period should be applied to patrol for managing the pipeline.

Moreover, risk value is also calculated from CoF and PoF with data. In this thesis, patrol plan is proposed to be decided with total risk value including current risk and potential risk about the future. In the concept of risk, the risk does not change with time in general. On the other hands, in the RBP methodology, the concept of potential risk is proposed that the risk of the pipeline and circumstance is increased with time if the patrol is not performed in the area that pipeline is buried. Because potential risk is increased with time, the total risk is increased continuously as well if patrol is not performed. This concept of total risk with potential risk is represented in Figure 4-5. The risk target can be decided based on the safety regulation, safety manager or company, the circumstance of pipeline, etc. Exponential function is recommended as the function of the potential risk because the closer the risk

get to the target, the risk should be increased rapidly for considering penalty that the patrol is not performed. Additionally, the patrol plan is recommended that the patrol is performed before the total risk go beyond ALARP (As Low As Reasonably Practicable) used in QRA methodology, which is defined as the region between ¼ and ¾ of the risk target in this methodology. So, the patrol should be performed to resolve the increased risk potentially (lower the risk), before the total risk value reach the maximum risk of ALARP region.

Table 4-8. Probability category

Category	GFF (year)
1	$GFF \leq$ 1E-4
2	1E-4 $< GFF \leq$ 1E-3
3	1E-3 $< GFF \leq$ 1E-2
4	1E-2 $< GFF \leq$ 1E-1
5	1E-1 $< GFF \leq$ 1E-0

Table 4-9. Consequence category

Category	Impacted area (IA) (m^2)
A	$IA \leq 1$
B	$1 < IA \leq 10$
C	$10 < IA \leq 100$
D	$100 < IA \leq 1000$
E	$IA > 1000$

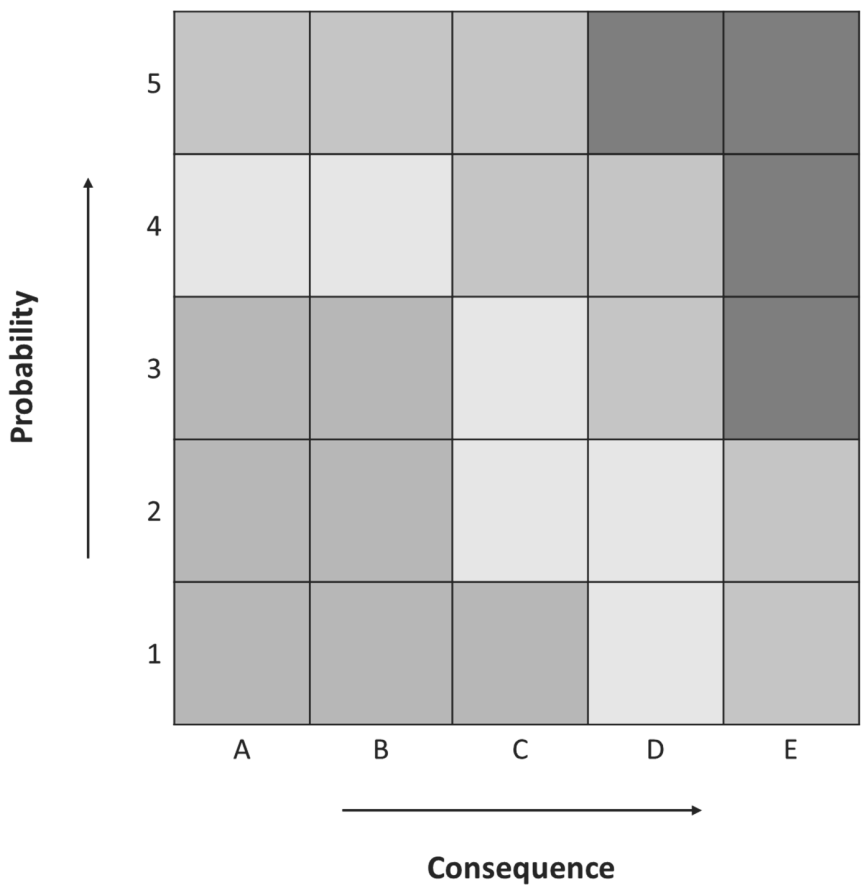

Figure 4-4. Risk matrix.

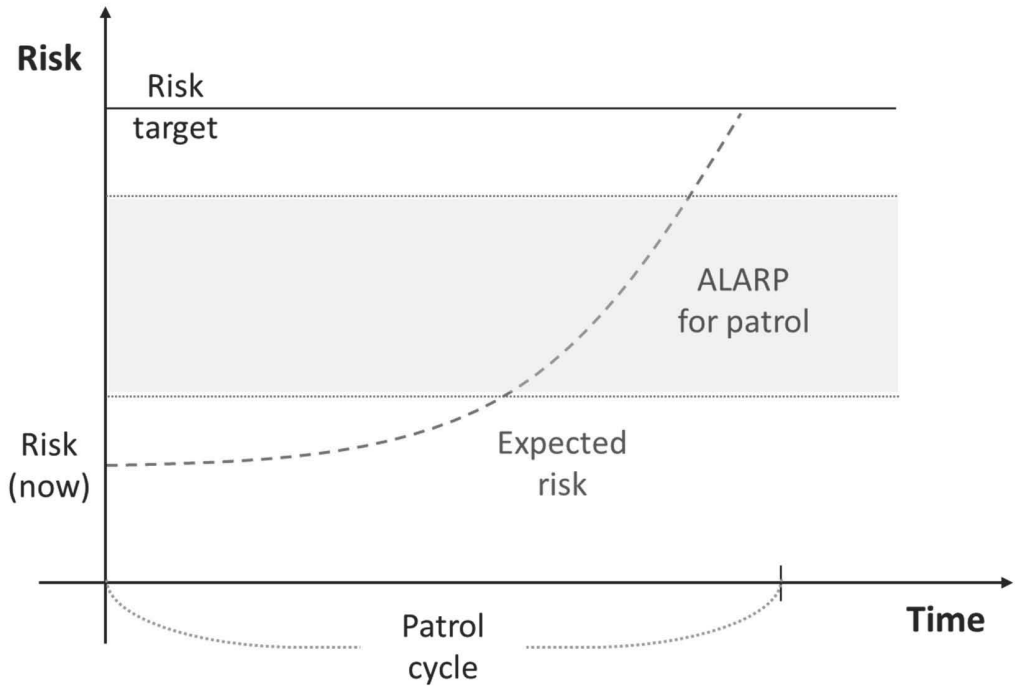

Figure 4-5. The graph of total risk with time including the potential risk for patrol plan.

4.3. The application of RBP methodology

4.3.1. NG pipeline in Ulsan

The proposed risk-based patrol methodology is applied to the pipeline of natural gas in part of Ulsan. The pipeline is divided into sections to be managed by safety inspectors. The information of the pipeline according to section number can be shown in Table 4-10. Total twenty sections are arranged with the information including section number, material, diameter, operating pressure. As explained previous section, the diameter and pressure are used to calculate the CoF, and the length and diameter are used to obtain the PoF value.

Table 4-10. Pipeline information in Ulsan.

	Length (km)	Material	Diameter (mm)	Operating pressure (kg/cm^3)	Population density ($person/m^2$)	Excavation work	Seismic zone	Buried area
Section 1	52.06	PE	63	0.32	0.01145	95	Zone C	School
Section 2	69.8	PLP	50	0.025	0.01709	18	Zone C	Drive
Section 3	75.2	PLP	150	5.1	0.01926	63	Zone C	Agricultural
Section 4	64.3	PE	110	0.5	0.00939	4	Zone C	
Section 5	74.25	PE	110	38.7	0.01672	6	Zone C	
Section 6	68.38	PLP	150	0.407	0.00320	44	Zone C	School
Section 7	71.93	PLP	300	38.7	0.00814	26	Zone C	
Section 8	64.9	PE	110	8.67	0.01409	24	Zone C	Drive
Section 9	70.5	PE	225	0.9	0.00653	34	Zone C	
Section 10	84.89	PLP	50	0.71	0.00301	28	Zone C	
Section 11	80.57	PE	225	0.02	0.01709	27	Zone C	Agricultural
Section 12	77.1	PE	63	8.67	0.00560	36	Zone C	
Section 13	74.6	PLP	300	0.82	0.00407	20	Zone C	
Section 14	65.44	PLP	500	7.64	0.01074	4	Zone C	
Section 15	61.96	PLP	50	0.9	0.00986	88	Zone C	
Section 16	74.29	PE	160	1	0.01540	21	Zone C	School
Section 17	66.63	PLP	100	2.54	0.03079	37	Zone C	School
Section 18	62.2	PE	110	0.7	0.01477	27	Zone C	
Section 19	61.82	PE	400	1	0.04220	18	Zone C	
Section 20	48.92	PLP	100	4.1	0.00889	63	Zone C	railway area

4.3.2. Risk calculation

4.3.2.1. Calculation of CoF and PoF

Impacted radius is calculated from equation (4-3) with diameter, operating pressure. From the radius, impacted area is calculated to decide CoF value. Based on the value, the CoF category is decided as well. The results can be shown in Table 4-11. As a result of calculation of CoF, Category A and B have one section respectively, and Category C has 6 sections. Also, 7 section and 4 section are positioned in Category D and E each.

Next, PoF is calculated form GFF with risk factors. The results of PoF are arranged in Table 4-12. GFF are decided from the diameter based on Table 4-2. And risk factors including population density, excavation work, seismic area, buried area are decided from the data of pipeline based on the range of each factor. In the case of population density, an average value of the overall Ulsan city (0.006448/m^2) is used as average value (P_a). Likewise, an average value of excavation work (8.83E-06) per m^2 in Ulsan city is used as the average value (E_a) in risk factor of excavation work. As a result, category 3 has two sections, and 14 sections, 4 sections are classified as category 4 and 5, respectively.

Table 4-11. The results of CoF

	Impact radius [m]	Impact area [m^2]	CoF category
Section 1	3.626	10.32	C
Section 2	0.804	0.51	A
Section 3	34.467	932.58	D
Section 4	7.914	49.17	C
Section 5	69.627	3805.65	E
Section 6	9.737	74.42	C
Section 7	189.893	28306.46	E
Section 8	32.956	852.58	D
Section 9	21.719	370.29	D
Section 10	4.287	14.43	C
Section 11	3.238	8.23	B
Section 12	18.875	279.66	D
Section 13	27.641	599.78	D
Section 14	140.620	15522.63	E
Section 15	4.826	18.29	C
Section 16	16.280	208.05	D
Section 17	16.216	206.43	D
Section 18	9.364	68.84	C
Section 19	40.700	1300.33	E
Section 20	20.603	333.21	D

Table 4-12. The results of PoF

	GFF	Population density	Excavation work	Seismic zone	Buried area	PoF	PoF category
Section 1	0.0003	1.2	3	1.2	2	0.13494	5
Section 2	0.001	1.5	2	1.2	1.8	0.45230	5
Section 3	0.00015	1.5	3	1.2	1.5	0.09137	4
Section 4	0.00015	1.2	1	1.2	1	0.01389	4
Section 5	0.00015	1.5	1	1.2	1	0.02005	4
Section 6	0.00015	0.9	1	1.2	2	0.02216	4
Section 7	0.0001	1.2	2	1.2	1	0.02072	4
Section 8	0.00015	1.5	2	1.2	1.8	0.06308	4
Section 9	0.0001	1.2	1	1.2	1	0.01015	4
Section 10	0.001	0.9	0.8	1.2	1	0.07334	4
Section 11	0.0001	1.5	3	1.2	1.5	0.06526	4
Section 12	0.0003	0.9	2	1.2	1	0.04996	4
Section 13	0.0001	0.9	1	1.2	1	0.00806	3
Section 14	0.00005	1.2	0.8	1.2	1	0.00377	3
Section 15	0.001	1.2	3	1.2	1	0.26767	5
Section 16	0.0001	1.5	3	1.2	2	0.08023	4
Section 17	0.0003	2	3	1.2	2	0.28784	5
Section 18	0.00015	1.5	3	1.2	1	0.05038	4
Section 19	0.00005	2	2	1.2	1	0.01484	4
Section 20	0.0003	1.2	2	1.2	1.8	0.07608	4

Table 4-13. Risk result

	PoF	CoF	Risk
Section 1	0.13494	1.182E-03	1.595E-04
Section 2	0.45230	8.683E-05	3.927E-05
Section 3	0.09137	1.797E-01	1.641E-02
Section 4	0.01389	4.617E-03	6.412E-05
Section 5	0.02005	6.363E-01	1.276E-02
Section 6	0.02216	2.380E-03	5.273E-05
Section 7	0.02072	2.305E+00	4.775E-02
Section 8	0.06308	1.202E-01	7.581E-03
Section 9	0.01015	2.418E-02	2.455E-04
Section 10	0.07334	4.336E-04	3.180E-05
Section 11	0.06526	1.406E-03	9.177E-05
Section 12	0.04996	1.567E-02	7.829E-04
Section 13	0.00806	2.439E-02	1.965E-04
Section 14	0.00377	1.667E+00	6.285E-03
Section 15	0.26767	1.803E-03	4.827E-04
Section 16	0.08023	3.204E-02	2.571E-03
Section 17	0.28784	6.356E-02	1.829E-02
Section 18	0.05038	1.017E-02	5.123E-04
Section 19	0.01484	5.488E-01	8.142E-03
Section 20	0.07608	2.963E-02	2.254E-03

4.3.2.2. Risk matrix

As a result of CoF, PoF calculation, the categories of probability and consequence are classified. Risk matrix are decided with the classification. The results of risk matrix are represented in Figure 4-6 and Table 4-14. The majority of pipeline sections have medium-high risk (70%), and others have high risk (25%), also only one section has medium risk (5%).

Minimum patrol period is specified depending on risk level. When the risk is the smallest, the patrol is conducted once a year (low risk). On the other hand, the patrol is performed once a month when it is the largest (high risk). The period is decided from the reference (Lee et al., 2017) that the maximum period (once a month) is specified based on the result of the study that the patrol duration can be lowered by 99% from the current level (once a day), and the minimum period is decided from the overseas regulations (once a year). As a result, the patrol of NG pipeline can be performed with different cycle based on each risk level.

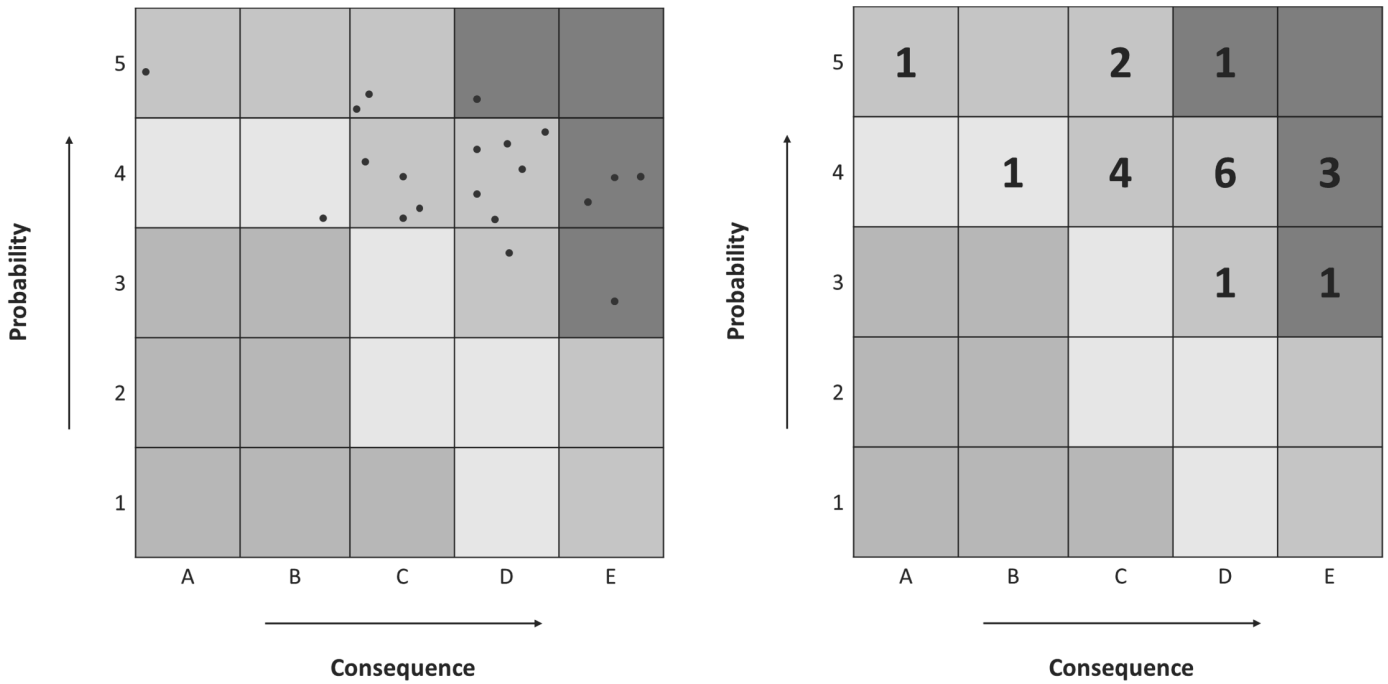

Figure 4-6. Results of risk matrix.

Table 4-14. Risk category with patrol duration.

Risk	Total number	Proportion	Patrol duration
High	5	25%	Once a month
Medium-high	14	70%	Once a quarter
Medium	1	5%	Once in six months
Low	0	0%	Once a year

4.3.2.3. Patrol plan

Patrol plan can be decided with the risk value (Table 4-13), and ALARP region. In this thesis, two sections in medium-high risk level are used to perform the case study of patrol plan. Section 8 and 12 are selected to be compared, because the sections have different risk value in same risk level.

In the case study, exponential function with constant 0.02 (risk value $\times$ $e^{0.02t}$) is used as function of potential risk. Also, risk target value is set as 2.0E-2. As explained, the factor can be changed according to safety inspector, regulation of company, circumstance near pipeline, etc. The result of patrol plan is represented in Figure 4-7. Although minimum patrol period of both sections is once a six-month, the risk of both section considering potential risk increases by risk target value before the six months (180 days). The risk of section 8 is reached to the maximum value of ALARP region on the 41th day, while section 12 reaches the value on the 148th day. Therefore, the pipeline in section 8 should be patrolled within 41 days, and within 148 days in the case of section 12. On the other hand, although both sections have same minimum period, the risk value of section 8 is higher than the one in section 12. So, the pipeline of section 8 should be managed with patrol more frequently within the period.

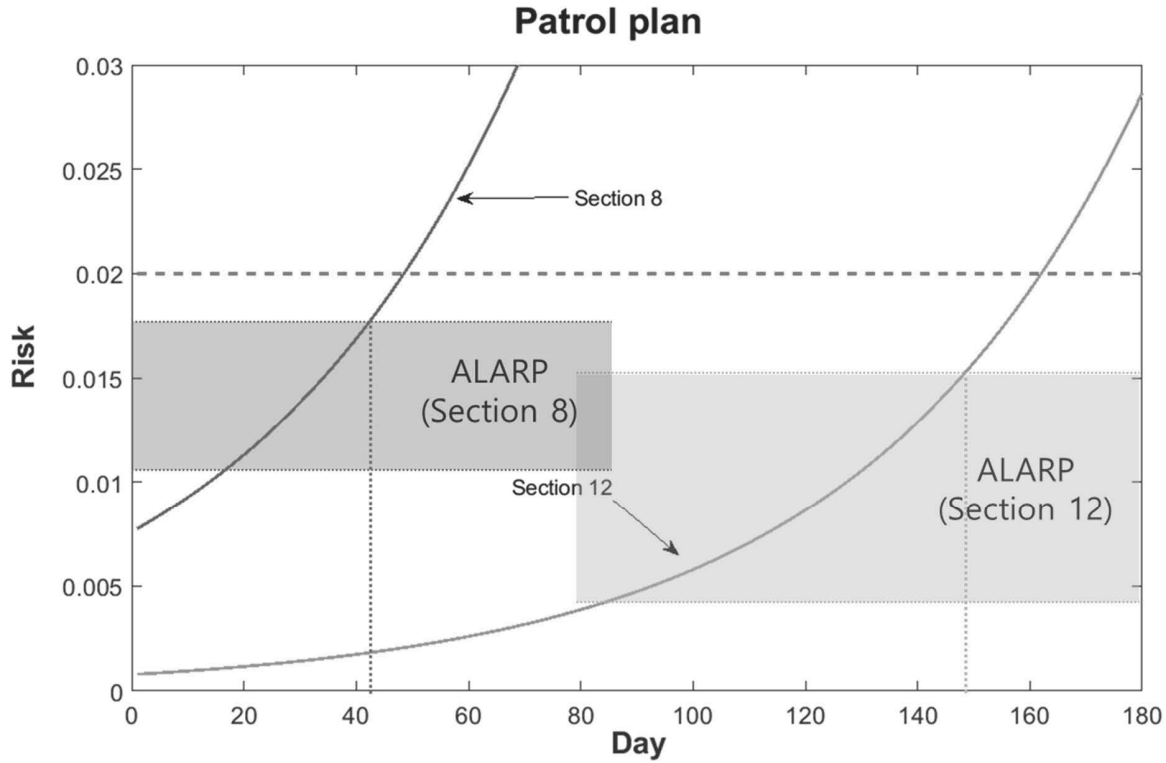

Figure 4-7. The result of Patrol plan.

4.4. Chapter conclusion

In this chapter, the methodology of risk-based patrol (RBP) is proposed to manage the NG pipeline for maintenance. The RBP methodology is reconstituted with using risk-based inspection (RBI) methodology for pipeline. The RBP methodology are based on the concept of risk that is the product of probability of failure (PoF) and consequence of failure (CoF). The CoF is calculated from the potential impact radius (PIR) model with simplicity. The PoF are obtained from the product of generic failure frequency (GFF) and risk factor. Risk factor is the factor that affect the risk of pipeline. Excavation factor, population density factor, seismic area factor, buried area factor are defined to modify the PoF to considering the factors. The risk matrix and risk value are decided with the results of PoF and CoF category. Furthermore, total risk is calculated with current risk value and potential risk.

The methodology is applied to NG pipeline in Ulsan as case study. As a result, most sections of pipeline have medium-high risk level (70%) in risk matrix with once a six-month as patrol period. Moreover, the risk values are calculated from PoF and CoF as well, and patrol plan are decided with exponential function as potential risk based on the risk values. Two sections of pipeline are studied on the patrol plan with different risk values in same risk level to confirm the difference between them.

CHAPTER 5. Concluding Remarks

5.1. Conclusion

In this thesis, risk-based design and management of chemical processes are studied according to stage of process life cycle. The risk-based methodologies are proposed and applied in conceptual design stage, basic design stage, maintenance stage to manage the safety considering process life cycle with process characteristics. Risk-based design is proposed and applied in the stage of conceptual design. Risk-based management with improved risk assessment considering further characteristic is proposed and applied in basic design stage. Also, risk-based patrol is proposed and applied to manage the safety of natural gas pipeline in operation stage.

First, in conceptual design stage, the risk-based design methodology is proposed to consider safety/risk by using inherently safe design (ISD) methodology with quantitative risk assessment (QRA). The methodology is applied to organic Rankine cycle (ORC) design for utilizing liquefied natural gas (LNG) cold energy to consider the safety of ORC in conceptual design. Design parameters of the ORC are organized from the previous studies to decide main parameter to study in this thesis. Working fluid is selected as main parameter in the ORC design. Six working fluids including pure component, binary components, ternary components are used as candidate to find optimal working fluid and condition. Two aspects are considered that one is thermodynamic aspect mainly used in previous studies, and another is safety aspect. For considering both aspects simultaneously, multi-objectives

optimization (MOO) methodology is used to obtain optimal solutions. As a result, the optimal solutions using MOO with parameters for each aspect including exergy efficiency and risk distance are obtained according to each working fluid. With the result, safety and efficiency can be compared with quantitative value for ORC design. For example, the risk distance of ORC with C2 is about 25% lower than one with C3 when the exergy efficiency is same. Moreover, among the six working fluids, R14-C_3H_8 is decided as the optimal working fluid based on the results that the Pareto optimal solutions of R14-C_3H_8 is safer and more efficient than other working fluids based on the results that the solutions, which have the ranges of exergy efficiency and risk distance of ORC with R14-C_3H_8 are 16.47–22.52 % and 19–63 m, are the closest with an ideal solution. Likewise, the ORC process with considering the risk value as well as thermodynamic efficiency can be designed and selected based on the risk-based design methodology in the stage of conceptual design.

Secondly, in basic design stage, the risk-based management with improved risk assessment considering seismic effect are proposed to treat the risk of earthquake that some processes are susceptible. The general QRA are improved by adding the frequency of initiating event from seismic effect with additional effects including domino-effect, multi-hazard effect by using Bayesian network (BN). The improved QRA methodology is applied to CO_2 injection system for geological storage on topside platform to be constructed in Pohang basin where the earthquake can occur consistently. The frequency analysis is performed with the information and data organized from references, also the consequence

analysis is performed to quantify the effect of events such as jet fire, pool fire and so on. After that, the additional frequency is analyzed and calculated to consider the effect of seismicity with using BN. The maximum value of additional frequency from seismic effect is 9.906×10^{-6} /Year, while 1.317×10^{-5}/Year in the case of domino effect. As a result, the risk of CO2 injection system is assessed by both methodologies (general, improved) to be compared to study additional risk from the seismic effect. Risk integral of improved QRA is 9.667×10^{-4}/Year while the value of general QRA is 9.303×10^{-4}/Year, which the value is increased by about 4%. With further study of sensitivity analysis, by the seismic effect, the risk integral of the system is increased by up to 35 % with 85 percentile value of annual exceedance probability (AEP). The result can explain that the risk from seismic effect should be considered when the process risk is assessed quantitatively that have vulnerable characteristics to earthquake.

Lastly, in the stage of operation, the risk-based patrol methodology to manage the risk of pipeline are proposed to consider the risk systematically and quantitatively for safety management. The risk-based patrol (RBP) methodology has similar structure of risk-based inspection (RBI) methodology, which calculate the risk with the probability of failure (PoF) and consequence of failure (CoF), but RBP consider the weight factor called by 'risk factor' that can affect the risk of the ground the pipeline buried or the pipeline itself. The RBP is applied to NG pipeline in Ulsan in South Korea for case study. As a result, the risk level of the pipeline is decided with the result of CoF and PoF

to apply the different minimum patrol period according to risk level. Specifically, most sections of pipeline, which is total 14 sections, are decided as medium-high risk level that the patrol should be performed once a quarter as regulation of patrol period. Also, patrol for risk management is planed based on the total risk value with the potential risk, which is the concept of risk increased with time if the patrol is not performed potentially. For example, section 8 and 12 have same risk level (medium-high), but the patrol plans are decided differently with depending on total risk value including current risk value and potential risk. The current risk of section 8 is 7.581×10^{-3}/Year, while the section 12 is 7.824×10^{-4}/Year, and the potential risk is calculated with the exponential function (risk value $\times e^{0.02t}$). As a result, patrol plan is specified based on the ALARP region that the patrol should be performed within 41th day from now in the case of section 8, while the 148th day in the case of section 12. The results mean that the risk level specify the minimum patrol period, and the risk value decide the patrol plan. To sum up, the patrol can be managed and performed with the risk value by applying the RBP methodology in reasonable manner.

5.2. Future works

Composition of working fluid; The composition of working fluids can be specified as the decision variable of optimization problem for organic Rankine cycle (ORC) design. The compositions are specified from previous studies that analyze the exergy destruction in condenser for minimizing exergy loss in this thesis. When the exergy loss is minimized, the exergy efficiency can be maximized. This is the reason why the composition is used in this thesis. However, the risk distance is changed depending on the composition values, and the value of risk distance can be preferred even though the exergy efficiency cannot be maximized.

Risk factor; Risk factor is proposed to give the weight based on the condition of pipeline that affect the risk. Although the factors are chosen with considering the circumstance of risk management in natural gas pipeline, the index according to risk states is newly specified by author. Therefore, the risk factors and the index should be validated by the data of patrol results, the pipeline inspector, the confirmation of experts. With the steps, the risk-based patrol (RBP) methodology can be robust and reliable to be utilized in the natural gas industry.

Uncertainty; The RBP methodology can be improve with considering uncertainty. The uncertainty of RBP for risk-based pipeline management comes from the condition of ground and pipeline, also the circumstance of safety management according to subjective of management. Specifically, the

excavation factor has the uncertainty that the number of excavation works can be changed in this year unlike last year. Moreover, the function of potential risk can be improved with adding technique to consider the uncertainty.

References

American Institute of Chemical Engineers. Center for Chemical Process Safety., 2008. Guidelines for hazard evaluation procedures. CCPS.

American Institute of Chemical Engineers. Center for Chemical Process Safety., 2000. Guidelines for Chemical Process Quantitative Risk Analysis. CCPS.

American Petroleum Institute, 2016. API RP 581 Risk-Based Inspection Methodology.

An, J., 2017. Design and Optimization of Carbon Dioxide Capture and Storage Process for Low-carbon Power Generation. Seoul National University.

Antonioni, G., Spadoni, G., Cozzani, V., 2007. A methodology for the quantitative risk assessment of major accidents triggered by seismic events. Journal of Hazardous Materials 147, 48–59.

Aspen Technology. (2013). Aspen Physical Property System: Physical Property Methods

Bao, J., Lin, Y., Zhang, R., Zhang, X., Zhang, N., He, G., 2018. Performance enhancement of two-stage condensation combined cycle for LNG cold energy recovery using zeotropic mixtures. Energy 157, 588–598.

BayesFusion, LLC. URL https://www.bayesfusion.com.

Blackford, J., Bull, J., Cevatoglu, M., Connelly, D., 2015. Marine baseline and monitoring strategies for carbon dioxide capture and storage (CCS). International Journal of Greenhouse Gas Control.

Blackford, J., Stahl, H., Bull, J., Berges, B., 2014. Detection and impacts of leakage from sub-seafloor deep geological carbon dioxide storage. Nature Climate.

Caramia, M., Dell'Olmo, P., 2008. Multi-objective management in freight logistics : increasing capacity, service level and safety with optimization algorithms. Springer.

Choi, I., Lee, S., Seo, Y., Chang, D., 2013. Analysis and optimization of cascade Rankine cycle for liquefied natural gas cold energy recovery. Energy 61, 179–195.

Cunha, S.B. da, 2016. A review of quantitative risk assessment of onshore pipelines. Journal of Loss Prevention in the Process Industries.

Damen, K., Faaij, A., Turkenburg, W., 2006. Health, Safety and Environmental Risks of Underground Co2 Storage – Overview of Mechanisms and Current Knowledge. Climatic Change 74, 289–318.

Dan, S., Lee, C.J., Park, J., Shin, D., Yoon, E.S., 2014. Quantitative risk analysis of fire and explosion on the top-side LNG-liquefaction process of LNG-FPSO. Process Safety and Environmental Protection 92, 430–441.

Deb, K., Pratap, A., Agarwal, S., Meyarivan, T., 2002. A Fast and Elitist Multiobjective Genetic Algorithm: NSGA-II, IEEE Transactions on Evolutionary Computation.

Det Norske Veritas, 2010. DNV RP G101, Recommended Practice: Risk Based Inspection of Offshore Topside Static Mechanical Equipment.

Det Norske Veritas, 2010. DNV-RP-J202, Recommended Practice: Design and Operation of CO_2 Pipelines.

Di Domenico, J., Vaz Jr., C.A., de Souza Jr., M.B., 2014. Quantitative risk assessment integrated with process simulator for a new technology of methanol production plant using recycled CO2. Journal of Hazardous Materials 274, 164–172.

Dodds, K., Waston, M., Wright, I., 2011. Evaluation of risk assessment methodologies using the In Salah CO2 storage project as a case history. Energy Procedia 4, 4162–4169.

Dou, Z., Jiang, J.-C., Wang, Z.-R., Pan, X.-H., Shu, C.-M., Liu, L.-F., 2017. Applications of RBI on leakage risk assessment of direct coal liquefaction process. Journal of Loss Prevention in the Process Industries 45, 194–202.

Edwards, D.W., Lawrence, D.W., 1993. Assessing the inherent safety of chemical process routes: is there a relation between plant costs and inherent safety? Transactions of IChemE 71, 252–258.

EI, 2006. EI Research Report: Ignition Probability Review, Model Development and Look-up Correlations, Energy Institute.

Eini, S., Javidi, M., Shahhosseini, H.R., Rashtchian, D., 2018. Inherently safer design of a reactor network system: A case study. Journal of Loss Prevention in the Process Industries 51, 112–124.

Eini, S., Shahhosseini, H., Delgarm, N., Lee, M., Bahadori, A., 2016. Multi-objective optimization of a cascade refrigeration system: Exergetic, economic, environmental, and inherent safety analysis. Applied Thermal Engineering 107, 804–817.

Eini, S., Shahhosseini, H.R., Javidi, M., Sharifzadeh, M., Rashtchian, D., 2016. Inherently safe and economically optimal design using multi-objective optimization: The case of a refrigeration cycle. Process Safety and Environmental Protection 104, 254–267.

Engebø, A., Ahmed, N., Garstad, J.J., Holt, H., 2013. Risk Assessment and Management for CO2 Capture and Transport Facilities. Energy Procedia 37, 2783–2793.

Fabbrocino, G., Iervolino, I., Orlando, F., Salzano, E., 2005. Quantitative risk analysis of oil storage facilities in seismic areas. Journal of Hazardous Materials 123, 61–69.

Gallina, V., Torresan, S., Critto, A., Sperotto, A., Glade, T., Marcomini, A., 2016. A review of multi-risk methodologies for natural hazards: Consequences and challenges for a climate change impact assessment. Journal of Environmental Management.

Gross, R.E., Mitchell, E.M., Harris, S.P., 2012. Evaluation of Maintenance Intervals for Spring-Operated Relief Valves Using a Risk-Based Inspection Technique. Journal of Pressure Vessel Technology 134, 061601.

Hassim, M., Hurme, M., 2010. Inherent occupational health assessment during process research and development stage. Journal of Loss Prevention in the Process Industries 23, 127–138.

Heikkilä, A.M., 1999. Inherent safety in process plant design. An index-based approach. VTT Publications 129.

Hvidevold, H.K., Alendal, G., Johannessen, T., Ali, A., Mannseth, T., Avlesen, H., 2015. Layout of CCS monitoring infrastructure with highest probability of detecting a footprint of a CO2 leak in a varying marine environment. International Journal of Greenhouse Gas Control 37, 274–279.

Jafari, M., Zarei, E., Badri, N., 2012. The quantitative risk assessment of a hydrogen generation unit. international journal of hydrogen energy 37, 19241–19249.

Kabir, G., Sadiq, R., Tesfamariam, S., 2016. A fuzzy Bayesian belief network for safety assessment of oil and gas pipelines. Structure and Infrastructure Engineering 12, 874–889.

Kamsu-Foguem, B., 2016. Information structuring and risk-based inspection for the marine oil pipelines. Applied Ocean Research 56, 132–142.

Kanbur, B.B., Xiang, L., Dubey, S., Choo, F.H., Duan, F., 2017. Cold utilization systems of LNG: A review. Renewable and Sustainable Energy Reviews 79, 1171–1188.

Khan, F.I., Amyotte, P.R., 2004. Integrated inherent safety index (I2SI): A tool for inherent safety evaluation. Process Safety Progress 23, 136–148.

Kim, H., Heo, G., Jung, S., 2016. QRA considering multi-vessel failure scenarios due to a natural disaster ??? Lessons from Fukushima. Journal of Loss Prevention in the Process Industries 44, 699–705.

Kim, K., Lee, U., Kim, C., Han, C., 2015. Design and optimization of cascade organic Rankine cycle for recovering cryogenic energy from liquefied natural gas using binary working fluid. Energy 88, 304–313.

Kletz, T.A., 1978. What you don't have, can't leak. Chemistry and Industry.

Konak, A., Coit, D.W., Smith, A.E., 2006. Multi-objective optimization using genetic algorithms: A tutorial. Reliability Engineering & System Safety 91, 992–1007.

Koornneef, J., Spruijt, M., Molag, M., Ramírez, A., Turkenburg, W., Faaij, A., 2010a. Quantitative risk assessment of CO2 transport by pipelines—A review of uncertainties and their impacts. Journal of Hazardous Materials 177, 12–27.

Koornneef, J., Spruijt, M., Molag, M., Ramírez, A., Turkenburg, W., Faaij, A., 2010b. Quantitative risk assessment of CO2 transport by pipelines-A review of uncertainties and their impacts. Journal of Hazardous Materials 177, 12–27.

Landucci, G., Antonioni, G., Tugnoli, A., Cozzani, V., 2012. Probabilistic assessment of domino effect triggered by fire: Implementation in quantitative risk assessment. Chemical Engineering Transactions 26, 195–200.

Lee, C.-J., Lee, Y., Lee, G., Lee, W., Park, J.-M., Gae, H., 2017. A Study on the Improvement of Safety for Urban gas facilities.

Lee, U., Kim, K., Han, C., 2014a. Design and optimization of multi-component organic rankine cycle using liquefied natural gas cryogenic exergy. Energy 77, 520–532.

Lee, U., Park, K., Jeong, Y.S., Lee, S., Han, C., 2014b. Design and Analysis of a Combined Rankine Cycle for Waste Heat Recovery of a Coal Power Plant Using LNG Cryogenic Exergy. Industrial & Engineering Chemistry Research 53, 9812–9824.

Lee, Y., Lee, S., Shin, S., Lee, G., Jeon, J., Lee, C., Han, C., 2015. Risk-Based Process Safety Management through Process Design Modi fi cation for Gas Treatment Unit of Gas Oil Separation Plant. Industrial & Engineering Chemistry Research.

Lentini, J.J., 2013. Scientific protocols for fire investigation. CRC Press.

Leong, C.T., Shariff, A.M., 2009. Process route index (PRI) to assess level of explosiveness for inherent safety quantification. Journal of Loss Prevention in the Process Industries 22, 216–221.

Li, X., Chen, G., Zhu, H., 2016. Quantitative risk analysis on leakage failure of submarine oil and gas pipelines using Bayesian network. Process Safety and Environmental Protection 103, 163–173.

Liang, C., Ghazel, M., Cazier, O., El-Koursi, E.-M., 2017. Risk analysis on level crossings using a causal Bayesian network based approach. Transportation Research Procedia 25, 2172–2186.

Little, M., Jackson, R., 2010. Potential impacts of leakage from deep CO2 geosequestration on overlying freshwater aquifers. Environmental science & technology.

Liu, Y., Guo, K., 2011. A novel cryogenic power cycle for LNG cold energy recovery. Energy 36, 2828–2833.

Mancuso, A., Compare, M., Salo, A., Zio, E., Laakso, T., 2016. Risk-based optimization of pipe inspections in large underground networks with imprecise information. Reliability Engineering & System Safety 152, 228–238.

Martinez-Gomez, J., Nápoles-Rivera, F., Ponce-Ortega, J.M., El-Halwagi, M.M., 2017a. Optimization of the production of syngas from shale gas with economic and safety considerations. Applied Thermal Engineering 110, 678–685.

Martínez-Gomez, J., Peña-Lamas, J., Martín, M., Ponce-Ortega, J.M., 2017. A multi-objective optimization approach for the selection of working fluids of geothermal facilities: Economic, environmental

and social aspects. Journal of Environmental Management 203, 962–972.

Martinez-Gomez, J., Ramírez-Márquez, C., Alcántara-Ávila, J.R., Segovia-Hernández, J.G., Ponce-Ortega, J.M., 2017b. Intensification for the Silane Production Involving Economic and Safety Objectives. Industrial & Engineering Chemistry Research 56, 261–269.

Martinez-Gomez, J., Sánchez-Ramírez, E., Quiroz-Ramírez, J.J., Segovia-Hernandez, J.G., Ponce-Ortega, J.M., El-Halwagi, M.M., 2016. Involving economic, environmental and safety issues in the optimal purification of biobutanol. Process Safety and Environmental Protection 103, 365–376.

Martins, M.R., Schleder, A.M., Droguett, E.L., 2014. A Methodology for Risk Analysis Based on Hybrid Bayesian Networks: Application to the Regasification System of Liquefied Natural Gas Onboard a Floating Storage and Regasification Unit. Risk Analysis 34, 2098–2120.

Medina-Herrera, N., Jiménez-Gutiérrez, A., Mannan, M.S., 2014. Development of inherently safer distillation systems. Journal of Loss Prevention in the Process Industries 29, 225–239.

Medina, H., Arnaldos, J., Casal, J., 2009. Process design optimization and risk analysis. Journal of Loss Prevention in the Process, 566–573.

Mehrpooya, M., Moftakhari Sharifzadeh, M.M., Rosen, M.A., 2016. Energy and exergy analyses of a novel power cycle using the cold of LNG (liquefied natural gas) and low-temperature solar energy. Energy 95, 324–345.

Meng, Y., Lu, C., Yan, Y., Shi, L., Liu, J., 2015. Method to analyze the regional life loss risk by airborne chemicals released after devastating earthquakes: A simulation approach. Process Safety and Environmental Protection 94, 366–379.

Metcalfe, R., Bond, A., Maul, P., Paulley, A., 2013. Whole-System Process Modelling of CO2 Storage and its Application to the In Salah CO2 Storage Site, Algeria. Energy Procedia 37, 3859–3866.

Nicol, A., Carne, R., Gerstenberger, M., Christophersen, A., 2011. Induced seismicity and its implications for CO2 storage risk. Energy Procedia.

Noori, S.A., Price, J.W.H., 2006. A risk approach to the management of boiler tube thinning. Nuclear Engineering and Design 236, 405–414.

Oil and Gas Producers, 2010. Process Release Frequencies, International Association of Oil and Gas Producers.

Oldenburg, C.M., Jordan, P.D., Nicot, J.P., Mazzoldi, A., Gupta, A.K., Bryant, S.L., 2011. Leakage risk assessment of the In Salah CO2storage project: Applying the Certification Framework in a dynamic context, in: Energy Procedia. pp. 4154–4161.

Palaniappan, C., Srinivasan, R., Halim, I., 2002. A material-centric methodology for developing inherently safer environmentally benign processes, in: Computers and Chemical Engineering. pp. 757–774.

Patel, S.J., Ng, D., Mannan, M.S., 2010. Inherently safer design of solvent processes at the conceptual stage: Practical application for substitution. Journal of Loss Prevention in the Process Industries 23, 483–491.

Pawar, R.J., Bromhal, G.S., Carey, J.W., Foxall, W., Korre, A., Ringrose, P.S., Tucker, O., Watson, M.N., White, J.A., 2015. Recent

advances in risk assessment and risk management of geologic CO2 storage. International Journal of Greenhouse Gas Control 40, 292–311.

Pedersen, N., 2012. Modeling of jet and pool fires and validation of the fire model in the CFD code FLACS.

Qiang, W., Yanzhong, L., Jiang, W., 2004. Analysis of power cycle based on cold energy of liquefied natural gas and low-grade heat source. Applied Thermal Engineering 24, 539–548.

Rhee, H., Seo, J., Sheen, D., Choi, I., 2012. Probabilistic seismic hazard analysis on Metropolitan cities and counties in Korea. Journal of the Geological Society of Korea.

Rohmer, J., Seyedi, D., 2010. Coupled large scale hydromechanical modelling for caprock failure risk assessment of CO2 storage in deep saline aquifers. Revue de l'Institut Français du.

Seo, J.K., Cui, Y., Mohd, M.H., Ha, Y.C., Kim, B.J., Paik, J.K., 2015. A risk-based inspection planning method for corroded subsea pipelines. Ocean Engineering 109, 539–552.

Shariff, A.M., Leong, C.T., 2009. Inherent risk assessment — A new concept to evaluate risk in preliminary design stage. Am Dental Assoc 7, 371–376.

Shi, X., Che, D., 2009. A combined power cycle utilizing low-temperature waste heat and LNG cold energy. Energy Conversion and Management 50, 567–575.

Smith, J., Durucan, S., Korre, A., Shi, J., 2011. Carbon dioxide storage risk assessment: Analysis of caprock fracture network connectivity. International Journal of Greenhouse.

Stephens, M.J., Leewis, K., Moore, D.K., 2002. A Model for Sizing High Consequence Areas Associated With Natural Gas Pipelines, in: 4th International Pipeline Conference, Parts A and B. ASME, pp. 759–767.

Tan, Z., Li, J., Wu, Z., Zheng, J., He, W., 2011. An evaluation of maintenance strategy using risk based inspection. Safety Science 49, 852–860.

Tucker, O., Holley, M., Metcalfe, R., Hurst, S., 2013. Containment Risk Management for CO2 Storage in a Depleted Gas Field, UK North Sea. Energy Procedia 37, 4804–4817.

Vilarrasa, V., Carrera, J., 2015. Geologic carbon storage is unlikely to trigger large earthquakes and reactivate faults through which CO2 could leak. Proceedings of the National Academy of Sciences.

Vinod, G., Sharma, P.K., Santosh, T.V., Hari Prasad, M., Vaze, K.K., 2014. New approach for risk based inspection of H2S based Process Plants. Annals of Nuclear Energy 66, 13–19.

Wahid, H., Ahmad, S., Nor, M.A.M., Rashid, M.A., 2017. Prestasi kecekapan pengurusan kewangan dan agihan zakat: perbandingan antara majlis agama islam negeri di Malaysia. Jurnal Ekonomi Malaysia 51, 39–54.

Wang, H., Shi, X., Che, D., 2013. Thermodynamic optimization of the operating parameters for a combined power cycle utilizing low-temperature waste heat and LNG cold energy. Applied Thermal Engineering 59, 490–497.

Witkowski, A., Rusin, A., Majkut, M., Rulik, S., Stolecka, K., 2015. Advances in Carbon Dioxide Compression and Pipeline Transportation Processes. Springer.

Zhang, L., Huang, H., Wang, Y., Ren, B., Ren, S., Chen, G., Zhang, H., 2014. CO_2 storage safety and leakage monitoring in the CCS

demonstration project of Jilin oilfield, China. Greenhouse Gases: Science and Technology 4, 425–439.

Zoback, M.D., Gorelick, S.M., 2012. Earthquake triggering and large-scale geologic storage of carbon dioxide. Proceedings of the National Academy of Sciences 109, 10164–10168.

Nomenclature

Acronyms

ALARP	As low as reasonably practicable
AEP	Annual exceedance probability
BN	Bayesian network
DAG	Directed acyclic graph
FTA	Fault tree analysis
PGA	Peak ground acceleration
ETA	Event tree analysis
HAZID	Hazard identification
IDLH	Immediately dangerous to life or health concentrations
PSA	Probabilistic safety assessment
QRA	Quantitative risk analysis
ISD	Inherent Safety Design
LINMAP	Linear Programming Technique for Multidimensional Analysis of Preference
LNG	Liquefied Natural Gas
MOO	Multi-Objective Optimization
ORC	Organic Rankine Cycle
TOPSIS	Technique for Order Preference by Similarity to an Ideal Solution

Variables

$\dot{n_{wf}}$	Mole flow rate of working fluid (kmol/s)
P_{wf}	Inlet turbine pressure of working fluid (bar)
d_{i+},d_{i-}	Distance from ideal/non-ideal solution
F_j^{ideal},$F_j^{non-ideal}$	Ideal/non-ideal solution in objective j
$\dot{m}_{vapor}$	Gas discharge rate, choked flow (kg/s)
$\dot{m}_{liquid}$	Liquid discharge rate (kg/s)
$\dot{m}_{total}$	Released mass due to continuous release (kg/s)
h_L	Liquid head (assume 0 m)

C_D	Discharge coefficient (for liquid, gases 1)
C_T	Fuel mole fraction concentration in a stoichiometric fuel air mixture (unitless)
D_{max}	Maximum diameter of fireball (m)
D_{risk}	Risk distance (m)
E_r	Radiant flux at the receiver (kJ/m^2 s)
$\dot{E}$	exergy rate (kJ/s)
F_{21}	View factor (dimensionless)
F_p	Point source view factor (m^{-2})
H_{TNT}	Heat of combustion of TNT (4686 kJ/kg)
H_{comb}	Energy of combustion of the fuel (kJ/kg)
L_{flame}	Length of the visible turbulent flame measured from break point (m)
M_a	Air molecular weight (kg/kmol)
M_f	Fuel molecular weight (kg/kmol)
P_a	Upstream absolute pressure (bar)
P_g	Upstream gauge pressure (kPa)
P_i	Probability of event i
Q*	Released mass due to instantaneous release (kg)
R_g	gases constant (8314 J/kg-mol/K)
$R_{overall}$	Individual risk (m/yr)
T_a	Air temperature (K)
X_s	Path length distance (m)
a,b,c_i	UVCE constants for overpressure peak calculations
d_j	Diameter of the jet, physical diameter of the nozzle (m)
g_c	Gravitational constant (unitless)
$k_1,\ k_2$	Probit constants depending of type of effect (unitless)
t_{BLEVE}	Duration of fireball (s)
t_e	Time to exposure to concentration C (min)
A	Hole cross-sectional area (m^2)
C	Air toxic concentration (ppm)
Dose	Dose received by a individual assuming total duration exposure

E	Radiative emissive flux (kJ/m^2 s)
L	Distance from incident to objective (m)
M	molecular weight (kg/kmol)
P	Probability (percent)
R	Radiative fraction of the heat of combustion (unitless)
RH	Relative humidity (percent)
H	enthalpy (kJ)
S	entropy (kJ/K)
$\dot{W}$	power (kJ/s)
$\dot{Q}$	heat transfer rate (kJ/s)
V	Causative variable (dose, thermal radiation, overpressure)
W	Equivalent mass of TNT (kg)
Y	Probit variable
Z	Scaled range TNT equivalency model (m/kg$^{1/3}$)
g	Acceleration due to gravity
k	Specific heats relation
n	Material toxicity related constant (unitless)
t	Time of interest in instantaneous release (s)
u	Wind velocity (m/s)
x	Downwind direction (m)
y	Cross-wind direction (m)
z	Distance above the ground (m)
f	Frequency rate considering seismic effect
f_0	Frequency rate from historic data
f_α	Frequency rate from seismic effect including multi-hazard and domino-effects
$f_{h,i,j}$	Frequency rate of leak event from historic data
$f_{s,i,j}$	Frequency rate from direct seismic effect
$f_{d,i,j}$	Frequency rate from effect by domino-effects and by multi-hazard effects
F_i	Frequency of event I
F_N	Frequency of all events

IR_i	Individual risk by event I
N_i	The number of fatalities resulting from event I
N_p	The number of people
P_{fi}	Probability of fatality by event I
P_{PGA}	Leak probability of the tank according to PGA value

Greek symbol

η_e	Empirical explosion efficiency (unitless)
η_{exergy}	exergy efficiency (unitless)
η_j	Fraction of total energy converted to radiation (unitless)
σ_x	Dispersion coefficient in x direction (m)
σ_y	Dispersion coefficient in y direction (m)
σ_z	Dispersion coefficient in z direction (m)
τ_a	Atmospheric transmissivity (transmitted energy fraction: 0-1)

Abstract in Korean (국문초록)

화학공정의 안전성은 그 중요성으로 인해 설계 단계부터 오퍼레이션 및 유지, 관리 단계까지 전 공정주기에서 여러 안전관리기법이 활용되고 적용되고 있다. 그러나 대부분의 기법은 정성적이고, 일부 정량적인 기법의 경우에는 화학공정의 복잡성 증가로 인해 적절한 위험성을 평가하는데 한계를 가지고 있다. 따라서 공정주기 및 공정 특성을 고려한 정량적 공정 안전 관리방법의 필요성과 중요성이 크다. 따라서, 본 논문에서는 화학공정의 안전을 관리하기 위해 공정주기 및 공정 특성을 고려한 위험도 기반의 설계 및 관리 방법을 제안한다.

첫째, 개념 설계 단계에서 공정 안전을 고려하기 위한 위험도 기반의 설계 방법을 제안하고, 이를 적용하였다. 정량적 위험성 평가 기법을 활용한 내재적 안전 설계 방법론을 사용하여, 공정의 안전성을 정량적으로 고려되도록 하였다. 위험도 기반 설계 방법론은 액화 천연 가스의 냉기 활용 수단 중 하나인 유기 랭킨 사이클의 설계에 적용하였으며, 열역학 측면과 안전성 측면을 동시에 고려하여 설계될 수 있도록 하였다. 두 가지 측면을 동시에 고려하기 위한 방법으로는 다목적 최적화 방법론을 적용하였다. 주요 설계 인자인 작동 유체의 조건들을 변수로 설정하고, 최종적으로 세 가지 카테고리 (순수 성분, 이원 성분, 삼원 성분)의

총 여섯 가지 작동 유체에 대해서 운전 조건에 따른 결과를 비교 분석하였다. 결과적으로 개념 설계 단계에서 위험도 기반 설계 방법론을 기반으로 위험도를 정략적으로 고려하여 유기 랭킨 사이클 공정을 설계할 수 있게 하였다.

둘째, 기본 설계 단계에서 지진 영향을 고려한 위험도 평가를 통한 위험도 기반 관리를 제안하고, 이를 적용하였다. 기존의 정량적 위험성 평가 기법을 베이지안 네트워크 기법을 사용하여 도미노 효과 및 다중 위험 영향을 포함한 지진 영향으로 인한 위험성을 평가할 수 있도록 개선하였다. 구체적으로, 빈도 분석이 인과 관계를 기반으로 하기 때문에, 인과 관계를 분석 가능한 베이지안 네트워크 기법을 활용함으로써 도미노 효과와 다중 위험 영향을 효과적으로 고려할 수 있었다. 해당 방법론은 지진의 영향을 받기 쉬운 지중 저장을 위한 탑사이드 플랫폼에 설치된 이산화탄소 주입공정 시스템에 적용하였다. 결과적으로, 기본 설계 단계에서 지진 지역에 설치되는 화학 공정의 안전성을 개선된 정량적 위험성 평가 기법을 활용하여 평가하고, 이를 기반으로 관리될 수 있게 하였다.

마지막으로, 오퍼레이션 단계에서 위험도를 고려한 배관 관리를 위하여 위험도 기반 순찰 방법론을 제안하고 적용하였다. 위험도

기반의 순찰 방법론은 천연 가스 파이프 라인의 정량적 위험도를 기반으로 하여, 차별적 안전 관리를 위하여 제안되었다. 방법론의 전체 구조는 실패 확률과 실패 결과로 구성된 위험도 기반 검사 방법론의 구조를 기반으로 구성하였으며, 순찰 측면에서의 위험도 평가의 목적에 맞게 천연가스 파이프 라인의 위험도에 영향을 미치는 위험 요소를 고려하기 위한 인덱스를 제안하였다. 결과적으로, 오퍼레이션 단계에서, 천연가스 파이프라인에 대한 위험도 매트릭스 결과에 따른 위험도 수준을 기준으로 최소 순찰주기가, 위험도 값을 기준으로 순찰 계획이 산출될 수 있게 하였다.

주요어: 공정주기; 공정 설계; 위험도 기반 설계; 정량적 위험성 평가; 위험도 기반 관리;

학 번: 2014-21587